

Structural and functional largescale brain network dynamics: Examples from mental disorders



Justyna Beresniewicz

Thesis for the degree of Philosophiae Doctor (PhD)
University of Bergen, Norway
2023

UNIVERSITY OF BERGEN



Structural and functional largescale brain network dynamics: Examples from mental disorders

Justyna Beresniewicz



Thesis for the degree of Philosophiae Doctor (PhD)
at the University of Bergen

Date of defense: 10.03.2023

© Copyright Justyna Beresniewicz

The material in this publication is covered by the provisions of the Copyright Act.

Year: 2023

Title: Structural and functional largescale brain network dynamics: Examples from mental disorders

Name: Justyna Beresniewicz

Print: Skipnes Kommunikasjon / University of Bergen

Scientific environment

This PhD-project has evolved in the scientific milieu of the Bergen fMRI research group at the Department of Biological and Medical Psychology (IBMP), University of Bergen (UIB), and the International Graduate School of Integrated Neuroscience (IGSIN) at the Faculty of Psychology (UIB) and the Norwegian Research School in Neuroscience (NRSN). The highly interdisciplinary neuroimaging research environment in Bergen (University of Bergen/ Haukeland University Hospital), includes in addition to the Bergen fMRI group, the Mohn Medical Imaging Visualization Center (MMIV) and the Bergen part of the NORMENT Center of Excellence (organized to the University of Oslo). The Bergen fMRI group has provided all necessary resources needed to complete the work in the thesis, including e-Infrastructure (Safe, University of Bergen), Infrastructure such as access state-of-the-art MRI scanners (Haukeland University Hospital) as well as other data material and data processing tools. A scheduled research stay abroad (Section on Development and Affective Neuroscience at the National Institute of Mental Health, USA) funded by the University of Bergen and the Meltzer Foundation, had to be canceled due to the COVID19 pandemic.

The main supervisor of the project is Associate Professor Renate Gruner, Department of Physics and Technology (UIB). The co-supervisor of this project is Professor Kenneth Hugdahl, Department of Biological and Medical Psychology, University of Bergen, Division of Psychiatry/ Dept of Radiology, Haukeland University Hospital. The project was funded by European Research Council (ERC) Advanced Grant # 693124 (“ONOFF - Perception of voices that do not exist: tracking the temporal signatures of auditory hallucinations”) to Professor Hugdahl.



Acknowledgments

I started my scientific journey in Norway as a master's student in 2015 thanks to the Erasmus exchange between the Institute of Medical Electronics, Lodz University of Technology, and the Department of Biomedicine, University of Bergen. My PhD time has been undoubtedly the most challenging period in my life, and therefore, I am very grateful for all the fantastic people that helped me through these years. Without you all, it would not be possible!

Firstly, I would like to thank my supervisors, Renate Gruner and Kenneth Hugdahl. The Ph.D. supervisor's role is much different from a boss's, and you both were much more than bosses to me. Thank you both for your patients while combating all the challenges of that PhD. Renate, you are a fantastic role model of a successful woman in science that I so much needed. Your optimism and kindness gave me a lot of motivation, especially in situations that looked hopeless.

Kenneth, by your side, young people flourish. Your open mind and enthusiasm towards new ideas and technologies inspired me to start a Ph.D. In addition, you showed me how to be a scientist and what it means to be a great leader.

I want to express my gratitude to Frank Riemer for his scientific advice and help with fMRI projects. Frank, your help was invaluable, and I cannot express enough how much I appreciate it! I always enjoyed our meetings and felt like I could discuss anything with you freely.

I want to thank all the articles' coauthors for their invaluable input while performing the projects and during manuscripts preparations. Additionally, I want to thank radiographers at Haukeland University Hospital. Thank you for helping in data collection most effectively and professionally and making the hours at the scanner the day's highlight. It was a pleasure to work with you all.

I would also thank all other administrative and research employees of IBMP: Alex Craven, Karsten Specht, Marco Hirnstein, Linn Sørensen, Robert Murison, Hege Folkedal, Vivian Fosse, Anna Marie Kinn Rød, Nina Harkestad and Lydia Brunvoll Sandøy. Thank you for being helpful, making everyday struggles more effortless, and creating a great working environment.

Lastly, but very importantly, I would love to thank my fantastic friends and family. I want to thank a lot to PhDs and postdocs of IBMP. You were my therapists, supervisors, friends, and the best support network I could ever wish for. I always felt like I could talk my heart out with you without fear of judgment.

Gerard, Isabella, Andrea, and Sarah, thank you for our countless phone conversations during the COVID pandemic when I could vent, cry, laugh, and discuss my Ph.D. and life struggles with you. Big thank you to Andrea for always being my voice of logic and reason! Isabela, your kind heart and empathy are so unique and precious. Gerard and Sarah, thank you for your help, support, and guidance! Thank you all for being by my side, especially at the end of my Ph.D. journey. Big thanks to Albin Severinson, with whom I had the pleasure of building the UiBdoc. I learned a lot from you, Albin, and I genuinely believe we could change the world together.

I would love to thank my partner Dan Inge for being my window out from the research bobble. You have always been my anchor, and I am excited about our new life challenges together. You gave me a family here in Norway, whom I love so much. Thank you to Boleslaw Srebro for being an inspiration and support from the very beginning of my journey in Norway. Special thanks to my mother and grandparents in Poland for never doubting me, always being my biggest fans, and pushing me to be my best in whatever I do in life.

Abstract

The human brain is organized in various networks both functionally and structurally. However, despite the extensive research on brain connectivity, which was made possible due to the development of *in vivo* brain imaging techniques, the neuroscientific field is still far from fully comprehending networks function and dynamics.

Detailed knowledge about the relationship between various brain networks is essential for understanding the function of the healthy brain. However, many studies on mental disorders such as schizophrenia suggest that it might be caused by abnormal brain network functioning and structural aberrations. Therefore, the knowledge of the brain network's dynamics and structure might be critical for revealing the underpinnings of mental disorders such as schizophrenia. The presented thesis had three main goals, resulting in three structural and functional imaging studies.

Firstly, the brain's structural connectivity affected by schizophrenia has been investigated to determine the nature and extent of its changes. Hence, Diffusion Tensor Imaging (DTI) and tract-based spatial statistics (TBSS) were employed to explore white matter differences between subtypes of schizophrenia patients compared to healthy controls. This study revealed widespread FA-value reduction in the hallucinating schizophrenia subjects' white matter compared to non-hallucinating ones.

Since widespread aberrations of the white matter should affect the function of the large-scale brain networks, the second goal was to explore the two main functional brain networks, Default Mode Network (DMN) and Extrinsic Mode Network (EMN). This is because dysfunction of DMN and EMN networks has been previously suggested to be significant for the generation of symptoms of schizophrenia disorder, such as Auditory Verbal Hallucinations (AVH). Since the concept of EMN is relatively new and not yet deeply explored, and additionally protocol used in that study has not been previously utilized to study EMN and DMN, it was first necessary to test the design in

a group of healthy participants. This study used the novel protocol based on the classic block design fMRI experiment with three different visual tasks: mental rotation, working memory, and mental arithmetic. The results of study II proved the existence of the EMN that is anti-correlated with the DMN and is domain-general.

Lastly, the neuroimaging studies of the participants suffering from mental disorders such as schizophrenia require relatively short and effective examination protocols. Therefore, the last project investigated both similarities and differences in DMN activity between two experimental designs: block design and resign state. A classic block design experiment would be a good candidate for the investigation reflecting the fluctuating activity of the brain during typical daily activity. The results of Study III showed that the activity of the DMN was generally similar in the two experiments, though with some discrepancies. These differences were in the DMN architecture itself and concerning the relations of the DMN with other brain networks. These findings, in combination with the results of study number two suggest that the block design experiment could be the most effective for studying the function of the brain in schizophrenia.

The studies incorporated in that thesis add to the current findings on the white matter alterations in schizophrenia disorder and contribute to a better understanding of the function and dynamics of the large-scale brain networks: EMN and DMN. Last but not least, the performed studies give a good background for future clinical studies on schizophrenia disorder.

List of Studies

- I. Beresniewicz, J., Craven, A. R., Hugdahl, K., Løberg, E.-M., Kroken, R. A., Johnsen, E., & Grüner, R. (2021). White matter microstructural differences between hallucinating and non-hallucinating schizophrenia spectrum patients. *Diagnostics, 11*(1), 139

- II. Riemer, F., Grüner, R., Beresniewicz, J., Kazimierczak, K., Ersland, L., & Hugdahl, K. (2020). Dynamic switching between intrinsic and extrinsic mode networks as demands change from passive to active processing. *Scientific Reports, 10*(1), 1-10

- III. Beresniewicz J., Riemer F., Kazimierczak K., Ersland L., Hugdahl K., Grüner R. Similarities and differences between intermittent and continuous resting-state fMRI. Manuscript submitted

Parts of the work in this thesis has additionally been presented at relevant national and international conferences in the field.

Reprints of “White matter microstructural differences between hallucinating and non-hallucinating schizophrenia spectrum patients” and “Dynamic switching between intrinsic and extrinsic mode networks as demands change from passive to active processing” are presented with permissions granted through open access publishing.

List of abbreviations

Abbreviation	Definition
ACC	Anterior Cingulate Cortex
ANOVA	Analysis of Variance
AVH	Auditory Verbal Hallucinations
BOLD	Blood-oxygen-level-dependent
CEN	Central Executive Network
DDD	Defined Daily Dose
DMN	Default Mode Network
DTI	Diffusion Tensor Imaging
DWI	Diffusion Weighted Imaging
EEG	Electroencephalography
EMN	Extrinsic Mode Network
ENIGMA	Enhancing Neuro Imaging Genetics through Meta-Analysis
ERC	European Research Concil european resuscitation council
FA	Fractional Anisotropy
FD	framewise displacement
fMRI	Functional Magnetic Resonance Imaging
HRF	Hemodynamic Response Function
ICA	Independent Component Anlalysis
MD-system	Multiple Demand system
MNI	Montreal Neurological Institute
MPFC	Medial prefrontal cortex
MPRAGE	Magnetization Prepared - RApid Gradient Echo
MR	Magnetic Resonance
MRI	Magnetic Resonance Imaging
PALM	Permutation Interface for the General Linear Model
PANSS	Positive and Negative Syndrom Scale
PCC	Posterior Cingulate Cortex
PET	Positron emisjon tomografi
SLF	Superior Longitudinal Fasciculus
SMA	Supplementary Motor Area
SN	Salience Network
SPM	Statistical parametric mapping
TBSS	Tact Based Spatial Statistics
TE	Time to Echo
TR	Repetition Time

WCST

Wisconsin Card Sorting Test

List of figures

Figure 1- The Default Mode Network.....	7
Figure 2- The Extrinsic Mode Network.....	8
Figure 3- Diffusion in different tissue structures.	15
Figure 4- Diffusion tensors of isotropic and anisotropic diffusion.	16
Figure 5- The HRF function.....	18

Contents

SCIENTIFIC ENVIRONMENT	I
ACKNOWLEDGEMENTS.....	II
ABSTRACT.....	IV
LIST OF PUBLICATIONS.....	VI
LIST OF ABBREVIATIONS.....	VII
LIST OF FIGURES.....	VII
CONTENTS.....	X
1. INTRODUCTION	1
1.1 STRUCTURAL AND FUNCTIONAL BRAIN NETWORKS	1
1.1.1 <i>Structural networks</i>	4
1.1.2 <i>The Default Mode Network</i>	5
1.1.3 <i>The Extrinsic Mode Network</i>	7
1.2 FUNCTIONAL NETWORK DYNAMICS AND INTERACTIONS.....	9
1.3 BRAIN NETWORK AND IMPLICATIONS FOR MENTAL DISORDERS.....	11
1.4 MAGNETIC RESONANCE IMAGING AND BRAIN NETWORK.....	13
1.4.1 <i>Diffusion Weighted Imaging</i>	14
1.4.2 <i>Functional MRI</i>	17
2. SPECIFIC BACKGROUND AND AIMS OF THE STUDY	20
3. METHODS	23
3.1 PARTICIPANTS.....	23
3.2 MRI DATA ACQUISITION	24
3.3 FUNCTIONAL NEUROIMAGING – COGNITIVE TASKS	25
3.4 IMAGE PROCESSING PIPELINES.....	26

3.5	STATISTICAL EVALUATIONS	29
4.	RESULTS	33
4.1	PAPER I – DIFFUSION TENSOR IMAGING IN MENTAL DISORDERS	33
4.2	PAPER II – NOVEL APPROACH TO NEUROIMAGING OF EFFORTS	34
4.3	PAPER III – SIMPLIFYING MAPPING OF RESTING-STATE	34
5.	DISCUSSION	36
5.1	LARGE SCALE NETWORK ALTERATION IN MENTAL DISORDERS SUCH AS SCHIZOPHRENIA.....	37
5.2	EMN AS A TASK TASK-POSITIVE NETWORK INDEPENDENT ON THE SENSORY MODALITY.....	39
5.3	EMN UP-REGULATION INDEPENDENT ON THE TASK SPECIFICS.	40
5.4	EMN MODULATED BY THE ENVIRONMENTAL DEMANDS	40
5.5	DMN AND EMN DYNAMICS COMPLEXITIES.....	41
5.6	DMN ACTIVITY PATTERN DEPENDING ON THE FUNCTIONAL MRI EXPERIMENTAL DESIGN ..	42
5.7	DMNs CONNECTIVITY DEPENDING ON THE FUNCTIONAL MRI EXPERIMENTAL DESIGN	43
5.8	THE BLOCK DESIGN EXPERIMENT AS A PROXY OF A DAILY BRAIN ACTIVITY	44
5.9	LIMITATIONS.....	45
5.10	CONCLUSION AND FUTURE DIRECTIONS.	47
6.	REFERENCES	49

1. Introduction

Modern neuroimaging and subsequent advanced data processing have provided unique insight into the living human brain. Still, the structural complexity and function of the healthy, thinking brain are still only poorly understood. There is a need for modifying current approaches to explore remaining questions. Understanding human cognition may in turn develop into biomarkers for understanding mental disorders. In this thesis summary, basic concepts of neuroimaging are described, alongside an introduction to the current state-of-the-art and the thesis aims.

1.1 Structural and Functional Brain Networks

The human brain is structurally and functionally arranged into a collection of specialized networks that flexibly interact to support various cognitive functions (Damien A Fair, Cohen et al., 2009). The properties of those complex networks have been identified with consistency in several modalities of neuroimaging data and over a range of spatial and time scales (Bassett & Bullmore, 2009).

Brain networks can be specified based on structural connectivity or functional interdependence, being a common activity in various brain structures that are mutually dependent under variation of a functional or behavioral parameter (Bressler & Menon, 2010). Functional neuroimaging uses functional Magnetic Resonance Imaging (fMRI) blood-oxygenation-level-dependent (BOLD) signal contrast to identify nodes of large-scale functional networks by relating temporally joint activation of brain areas to various cognitive processes and mental states. The identification of functional network edges comes from the analysis of functional interdependence (or functional connectivity), which assesses interactions among network nodes (Bressler & Menon, 2010). Functional connectivity of the brain is most often studied using resting-state functional Magnetic Resonance Imaging (rs-fMRI).

The brain structural network organization is based on white matter microstructure that physically interconnects brain regions. The most often used approach to study structural brain connectivity is diffusion-based magnetic resonance imaging methods, such as diffusion tensor imaging (DTI). This method allows determining major fiber bundles of the brain *in vivo* by identifying the principal direction of diffusion between fiber bundles (Bressler & Menon, 2010). The main difference between functional and structural connectivity is that functional connectivity is purely correlative, while structural connectivity reflects measurable physical connections. Therefore, functional connectivity between two regions may be seen even when structural connections are weak or absent. However, in most cases, these two aspects of brain connectivity show at least some level of convergence (Eickhoff & Müller, 2015).

Structural networks provide a complex architecture that facilitates dynamic interactions between brain areas that provides the underpinning for functional networks. It has been long assumed that cognitive functions and mental states are driven by the operations of distinctive brain areas either in isolation or in simple interactions. However, more recent findings have shifted focus in favor of the view that cognition results from the dynamic interactions of distributed brain areas acting in large-scale networks (Bressler & Menon, 2010). Therefore, a functional brain network can be defined as interconnected brain areas that interact to perform circumscribed cognitive and mental functions.

One of the most studied and known functional large-scale brain networks, the Default Mode Network (DMN), shows deactivation during engagement in cognitive tasks and increased activity during awake resting (Bressler & Menon, 2010). Therefore, the DMN is often referred to as a resting-state network (Greicius, Krasnow et al., 2003; Raichle, MacLeod et al., 2001). The large-scale functional brain network that contrasts the DMN has been described by Kenneth Hugdahl, Marcus E. Raichle et al. (2015a). They proposed the existence of a generalized task-related cortical network that is up-regulated when the performed task needs the allocation of generalized non-specific

cognitive resources, independent of the specifics of that task. Hugdahl and Raichle called this network the extrinsic mode network (EMN).

A deeper understanding of large-scale functional and structural brain networks is required to characterize the basics of normal cognitive processes and would give novel insights into psychiatric and neurological disorders. For instance, clinical studies in Alzheimer's disease and schizophrenia have identified abnormalities of network configuration (Bassett & Bullmore, 2009). Moreover, Hugdahl et al. (2015a) suggested that failure of up-and down-regulation dynamics of the large-scale functional networks, such as DMN and EMN, may provide neural underpinnings for cognitive impairments seen in many mental disorders, such as, for example, in schizophrenia.

The spatial organization of brain white matter is composed of densely packed axons organized into fiber tracts, also named bundles of fascicles. These tracts form a complex but well-organized architecture within and across the hemispheres (Mandonnet, Sarubbo et al., 2018). Diffusion-weighted magnetic resonance imaging (DWI) and tractography techniques allow visualization of the three-dimensional "skeletons" of the white matter. The white matter tracts are broadly classified into three main groups according to their connectivity, and these are projection, association, and commissural fibers (Wycoco, Shroff et al., 2013). Projection fibers connect the cortical areas with the deep gray nuclei, brainstem, cerebellum, and spinal cord. Association fibers connect different cortical regions within the same hemisphere. These major long tracts include superior and inferior occipitofrontal fasciculus, cingulum, uncinate fasciculus; superior longitudinal fasciculus and inferior longitudinal fasciculus. Commissural fibers of the corpus callosum and the anterior commissure connect similar cortical areas between the hemispheres, including the corpus callosum and the anterior commissure (Wycoco et al., 2013).

Disruptions of functional connectivity between distant brain regions can impair information processing associated with various neuronal processes. However, there is an existing body of evidence implying that defects in myelin insulation can lead to

impaired cognitive function in, for example, multiple sclerosis patients or cognitive decline in aging (Fields, 2008). Moreover, many psychiatric disorders such as schizophrenia, bipolar disorder, and post-traumatic stress syndrome have been associated with white matter abnormalities (Fields, 2008). These findings suggest that impaired cognitive ability, disorganized thinking, mood disorders, hallucinations, and accompanying psychiatric illness may result from slowed or desynchronized impulse conduction between distant cortical regions (Fields, 2008). Therefore, studying structural and functional connectivity in mental disorders is necessary to understand them fully.

The current thesis aims at examining structural connectivity of the schizophrenia brain using diffusion tensor MRI (DTI). Furthermore, using fMRI, the thesis aims to explore the dynamics of large-scale functional brain networks, namely DMN and EMN, as two complementary networks, and establish a framework for advancing the understanding the complex mental disorders.

Exploring structural connectivity in schizophrenia may provide a better understanding of possible anatomical underpinnings of the disorder and it may facilitate investigations of how structural aberrations relate to the brain functional changes. Furthermore, studies of functional large-scale brain networks may provide a better understanding of brain function in a healthy population. They hold the potential for improving design and analysis of future clinical trials. This could lead to a better understanding of the mechanisms behind symptoms of mental diseases.

1.1.1 Structural networks

The function of white matter pathways is not yet fully understood although it is studied in many different contexts. As mention above, it has been shown that the strength of functional connections is often reflected in the strength of structural connections (Honey, Sporns et al., 2009). In the context of connectivity of large-scale brain networks, the results of a recent study by Alves, Foulon et al. (2019) on structural connectivity of the DMN identified several white matter pathways to be connected to

key nodes of DMN such as the anterior and posterior portions of the cingulum, as well as the inferior longitudinal fasciculus, the second branch of the superior longitudinal fasciculus (SLF), the posterior segment of the arcuate fasciculus, the uncinate fasciculus and fibers of the frontal orbito-polar tract. Therefore, one may hypothesize that aberrations in white matter connectivity of the tracts identified by Alves et al. (2019) may affect activity of the DMN. Interestingly, several white matter connections mentioned by Alves et al. (2019) have been of interest in studies of mental disorders. These are in particular the SLF and the arcuate fasciculus, which were shown to be related to auditory verbal hallucinations in schizophrenia (Chawla, Deep et al., 2019; Ćurčić-Blake, Nanetti et al., 2015; Geoffroy, Houenou et al., 2014). Different anatomical models of SLF have been suggested, although most models emphasize the significance of tracts linking the frontal region to the temporal and parietal regions, regions that are eventually implicated in semantic processing (Catani, Jones et al., 2005; Glasser & Rilling, 2008). Madhavan, McQueeney et al. (2014) showed that SLF is developed from four subparts. Each subpart connects frontal and opercular regions with other brain regions, such as the superior parietal lobe, the angular gyrus, the supramarginal gyrus, and the superior temporal gyrus (Madhavan et al., 2014). The SLF was initially considered synonymous with the arcuate fasciculus, however today, the part of the SLF connecting frontal regions with the superior temporal gyrus is viewed as the arcuate fasciculus (Madhavan et al., 2014). The arcuate fasciculus includes a long segment directly connecting Broca's and Wernicke's areas and two short segments that indirectly connect anterior and posterior language areas via the inferior parietal lobule. Altogether, they form the dorsal language stream implicated in phonemic aspects of language (Johns, 2014).

1.1.2 The Default Mode Network

The Default Mode Network (DMN) is a well-known large-scale brain network that has been known and explored by the neuroscience community for more than two decades. The active brain regions were initially defined using task-based contrasts and included those that were deactivated during performance of a task when compared to a resting baseline condition. This was first described by Shulman, Fiez et al. (1997.) and

subsequently by Gusnard and Raichle (2001) and Raichle et al. (2001), who all observed that certain brain regions exhibited increased metabolic activity during rest and decreased activity when engaged in goal-directed (i.e. cognitively demanding) behavior.

It has been observed that the DMN is activated during in situations when thought can be understood to be directed toward inwards. Further, the DMN is more activated in subjects that tend to "daydream" more often (Buckner, Andrews-Hanna et al., 2008). This may lead to the hypothesis that the DMN is a core brain network associated with spontaneous cognition and that individuals have a strong tendency to engage or activate the DMN when they are not otherwise occupied by external tasks (Buckner et al., 2008). This notion seems to be supported by findings showing that up to 90% of the energy consumed by the brain is used to support the DMN (Raichle & Snyder, 2007). Moreover, the DMN continues to be activated during sleep and even during light anesthesia (Raichle, 2009).

Current evidence shows that the DMN is also involved in different forms of self-relevant mentalization processes. An increase in DMN activity has been related to theory of mind, such as thinking about one's desires, beliefs, and analyzing the intentions of others (Buckner et al., 2008). DMN activity increases have also been related to autobiographical thoughts such as thinking about the past and planning the future activities (Buckner et al., 2008). These findings may suggest that the DMN may contribute to adaptive behavior by allowing scenarios to be constructed and explored in the mind, with the aim to review past events and to create expectations about the future (Buckner et al., 2008).

Anatomically, the DMN has primarily been cortically defined as a set of network nodes distributed across the ventral and dorsal medial prefrontal cortices (BA 24, 10m, 10r, 10p, 32a, 32c, 9), posterior cingulate/retrosplenial cortex (BA 29/30, 23/31), inferior parietal lobule (BA 39, 40), lateral temporal cortex (BA 21), and hippocampal formation (Manning & Steffens, 2016), see Figure 1.

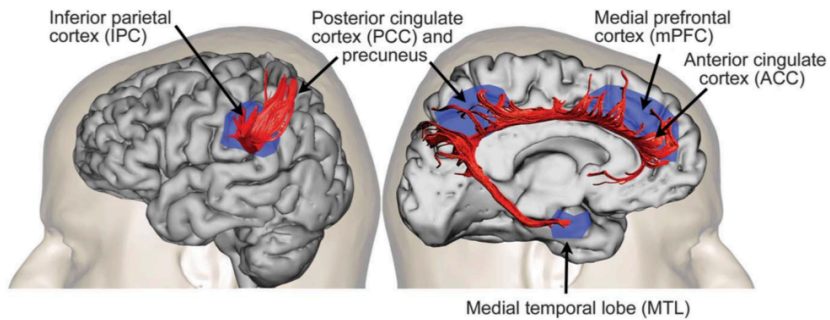


Figure 1- The Default Mode Network.

Lateral and medial view of the default mode network of the left hemisphere (Sandrone & Catani, 2013).

1.1.3 The Extrinsic Mode Network

Around the new Millennium, there were reports showing that different cognitive processes nevertheless engaged the same or similar brain regions. Firstly, Köhler, Moscovitch et al. (1998), see also Duncan and Owen (2000) suggested the existence of domain-specific versus domain-general brain structures involved in semantic memory, and suggested that there may also exist brain structures in order to handle requirements for generalized mental flexibility. Duncan (2013) suggested that the activation regularities across tasks constituted a multiple-demand (MD) system. The MD system is a common brain activity resulting from cognitive challenges in many domains, like perception, response selection, language, many varieties of memory, and problem-solving. In 2015, the theory of the existence of a generalized non-specific task-dependent network called the extrinsic mode network (EMN), which is a network complementary to the default mode network (DMN), was suggested by Hugdahl and Raichle (Hugdahl et al., 2015a).

The backdrop for the suggestion of the EMN was the observation of a common pattern of activation when comparing brain activation (fMRI) maps from different cognitive paradigms and different acquisition schemes in multiple studies in the same laboratory (Bergen fMRI Group laboratory, Bergen, Norway). The EMN was further explored

through a conjunction analysis that included statistical maps from nine studies: working memory (n -back task), response inhibition (Go/No-Go task), impulse control (Stroop color-words task), executive function (dichotic listening task), mental rotation (left-right, L/R, discrimination task), cognitive flexibility (WCST), attribution of beliefs to others (Theory of Mind test), mental arithmetic (addition task) and context updating (oddball auditory task) (Hugdahl et al., 2015a). Although these nine cognitive tasks indicate different cognitive processes and functions, they all demand assignment of intellectual capacity and mental effort (Hugdahl et al., 2015a). Commonality across task-pattern of activation revealed evidence of a general cortical activation network common across cognitive tasks, themes, and domains, cfr Figure 2.

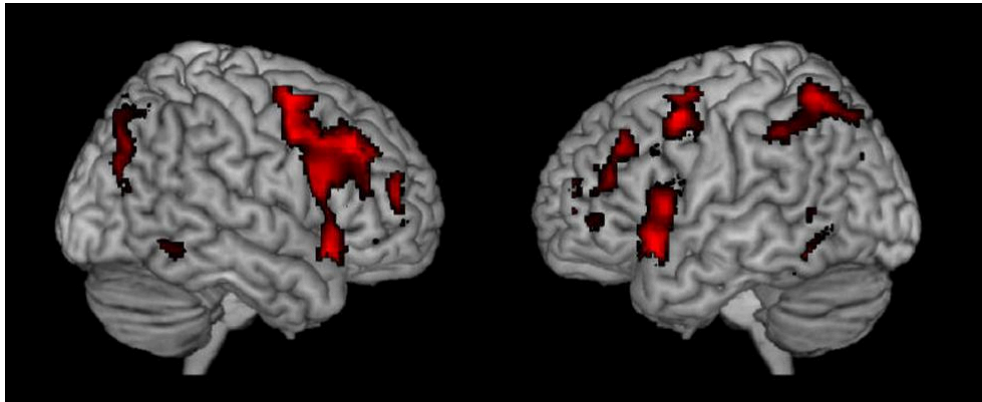


Figure 2- The Extrinsic Mode Network.

Resulting joint activations after conjunction analysis of the nine different studies working memory (n -back task), response inhibition (Go/No-Go task), impulse control (Stroop color-words task), executive function (dichotic listening task), mental rotation (left-right, L/R, discrimination task), cognitive flexibility (WCST), attribution of beliefs to others (Theory of Mind test), mental arithmetic (addition task) and context updating (auditory oddball task) (Hugdahl et al., 2015a).

The EMN nodes are regions not necessarily shared by all tasks. Critical regions in the EMN are the SMA, precentral sulcus, inferior frontal gyrus, insula, and inferior parietal lobule. The dynamics of the EMN would be characterized by a stable and unchanged overall architecture of the whole network. At the same time, peak amplitude and/or area extension of the EMNs regions will depend on the specifics of the tasks performed (Hugdahl et al., 2015a).

The EMN was introduced as an extension of the concept by Duncan (2013) MD system, suggesting a shared activation network across cognitive processes. According to Hugdahl et al. (2015a), EMN acts as a supervisory attention system and is not dependent on task difficulty. However, a certain level of novelty is required for EMN to engage because overlearned tasks, like language, do not activate the EMN, with the possible exception of an unfamiliar, second language (Hugdahl et al., 2015a). Further, the EMN broadly overlaps with the network for intrinsic alertness. Intrinsic alertness represents the internal cognitive control of wakefulness and arousal and is a basic level of attention (Sturm, Simone et al., 1999). This overlapping activation may suggest that EMN is also active at a fundamental level of brain function, which may indicate that it is always activated when a possible response is required or expected (Hugdahl et al., 2015a).

1.2 Functional Network Dynamics and Interactions

Since the discovery of the DMN, it has been assumed that the brain maintains a unique activation architecture during the absence of any external stimuli. In contrast, external stimuli will drive task-specific activations, e.g. the EMN, which are anti-correlated with the DMN (Hugdahl et al., 2015a). The phenomenon of anti-correlation refers to the observation that different brain systems and networks show strong negative correlations with one another, i.e., as activity within the DMN increases, activity in a task-specific, like the external attention system, decreases (Buckner et al., 2008). These observations led to the hypothesis that the brain may shift between two distinct modes of information processing. One mode, dominated by DMN activity, characterized by inward attention, detached from the external environment, and another mode dominated by the EMN activity characterized by external attention, with focused information extraction from the environment (Buckner et al., 2008). It has further been suggested that these systems may work as opposed to one another and thus represent functionally competing brain systems (Buckner et al., 2008).

Similar thoughts were advocated by Hugdahl et al. (2015a) who suggested that the EMN may represent a primary network for extrinsic neuronal activity, meaning, the brain's activity in response to specific stimuli or tasks, in contrast to intrinsic neuronal activity, which is the brain's activity in the absence of specific stimuli or tasks, characteristic of the DMN (Hugdahl et al., 2015a). While the intrinsic characteristics of the DMN is empirically well documented, the extrinsic characteristics of the EMN are less documented, but is suggested to be a network that is up-regulated in the presence of external, novel tasks. Hugdahl et al. (2015a) suggested that the DMN and EMN show a similar inverse relationship, obtained under both task-absent and task-present conditions, and not attributable to global signal fluctuations during resting-state (task absence) conditions. This suggestion was further validated in a study from 2019 in which Hugdahl, Kazimierczak et al. (2019) utilized an auditory task with varying cognitive demands in a standard fMRI block-design to test how the networks interact in transition points between rest and active processing conditions (Hugdahl et al., 2019). This study alternated task-present blocks with an equal number of task-absent blocks to capture network dynamics across time and changing environmental demands. The Hugdahl et al. (2019) study showed an initial rapid onset of activity in the EMN during active blocks, which remained throughout the duration of the block, and faded away during the first seconds of the task-absent block. DMN network activity showed an initial time-lag during task-absent blocks where neither the EMN nor the DMN was active, followed by the DMNs' up-regulation.

The autonomous character of the intrinsic DMN and extrinsic brain networks, such as the EMN, raises the question of how their relationship is regulated. Is there a separate control system that in some way directs which of these two brain systems is active? Or, are the two systems in direct competition with one another in a way that local competitive interactions between the systems define their levels of activity?

Two other networks that have been suggested to modulate the fluctuating activity of the DMN are the Central Executive Network (CEN) and the Salience Network (SN). Together with the DMN, these networks create a so called triple-network model where

the SN is responsible for switching between an active state when CEN is upregulated and a resting-state when DMN is upregulated, and the CEN is downregulated (van Oort, Tendolkar et al., 2017). The SN generally comprises of the dorsal anterior cingulate and anterior insular cortices (Uddin, 2017). Interestingly, it has been shown that one of the roles of the anterior insula is to activate the CEN and deactivate the DMN across visuo-auditory modalities and in a resting state (Sridharan, Levitin et al., 2008). The SN has been shown to be involved in bottom-up detection of salient events and plays an important role in switching between large-scale networks to facilitate the access of resources from attention and working memory (Di & Biswal, 2015). The results of the study by Di and Biswal (2015) show that high activity of the SN is associated with increased functional connectivity between the DMN and frontoparietal executive networks, like the CEN. According to Di and Biswal (2015), the SN not only modulates the separate activities of the two networks, but may also modulate the relationships between them. Furthermore, Di and Biswal (2015) argued that this hypothesis is somewhat plausible because the regions of the SN are generally the cognitive "driving hubs" which send information to other regions of the whole brain (Di & Biswal, 2015). In addition, the SN contains a particular type of neuron termed von Economo neurons. These neurons have large axons to facilitate rapid relay of SN signals to other brain regions, hence they may support particular functions of the SN during modulation of large-scale brain networks (Di & Biswal, 2015). Interestingly, both the CEN and SN, being task specific networks, have been recognized to partially share anatomical structure with the EMN (Hugdahl et al., 2019). However, the exact role of each of those networks within the dynamic interplay between EMN and DMN has not yet been fully explored.

1.3 Brain Networks and Implications for Mental Disorders

Brain functioning relies on highly intricate interactions between distributed brain areas, and it has been suggested that altered interactions of regions within networks are at the core of the pathophysiology of mental disorders (Braun, Schaefer et al., 2018). Recently it was shown that symptoms of diseases such as schizophrenia, depression,

autism, and other mental disorders are accompanied by brain connectivity alterations (Lubrini, Martín-Montes et al., 2018).

In 1911, schizophrenia was described by Bleuler as a neural conduction disorder which, from a modern-day perspective, may be interpreted as a disruption of functional connectivity (Collin, Turk et al., 2016). Many studies support the notion that disruptions of network connectivity may be underlying the pathophysiology of schizophrenia (Calhoun, Eichele et al., 2009; Fitzsimmons, Kubicki et al., 2013; Narr & Leaver, 2015). One of the most often studied functional networks in schizophrenia is the DMN and its connections with other brain networks, like the salience (SN) and central executive (CEN) networks (Narr & Leaver, 2015). However, existing studies report mixed findings of DMN hypo- and hyper-connectivity and different degree of intra-network connectivity (Narr & Leaver, 2015). In a review, Fornito, Zalesky et al. (2012) found that widespread reduced functional connectivity in schizophrenia patients is a robust finding, supported in a more recent meta-analysis by Brandl, Avram et al. (2019), which showed network dysconnectivity and gray matter volume reductions in the insula, lateral postcentral cortex, striatum, and the thalamus. Manoliu, Riedl et al. (2014) found evidence linking impaired insula, DMN, and central executive (CEN) network activity to psychosis. Further, Hugdahl et al. (2015a) suggested that: "*the cognitive impairment and hypo-activation seen in, e.g., schizophrenia patients when exposed to challenging cognitive tasks could be caused by failure of interactive regulation of the DMN and EMN networks, rather than a deficit with regard to a specific brain region.*" Hugdahl et al. (2015a) further suggested that the incidence of auditory verbal hallucinations (AVH), a symptom in schizophrenia, may be caused by abnormal functioning of cognitive control mechanisms. This can result from failure of down-regulation of the DMN resting-state network, or failure of a corresponding up-regulation of the EMN task-positive network (Hugdahl et al., 2015a).

For structural networks in schizophrenia patients, disruption of structural connectivity has been reported within almost all primary association and projection pathways, despite of the use of different data acquisition and processing methods, and statistical

analyses (Narr & Leaver, 2015). Although, as in the case of functional networks, the direction of the observed changes in distinct white matter tracts is often mixed in the results. It may seem as if aberrations of the white matter pathways in schizophrenia is rather widespread and not localized, i.e. not directly related to any particular white matter connection (Narr & Leaver, 2015). Focus in DTI studies of schizophrenia has therefore shifted towards comparing structural connections within and across anatomic or functional networks rather than focusing solely on white matter microstructural properties in particular pathways (Narr & Leaver, 2015).

The recent mega-analysis by KellyJahanshad et al. (2017) across 29 independent studies and 1963 patients showed that schizophrenia is characterized by widespread reduction of fractional anisotropy (FA) values, indicative of abnormal white matter integrity. Of the 25 studied regions, 20 showed significantly lower FA in patients than controls. The findings by Kelly et al. (2017) may give further support for a "global hypothesis" about white matter aberrations in schizophrenia.

1.4 Magnetic Resonance Imaging and Brain Networks

In 1970 several imaging modalities were introduced that allowed *in vivo* quantitative measurement of human brain function and structure. The most diverse and frequently used modality to study the brain *in vivo* is MRI, due to excellent soft tissue contrast, multiple imaging contrasts available in one session and the possibility of repeated measures since MRI is not based on ionizing radiation. MRI is based on the physical principles of magnetic resonance, which allows signal detection of the inherent magnetic properties of nuclei with odd numbers of protons and neutrons. Due to its high abundance in the brain, providing a strong signal, hydrogen (^1H), is the basis of most MRI investigations. A strong magnetic field, typically 1.5T or 3T in clinical MRI systems, is required to align the hydrogen nuclei parallel or opposing the applied magnetic field (B_0). The resulting net magnetization is manipulated by applying electromagnetic pulses (radiofrequency pulses) while dedicated magnetic field gradient coils are used to spatially encode the signal and record relaxation processes of the

nuclei spins. Tissues are characterized by different water concentrations, chemical environment and structure, and hence will relax at different time rates (T_1 , T_2). Different acquisition schemes, or pulse sequences, are available to generate the final anatomical images, or more advanced image contrast such as diffusion weighted imaging, or the blood-oxygenation level dependent (BOLD) contrast captured in fMRI studies. Common to these two latter approaches is that in addition to a more advanced data acquisition scheme, data modelling and analysis is mandatory to extract relevant information. Diffusion weighted imaging (or more specifically diffusion tensor imaging, DTI) and fMRI are often used together to investigate white matter brain connectivity (structural connectivity) and brain function under different cognitive and mental states (functional connectivity), respectively. These approaches are described in more details in the following sections.

1.4.1 Diffusion Weighted Imaging

Diffusion-weighted imaging (DWI) is an MRI method sensitive to diffusion of water molecules, also called Brownian motions, inside the selected voxels. The mobility of molecules is described by a coefficient, D , which is related to the root mean square displacement of the molecules over a given time. The Stokes-Einstein Equation describing the coefficient D shows that it is directly proportional to the absolute temperature in Kelvin, T , and the Boltzmann constant k (JK⁻¹). However, D is inversely proportional to the radius of the molecules' viscosity η . See Equation 1.1.

$$D = \frac{kT}{6\pi\eta R} \quad 1.1$$

Depending on the direction of the motion of a molecule, anisotropic and isotropic diffusion can be distinguished. When no obstructions (e.g. in the form of fat tissue) are present, the molecules can move freely in all directions. This is called isotropic diffusion. However, in an environment where obstructions are present, limiting the

motion of molecules, so-called anisotropic diffusion is observed. Examples of isotropic and anisotropic diffusion are shown in Figure 3.

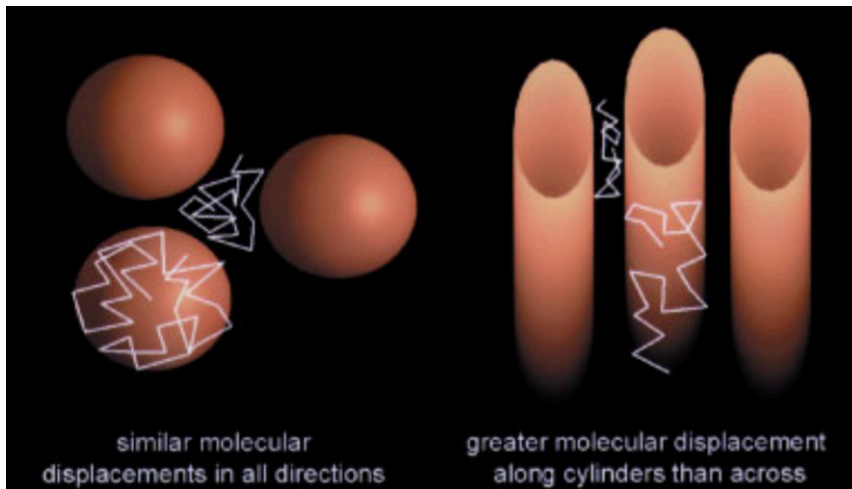


Figure 3- Diffusion in different tissue structures.

Examples of paths of molecules in the situation of isotropic (left) and anisotropic (right) diffusion (Beaulieu, 2002). In isotropic diffusion, the probability of displacement is equal in all direction, while a preferred displacement is evident in anisotropic diffusion.

The degree of a hindrance to water diffusion will be determined by the size, shape, and composition of any physical obstruction, as well as the spacing between these obstructions. DTI is the magnetic resonance method utilizing magnetic field gradients, allowing the MR to be sensitized to the water molecules' thermally driven motion in the direction of the magnetic field gradient. Information about diffusivity in a given direction is contained within the diffusion tensor (Basser & Jones, 2002). A *tensor* is a mathematical entity that summarizes and represents diffusion in 3D space (Equation 1.2). The diffusion tensor is a matrix of 3x3 size, diagonally symmetric, where D is a tensor derived from directional diffusivities, λ_1 , λ_2 , λ_3 are the eigenvalues, and E is a matrix of the three eigenvectors. Minimum six encoded measurements are required to fill the matrix. The more measurements, the better is accuracy. Several indices can be computed to relate to diffusional properties by performing simple mathematical operations on the tensor.

$$D = \begin{pmatrix} D_{xx} & D_{xy} & D_{xz} \\ D_{yx} & D_{yy} & D_{yz} \\ D_{zx} & D_{zy} & D_{zz} \end{pmatrix} = E^T \begin{pmatrix} \lambda_1 & 0 & 0 \\ 0 & \lambda_2 & 0 \\ 0 & 0 & \lambda_3 \end{pmatrix} \quad 1.2$$

The three eigenvectors in the matrix represent the major, medium, and minor principal axis of an ellipsoid, which can graphicly represent the tensor. See figure 4.

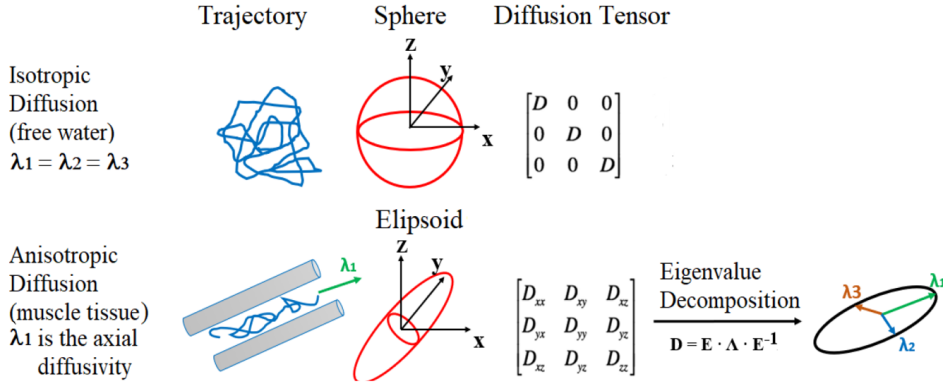


Figure 4- Diffusion tensors of isotropic and anisotropic diffusion.

The figure shows trajectories of the water molecules when in restricted and unrestricted environments (e.g., white matter) along with associated diffusion tensors (Pop & Stefu, 2020).

The Fractional Anisotropy (FA) is a rotational invariant metric that describes the amount of diffusion asymmetry within the voxel, defined in terms of its eigenvalues. FA is derived from the standard deviation of the three eigenvalues and ranges from zero (isotropy) to maximal anisotropy. See equation 1.3.

$$FA = \sqrt{\frac{3}{2}} \cdot \sqrt{\frac{(\lambda_1 - \bar{\lambda})^2 + (\lambda_2 - \bar{\lambda})^2 + (\lambda_3 - \bar{\lambda})^2}{\lambda_1^2 + \lambda_2^2 + \lambda_3^2}} \quad 1.3$$

Although FA-values carry information about white matter state at the cellular level, this information is averaged over large voxel volumes (O'Donnell & Pasternak, 2015). The MRI resolution is in mm which is a different scale than the scale of the cells probed by diffusing water which is in μm . Thus, while observing reduced FA values in specific brain areas, it cannot be presumed that this results only from abnormalities at the

cellular level. It should be kept in mind that while FA alterations can be seen as a general measure of white matter integrity, observed changes can be of multifactorial origin (e.g., cell death, edema, gliosis, inflammation, change in myelination, increase in connectivity of crossing fibers, etc.). The existence of multiple fiber populations with different fiber directions may also contribute to the average value of the signal, and the signal can be a mixture of changes in tissue myelination, fiber organization, and the number of axons (Mori & Zhang, 2006).

1.4.2 Functional MRI

The discovery of the blood oxygenation level dependent (BOLD) contrast was essential for the development of functional MRI (fMRI). Since its discovery over thirty years ago by Ogawa, Tank et al. (1992), the field of fMRI has grown in usage, sophistication, range of applications, and impact (Bandettini, 2012). fMRI allowed progress in neuroscientific research by providing scientists a non-invasive method for performing quantitative *in vivo* experiments on the normally functioning human brain. Today, fMRI has overtaken other modalities (e.g., Electroencephalography (EEG) or Positron Emission Tomography (PET)) as the predominant method for measuring cognitively induced changes in brain activity (Van Horn & Poldrack, 2009). The considerable advantage of fMRI over other methods such as PET is its ability to safely and noninvasively image neuronal activity with reasonably good spatial resolution (millimetres). This comes however to the prize of a relatively low temporal resolution (seconds). The fMRI method is based on the fact that activated neurons increase their demand for oxygenated blood to a specific brain region involved in a cognitive, sensory or motor task. The excess of oxygenated blood compared to de-oxygenated blood gives rise to the BOLD signal because of difference in magnetic susceptibility of oxygenated and de-oxygenated blood. The vascular response to an immediate neuronal activation can be described as a hemodynamic response function (HRF), see Figure 5. The HRF is a slow process (seconds) compared to the neuronal activity (milliseconds). The increase of blood flow following the neuronal activity takes about 5 seconds to reach its maximum. This activation peak is followed by a long (15-20 seconds) undershoot until it returns to the baseline.

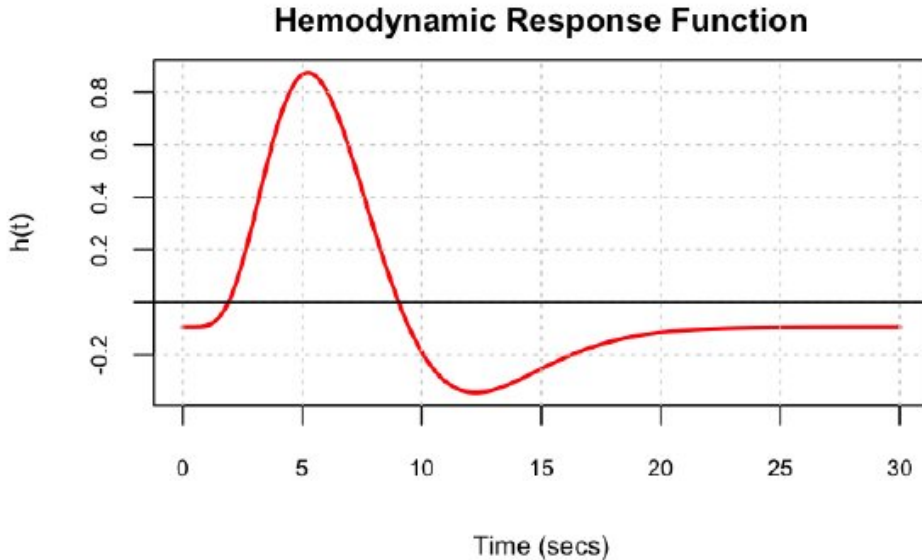


Figure 5- The HRF function.

The figure shows the BOLD response to a brief stimulus with initial deep shortly after stimulation, peak around 5 s after stimulation and post stimulus undershoot that start 10s after the stimulation (Stocco, 2014)

Depending on the experimental design and further the data model used in the post-processing of the fMRI images, different kinds of information about brain activity can be extracted. For cognitive tasks, typically an experimental block-design is used. In block-design experiments, fMRI signals across many subsequent trials (blocks) are recorded and modelled. To measure specific task-related activity, participants are scanned while performing a task and while performing a control condition, i.e. typically a resting or baseline condition (Gusnard & Raichle, 2001). The length of blocks vary largely from as short as 10 seconds to 30 seconds or longer (Stark & Squire, 2001). When activity in a particular region of the brain is of the same intensity during task processing and rest, it is assumed that this particular region is not involved in the task (Stark & Squire, 2001). However, periods of rest have frequently been associated with significant cognitive action, suggesting the crucial role of baseline tasks in the design and interpretation of fMRI studies (Stark & Squire, 2001).

In the last two decades, the interest in the brain activity during resting has become a focus. Resting-state fMRI measures of spontaneous low-frequency BOLD fluctuations (<0.1 Hz) has been in focus to investigate the functional architecture of the brain (Lee, Smyser et al., 2013). Resting-state fMRI has allowed for the identification of various resting-state networks (RSNs), which are spatially distinct areas of the brain that demonstrate synchronous BOLD fluctuations at rest. There have been various methods developed for analyzing resting-state data such as seed-based approaches, independent component analysis (ICA), graph methods, clustering algorithms, neural networks, and pattern classifiers (Lee et al., 2013). During resting state, fMRI experiment subjects lie inside the scanner and are asked to relax and often instructed to keep their eyes open. Most studies on resting-state functional connectivity are typically between 10-20 minutes, although shorter durations have also been used. In general, it has been shown that reliability of resting-state fMRI data is significantly improved by having longer scan durations (Birn, Molloy et al., 2013).

2. Background and Aims of the Thesis

The aim of this thesis was firstly to explore structural connectivity in a group of patients suffering from schizophrenia to explore the feasibility of such an approach for future studies relating functional and structural networks in mental disorders. The properties and dynamics of large-scale functional brain networks, in particular the DMN and EMN, as two complementary networks, was a second focus of the thesis. Studying both structural and functional connectivity in the context of mental health is valuable not only for better understanding of possible anatomical underpinnings of such disorders but also to better comprehend how structural aberrations relate to functional aberrations. In this context, three *in vivo* neuroimaging studies were designed and conducted with the following research questions were perused:

Study I: How does white matter connectivity differ between schizophrenia patients and controls, and between hallucinating and non-hallucinating subtypes of schizophrenia patients?

Many DTI studies have demonstrated a correlation between white matter integrity and schizophrenia (De Weijer, Mandl et al., 2011; Ellison-Wright & Bullmore, 2009; KellyJahanshad et al., 2018; Kubicki, McCarley et al., 2007; Leroux, Delcroix et al., 2017; Oestreich, McCarthy-Jones et al., 2016). Nonetheless, the association between AVH, a fundamental symptom in schizophrenia, and white matter integrity are not yet fully understood, and results are often contradictory. Several facts can explain the lack of convergence in the current literature. One source of variability between studies is the unstable nature of AVH (“state” vs. “trait”) (Hugdahl & Sommer, 2017; Kühn & Gallinat, 2012). Therefore, multiple assessments over an extended observation period would be required to classify patients correctly. Study I included evaluation of AVHs throughout a 12 months period, using the P3 item of the Positive and Negative Syndrome Scale (PANSS) (Kay, Fiszbein et al., 1987), which is a clinical interview questionnaire. The P3 item indicates hallucinatory behavior, and the score on the P3 item was used to classify patients as either hallucinators (AVH+) or non-hallucinators (AVH-). A second issue in Study I was hemispheric asymmetry and lateralization of white matter tracts. Majority of studies on white matter integrity have not compared

FA values between the left and right hemisphere (e.g., Ćurčić-Blake, Nanetti (Ćurčić-Blake et al., 2015)), or have just reported data from one hemisphere (e.g., Leroux, Delcroix (Leroux et al., 2017) , McCarthy-Jones, Oestreich (McCarthy-Jones, Oestreich et al., 2015)), or have limited the analysis to individual fiber tracts (e.g., De Weijer, Mandl (De Weijer et al., 2011) , Falkenberg, Westerhausen (Falkenberg, Westerhausen et al., 2019)). Paper I investigated possible hemispheric asymmetry between groups, and sub-groups.

Study II: How do the DMN and EMN networks interact across time when environmental demands switch from active to passive on a short-term basis?

Many studies of the relationship between task-negative (e.g. DMN) and task-positive (e.g. EMN, SN, CEN) cortical networks have utilized prolonged resting periods or a single task. A single-task paradigm is usually used to address a single cognitive domain (Corbetta, Patel et al., 2008; Lustig, Snyder et al., 2003; Shulman, Fiez et al.), e. g. working memory or attention. However, this would not capture the dynamics of resting-state or network interactions, where tasks change from one processing period to another across the experimental session. Therefore, in this study, three different tasks were chosen to represent three different cognitive domains. To activate visuospatial processing, a mental rotation task (Shepard & Metzler, 1971) was chosen because this task is shown to provide significant frontoparietal activations (Hugdahl, Thomsen et al., 2006; Jordan, Heinze et al., 2001; Tagaris, Kim et al., 1997). A working memory task was chosen since it also includes attention and executive control in addition to short-term memory (D'esposito, Detre et al., 1995; Hammar, Neto et al., 2016). A mental arithmetic task with adding numbers was chosen because it draws on a basic cognitive ability for number processing and mental abstractions

Study III: Is the architecture of resting-state network observed during a single prolonged resting period the same as the architecture of resting-state networks observed during repeated brief resting-periods in between task-processing periods?

Previous studies investigating this topic have generally estimated how well resting-state activity observed in task-processing experiments resembles resting-state activity observed in classic resting-state experiments (Damien A. Fair, Schlaggar et al., 2007; Ganger, Hahn et al., 2015). In contrast, Study III explored similarities and differences in resting-state network activity in two resting-state conditions: an intermittent and a continuous condition. In Study III, a standard fMRI block-design was utilized to explore how resting-state activity observed during absence of cognitive tasks differed from resting-state activity in the absence of a task. Study III focused on differences in DMN architecture between the two conditions since the DMN is one of the most well-known and researched resting-state networks. The central hypothesis of this study was that although DMN activity should be similar between the two conditions, different mental states induced in the two conditions may influence DMN activity and intra-network connectivity in different ways.

3. Methods

In this chapter, methodological aspects are described. Enrollment of participants are presented, alongside with an overview of data acquisition procedures, image processing pipelines, and evaluation of statistical significance.

3.1 Participants

The studies were conducted in accordance with the Declaration of Helsinki with respect to ethical standards and was approved by the Regional Committee for Medical Research Ethics in Western Norway (2014/1641/REK Vest and REK-VEST, #2010/3387-6). Written informed consent was obtained from all participants.

Adult, schizophrenia patients (N = 57, Study I) were recruited through an at the time ongoing overarching research project, the Bergen Psychosis Project 2 (Principal investigator Professor Erik Johnsen, Haukeland University Hospital, Bergen, Norway). All patients had symptoms of schizophrenia spectrum disorder, psychosis or paranoid psychosis according to the International Classification of Diseases ICD-10 diagnostic manual, and were under treatment using second-generation antipsychotic medication. In order to investigate potential changes in patient's experience of AVHs, longitudinal psychiatric evaluations were performed at regular intervals over a period of 12 months, typically eight evaluations per patient (median of six assessments per patient). The assessments were conducted by a limited number of certified clinicians to reduce interrater variability.

In Study I, the patients were assigned to two groups dependent on their experiences of hallucinations as assessed from the PANSS P3 score from all evaluations. Of the 57 patients, 44 were defined as having hallucinations (AVH+) as they scored 3 (mild symptom load) or higher on at least one psychiatric evaluation within the 12-months period. The remaining 13 patients were defined as non-hallucinating (AVH-). The strict criterion on hallucinations resulted in a small sample size for this group. Although

PANSS P3 assesses hallucinations in a spectrum of modalities (e.g., visual, tactile, olfactory), there is a focus on auditory verbal hallucinations in the questions given by the clinician, such that using PANSS P3 as a marker of AVH severity and since auditory hallucinations dominates over other modalities (McCarthy-Jones, Smailes et al., 2017; Nayani & David, 1996; Shinn, Pfaff et al., 2012). A PANSS P3 score of 3 is a cut-off criterion commonly used in other studies (e.g., Weber, Johnsen et al. (2020)), see also (Kay et al., 1987)

Age-, handedness- and gender-matched controls were recruited from the local municipality (N=57). Using an in-house developed questionnaire, these participants had to self-report on history of mental disorders and medicinal status. Also, for the investigations in Study II and III (same participants in both studies, N=47), healthy participants were recruited in the municipality through open announcements. Based on self-report, none of the participants had any history of psychiatric disorder or neurological disease. The participants demonstrated sufficient visual perceptive and color vision as assessed by their general performance on the provided tasks during a pre-scanning training session where examples of the fMRI tasks were demonstrated. Both the tasks during the pre-MRI training session and the actual tasks during scanning were presented using the E-Prime stimulus program.

3.2 MRI Data Acquisition

Two different 3T clinical MRI systems were used to acquire the imaging data used in the thesis. The selection of scanner was decided based on availability as well as access to various advanced scanning protocols that had been in use in various studies by the same group (Hjelmervik, Craven et al., 2020; Weber, Hjelmervik et al., 2021; Weber et al., 2020).

The data in Study I, were acquired using a whole-body 3T GE Medical Systems Signa HDx MRI system which was later upgraded to a Discovery MR750 system, while data collection for Study I was still ongoing. To assure that the scanner upgrade was not

affecting the reported results, a covariate was included in all statistical comparisons. Furthermore, patients as well as their age- and gender-matched control participants were always scanned on the same system. The diffusion weighted data reported in Study I were acquired using b-values of 0 s/mm² (average of six unweighted images) and 1000 s/mm² (spin echo echo planar imaging, 30 diffusion directions, TE/ TR = 84.4/ 14000 ms, voxel size of 1.7 x 1.7 x 2.4 mm, total acquisition time 8.4 min).

In Study II and III, a whole-body 3T Magnetom Prisma MR scanner (Siemens Healthcare, Germany) was used. The task-based fMRI data were acquired using a 2D gradient echo echo planar imaging sequence (TE/ TR = 30/ 2000 ms, 306 volumes with 35 acquired slices per volume, voxel size of approx. 3.6 mm³). A resting-state fMRI acquisition was recorded immediately after using the same imaging protocol but including 150 repeated volumes. T1 weighted, anatomical data were also acquired in each participant (MPRAGE, sagittal, TE/TR/TI = 2.28 ms/1.8 s/900 ms, flip angle of 8 degrees, voxel size of 1mm³, acquisition time of 7.40 min)

3.3 Functional Neuroimaging – Cognitive tasks

Study I and III did not involve analysis of cognitive tasks and are therefore not further discussed in this section. In Study II, however, three cognitive tasks were integrated and presented via an MR compatible goggles during image acquisition (fMRI). The acquisition was done as a traditional block design with presentations of ON-blocks (30 seconds) with one of the following three tasks: mental arithmetic, mental rotation and working memory. Responses to the tasks were recorded using an MR compatible response button system (NordicNeuroLab, Inc, <https://www.nordicneurolab.com/>). Response accuracy and response latency (RT in ms) were evaluated statistically for means, standard deviations, and hits ratio of correct responses to false alarms for all three tasks. Cohen's d-statistic for effect sizes in each task were calculated using hits ratios.

Summary of tasks, for details cfr. Study II:

- Mental arithmetic task: two digits from 1–9 presented on top of each other, in the purple font on a black background. The task was to mentally add the two numbers and press a hand-held button when the sum of the two digits was "11".
- Mental rotation task: based on the classic Shepard, and Metzler mental rotation task (Shepard & Metzler, 1971) with images of two 3D non-configurative objects in a white against black background displayed on each trial. The task was to decide whether the two shapes were two different objects or two shapes of the same object but rotated differently. A hand-held button was used to record responses.
- Working memory task: n-back task with presentations of incongruent Stroop color-words, like the word "red" written in blue ink. The task was to remember the color of the word presented two items back and press a hand-held button when the item currently seen matched the one presented two items back.

Each ON-block was alternated with OFF blocks (30 seconds, eyes open, fixation cross, cfr. details in Study II). Nine ON-blocks, i.e. three repetitions of each task, and nine OFF-blocks were thus presented. The subsequent resting-state fMRI acquisition was acquired as a long OFF-block using again an eyes-open instruction to the participant (fixation cross).

3.4 Image Processing Pipelines

All the data were de-identified prior to processing, and all processing was performed on secure storage solutions. Image processing pipelines were developed for the acquired imaging data, including both available software packages (i.e. SPM, CONN, FSL) in addition to in house scripting (Matlab, shell-scripting). For details on processing steps, cfr individual studies and description therein.

Pipeline for Diffusion weighted image processing

The processing of DTI-data (Study I) was performed using the FMRIB Software Library (FSL) software package (version 5.0; FMRIB Software Library and the corresponding Diffusion Toolbox). Data were inspected visually at all pre-processing

steps to identify artifacts and guarantee good image data quality. First, a binary brain-mask was created for each participant. Afterwards, the original data were corrected for head movements and eddy currents with outlier replacement and slice-to-volume outlier correction. FA-maps were subsequently calculated by fitting a diffusion tensor in each imaged voxel. After calculating the FA-images, voxel-wise statistical analysis of the FA-data was performed using the TBSS component of FSL (Smith, Jenkinson et al., 2006; Smith, Jenkinson et al., 2004). This involved aligning all FA-images onto a common space, i.e. the standard Montreal Neurological Institute (MNI) space atlas, and resampling to 1 mm³ spatial resolution. A resulting mean FA-image volume was created and further thinned, resulting in a mean FA-skeleton. The skeletonized mean FA-image volume was thresholded at 0.3 to suppress low mean FA-values and areas with low and/or high participant-variability. Next, the aligned FA data for all participants were projected onto the mean FA-skeleton by filling the skeleton with FA-values from the nearest relevant tract center. This resulted in a four-dimensional (4D) image file containing the projected, skeletonized FA data, then entered into statistical analyses. Symmetric mean FA-skeleton image volumes were created to perform hemispheric asymmetry analysis between patients and controls. In the analysis, the image volumes were flipped and subtracted from each other to create “left minus right” data.

Pipeline for task-related functional neuroimaging

The task-related fMRI data were preprocessed using conventional procedures, including rigid-realignment, normalization to MNI space, and smoothing (8mm³ Gaussian kernel). All steps were performed using SPM 12.

In the next step, first-level analysis of all subjects was conducted. The calculated motion parameters from the re-alignment procedure were utilized as a regressor. Framewise displacement was computed from the re-alignment parameters (Power, Barnes et al., 2012; Power, Mitra et al., 2014) to examine further and ensure the motion does not impact the results. The resulting t- contrast images were grouped by condition and further used in a statistical comparison.

Pipeline for resting-state functional neuroimaging

Before preprocessing of the task fMRI data, the seven most central image volumes of each of the nine OFF-blocks in the task-related fMRI series were extracted to construct a resting-state acquisition based on OFF-blocks. This 4D data set (referred to as “intermittent resting condition data”) was compared to the conventionally acquired resting-state data acquired immediately after the task-related fMRI acquisition (referred to as “continuous resting condition data”).

Each OFF-Block consisted of 17 image volumes. The first five volumes of the OFF-blocks were omitted to avoid including a transient state of the BOLD signal from ON-blocks to OFF-blocks. The last five volumes of the OFF blocks were omitted to avoid including volumes when participants could have anticipated the appearance of the next cognitive task due to fixed block-lengths. Pyka, Beckmann et al. (2009) suggested that after a cognitively demanding task, nonlinear increase in DMN may reflect increased self-referential processes. This process may be triggered by a minor increase in ability to predict task complexity and may not reflect the previous task-related magnitude of reallocation of cerebral resources. Omitting the last five volumes of the OFF blocks was to prevent this.

The following steps were taken to extract the data from the OFF blocks: The task-related fMRI data were first disentangled into individual volumes. The volumes of interest were then saved as separate 3D nifty images. Finally, the extracted "resting" 3D volumes were merged into the 4D images consisting of 63 volumes (total time two minutes and one second). The whole procedure was performed in Matlab R2017b (the MathWorks, Natick, MA), including the usage of various SPM12 functions.

All preprocessing was done using the CONN functional connectivity toolbox 17b (<https://web.conn-toolbox.org>). Preprocessing included functional realignment and unwrapping, functional centering to (0,0,0) coordinates, functional outlier detection (ART-based identification of statistical outliers scans for scrubbing), functional direct

segmentation and normalization, structural centering to (0,0,0) coordinates, structural segmentation and normalization, and functional smoothing.

Further, Spatial Independent Component Analysis (ICA) was conducted individually on the resting-state data from the intermittent and continuous resting-state conditions. The ICA calculation was performed using Group ICA for fMRI toolbox (GIFT v3.0b). Twenty independent components were extracted using the algorithm type ‘Infomax’ [90] with default settings. Extracted independent components were spatially sorted according to correlation coefficients with the template DMN component map from the ten components derived in the study by ((Bell & Sejnowski, 1995) (<https://www.fmrib.ox.ac.uk/datasets/brainmap+rsns/>)). The sorting procedure automatically picked the components best reflecting DMN in the two data sets.

3.5 Statistical Evaluations

Statistical evaluations were performed for all comparisons. Due to differences in the underlying data and study designs, statistical analysis had to be adopted accordingly. The details of the comparisons are presented in each study, an overall summary is provided in the following.

Comparison of the FA skeletons

The first statistical analysis of Study I tested whether voxel-wise FA-values between patient subgroups and their matched control groups differed from each other using the original FA-skeleton images. Secondly, significant group differences in the FA-values between the left- and right hemisphere FA skeleton were tested for, using left-minus-right subtracted symmetrical skeleton images.

In the case of both statistical analyses, there were three comparisons performed using two-sided *t*-tests :

1. Comparison between AVH+ and AVH- patients
2. Comparison between AVH+ patients and their matched controls

3. Comparison between AVH- patients and their matched controls

Additionally, the comparison between FA skeletons of two control groups was performed. This comparison aimed to confirm that observed FA dissimilarities between the patient groups were not driven by the differences in sample sizes or the influence of covariates of no interest.

Statistical analyses were conducted using permutation interface for the general linear model (PALM) using 10 000 permutations (Winkler, Ridgway et al., 2014). Permutation testing was used since it does not impose any assumptions on the distribution of the dependent variables and accounts for possible non-normality of FA-values (Nichols & Holmes, 2002). Finally, the individual FA-values were extracted from the significant clusters to illustrate group differences.

Comparison of fMRI activity maps

In Studies II and III, conjunction analysis was used to compare fMRI activity maps. The process was similar in Study II and III; however, different data types were used.

In Study II, the conjunction analysis aimed to show overlap in activity patterns across three tasks used in experiment, both in an active and resting-state condition. Hence, conjunction analysis was done using first-level contrast images (one for each subject and condition). In Study II, the tasks were additionally analyzed individually to assess the effect of each task. These individual maps were processed in MRICron and superimposed on each other.

The conjunction analysis in Study III aimed to show overlap between the DMN maps across the two resting conditions (intermittent and continuous). In the case of study III, the resultant mean participants' components with the highest correlation to the template DMN map were used to select individual components (one for each participant and each condition) to perform conjunction analysis. In the case of both Study II and III a second-order analysis (one-way ANOVA) was used to perform the conjunction

analysis. For details about the conjunction analysis routine and parameters used cfr. Study II and III.

Additionally, Study III tested the spatial overlap of the components with the highest and second-highest correlation to the template DMN map, using a probability map for all participants. The probability map was made using SPM12 for details on the procedure cfr. Study III .

Between-network dynamics

Study II explored not only the activity patterns of the EMN and DMN networks but also their temporal dynamics. To do this, the activity in ROIs functionally defined from the activation patterns seen in the conjunction, analyses were compared. These ROIs were chosen because they have shown significant activations during resting- and task-absent periods (Buckner & DiNicola, 2019; Cunningham, Tomasi et al., 2017; Deng, Wu et al., 2019; Michael D Fox, Abraham Z Snyder et al., 2005) and during active processing and task-presence (D'esposito et al., 1995; Fedorenko, Duncan et al., 2013; Hammar et al., 2016; Hugdahl et al., 2019; Le, Zhang et al., 2018), including tasks used in Study II. For this time-course analysis, the ROIs were created using MarsBaR from the thresholded SPM clusters. Mean voxel values over the ROI were then extracted for each subject from the motion-corrected intensity images in MNI-space. These images represent the actual BOLD signal change at each voxel rather than the modeled, HRF-corrected response. The images were then averaged over the cohort into a single time-course curve. The resultant time-course curve was rescaled as a percentage of total BOLD signal change.

In Study III, functional connectivity differences between the DMN and eight selected networks between two conditions were explored, chosen from the CONN atlas. The ROI-to-ROI functional connectivity analysis was performed with the CONN toolbox (<https://web.conn-toolbox.org>). Functional connectivity z- scores were calculated between the ROIs belonging to DMN and ROIs belonging to selected functional networks (DMN, Sensori/Motor, Visual, Salience, Dorsal Attention, Fronto Parietal,

Language, Cerebellar) for details cfr. Paper III. The resulting connectivity matrices for two conditions were further extracted and compared using the PALM and two-tailed paired t-test with 10 000 permutations.

4. Results

Firstly, the study of patients suffering from schizophrenia revealed that patients with episodes of auditory-verbal hallucinations assessed over a period of twelve months showed widespread, significant differences in recorded fractional anisotropy (FA) values. This opens the obvious question of possible structural-functional abnormalities in these patients. To investigate such a relation, a means to adequately acquire functional performance had to be established, which was the reason for suggesting the task-based fMRI design explored in Study II. Given the novelty of the design, it was necessary to first test the design in a group of healthy volunteers. The fMRI design was not only to investigate how the participants would perform when solving the tasks at hand, but also how the neural networks of solving the different cognitive tasks (EMN) compared to the opposing resting network condition (DMN).

The framework of switching among these networks opens a novel path for investigating brain network aberrations in mental disorders from a dynamic viewpoint. Making neuroimaging accessible to severely impaired patients requires scan times to be as short as possible, and hence it was promising that the results of Study III showed that much of the DMN network could be revealed by intelligently extracting data from regular task-related fMRI without the need to acquire additional data. In the following, the results in each individual study are described in some more detail.

4.1 Study I – Diffusion Tensor Imaging in Schizophrenia

The main finding in this study was that comparison of patients with episodes of auditory verbal hallucinations (AVH+) during the past 12 months (defined as PANSS P3 of at least three) showed widespread differences in fractional anisotropy (FA) values compared to patients without these symptoms during the twelve months observation period (AVH-). The involved structures were identified from the TBSS skeleton analysis and included bilateral anterior thalamic radiation, bilateral corticospinal tract, bilateral inferior fronto-occipital fasciculus, bilateral superior longitudinal fasciculus,

and the temporal part of the right inferior longitudinal fasciculus, forceps minor, and the cingulum bundle. For all significant clusters, the extracted FA-values were lower for the AVH+ group and higher for the AVH- group with control group falling in between these two groups, without being significantly different to either group.

4.2 Study II – Novel Approach to Neuroimaging of Effort

A novel paradigm for a task-related fMRI experiment, composed of three well established cognitive tasks, was suggested to reveal not only the neuronal activation in response to each task, but also the overlap across tasks. This was done in a means to identify a network involved in solving a wide range of tasks, an extrinsic mode network (EMN), to be contrasted to a resting-state network – the default mode network (DMN). The results of Study II revealed significant neuronal activation in the right SMA, right inferior occipital gyrus, right angular gyrus, left superior parietal lobule, right and left precentral gyrus, left anterior insula, and left middle frontal gyrus in response to tasks (ON-OFF). The mirrored contrast (OFF-ON) revealed activations in the left precuneus/posterior cingulate gyrus (PCC), left and right angular gyrus, and right central operculum. These main findings were apparent both in a general conjunction analysis across the three cognitive tasks, as well as for each of the tasks separately, suggesting they span the activation of the EMN network. There were additionally smaller variations in the analysis for each specific task, cfr. Study II for details.

4.3 Study III – Simplifying Mapping of Resting-state

Comparing resting-state activations from the two conditions “continuous resting condition” and “intermittent resting condition” revealed that both approaches provided independent components that overlap substantially with the template of the well-reported default mode network (DMN). The overlap was slightly weaker in the frontal (anterior) regions compared to the posterior regions.

Across the two conditions, six significantly different connections between DMN network ROIs and ROIs belonging to the eight selected networks were detected. The findings were significant differences in the connection between the intermittent resting condition DMN and the salience network, than for the continuous resting condition .

5. Discussion

In the current thesis, structural and functional large-scale brain network dynamics have been investigated in healthy volunteers and in patients affected by schizophrenia. The novelty of the presented work includes i) combining different approaches for data analysis including a wide range of statistical modelling approaches (conjunction analysis, independent component analysis and statistical template matching), ii) proposing and implementing a novel fMRI experimental design (working memory, mental rotation, mental arithmetic) to map the extrinsic mode network (EMN), iii) investigating the feasibility of a simplified approach to measuring resting-state (OFF) which holds the potential to more easily be implemented in a clinical setting due to its shorter acquisition time.

The study I on structural brain connectivity revealed widespread differences in white matter connectivity between hallucinating and non-hallucinating patients. Widespread white matter alterations may significantly impact large-scale brain functional network dynamics, such as the EMN and DMN.

Moreover, alterations of EMN/DMN network dynamics has been suggested to be related to symptoms, such as AVH in schizophrenia. This may suggest that the general approach for studying network connectivity in schizophrenia should focus more on the global aspect of connectivity, rather than focusing on particular brain functional and structural connections. Hence, studies number II and III aimed to investigate the dynamics of the DMN and EMN, which should allow for a better understanding of the functioning of those networks in the healthy brain and provide a basis for future clinical studies of schizophrenia. The results of studies II and III support the suggestions by Kenneth Hugdahl, Marcus E Raichle et al. (2015b) of the EMN being a general task-positive network independent of sensory modality and task specifics. Furthermore, the results provide some vital information about the dynamics between the EMN and DMN and those environmental demands modulating the interaction between the networks.

Additionally, studies II and III provide input on the choice of different fMRI study paradigm applications for future mental disorders studies, and suggest that the block-design may be an optimal one. The following section will discuss the central findings from all three studies.

5.1 Large Scale network Alteration in Schizophrenia

It has been suggested that disruption of large-scale brain network functional connectivity may be related to symptoms of schizophrenia (Hugdahl et al., 2015b). That could lead to the hypothesis that such disruptions should be reflected in brain structural connectivity and would also be relatively widespread instead of focused. Study I aimed to investigate a possible link between alterations of white matter integrity and AVH, as a symptom in schizophrenia. Study I showed widespread FA-differences between the AVH+ and AVH- subgroups in white matter pathways, confirming results of previous studies (Bopp, Zöllner et al., 2017; Zhang, Gao et al., 2018). AVH+ had reduced FA-values compared to AVH- patients in all significantly different between-group regions. In addition study I shows that, hemispheric asymmetry was significantly different between the AVH+ and AVH- subgroups in two small clusters in the SLF.

While abnormalities of white matter connecting frontal and temporal brain areas are a frequent finding in DTI-studies of AVH in schizophrenia (Ćurčić-Blake et al., 2015; Falkenberg, Westerhausen et al., 2020; Leroux et al., 2017; Oestreich et al., 2016), Hugdahl, Løberg et al. (2009) suggested that in AVH, the dynamic interplay between top-down (information processing) and bottom-up (stimulus processing) may be unbalanced (Hugdahl, 2009). In general, white matter tracts such as the arcuate fasciculus, inferior fronto-occipital fasciculus and the superior longitudinal fasciculus connect frontal and temporal regions. These pathways have vital roles in language and semantic speech processing (e.g., (Duffau, Gatignol et al., 2005; Friederici, 2009; Glasser & Rilling, 2008; Rilling, Glasser et al., 2008), attention, working memory, and emotions (Geschwind, 1970; Hagmann, Cammoun et al., 2006).

Hugdahl et al. (2009) further suggested that unimpaired prefrontal and temporal areas help healthy voice-hearers to resist being overwhelmed by their "voices" compared to hallucinating schizophrenia patients. As observed in Study I, decreased FA-values in frontotemporal and fronto-occipital pathways support the model proposed by Hugdahl et al. (2009). The abnormalities of white matter tracks connecting frontal and temporal lobes may affect information flow from the frontal cortex. This can cause that frontal cortex fails to inhibit bottom-up temporal lobe hyper-activation. Another key finding of Study I showed abnormalities in the anterior thalamic radiation and in the cingulum bundle that have been shown to be involved in emotion processing (Bubb, Metzler-Baddeley et al., 2018; Panksepp, 2004, 2005; Sun, Peräkylä et al., 2015). Emotion processing is a process that is central in AVHs they have typically negative character. There were no differences between patient groups when it came to negative scores. Therefore, the changes observed in the anterior thalamic radiation and cingulum bundle are likely not related to other negative symptoms but rather the emotional content of AVH.

The results of study I showing more pronounced leftward FA-asymmetry in the AVH-group could mean that the AVH+ patients had decreased between-hemisphere FA asymmetry than the AVH- group. Some studies have linked leftward asymmetry of the planum temporale and auditory cortex in healthy subjects to left hemispheric functional specialization for language (Hugdahl, Løberg et al., 2008; Jäncke, Wüstenberg et al., 2002). Hence, reduced leftward asymmetry in our AVH+ patients for major white matter pathways connecting frontal and temporal brain areas may hypothetically be related to dysfunction of language areas in AVH. Parts of the frontal SLF contain arcuate fasciculus and connect to the frontotemporal language association cortex (Kamali, Flanders et al., 2014). Further, many studies suggest that the left arcuate fasciculus, a critical pathway of the language network, exhibits reduced FA-values in AVH+ patients (Abdul-Rahman, Qiu et al., 2012; Catani, Craig et al., 2011; Čurčić-Blake, Ford et al., 2017; Seok, Park et al., 2007).

5.2 EMN as a Task-positive Network Independent of Sensory Modality

The second Study of the thesis assessed the hypothesis of the studies by Hugdahl et al. (2015a) and Hugdahl et al. (2019) that switching between resting and active processing periods results in DMN and EMN being correspondingly up- and down-regulated as environmental demands change from passive to active by using a new and unrelated paradigm. In this respect, the results presented in Study II, using a visually-cued paradigm, resemble those from a previous study by Hugdahl et al. (2019), where the auditory task was utilized. Although some notable differences were present, the most prominent similarities between the study II and the one by Hugdahl et al. (2019) were the overlapping activations in the SMA and insula regions. Therefore, it may be concluded that the EMN, is independent of sensory modality.

For both studies, there were differences in activations in the sensory areas, which were not independent of sensory modality. In the Hugdahl et al. (2019) study, activations during ON-blocks were observed in the auditory areas in the temporal lobes. In contrast, the present study showed activations in visual regions in the occipital cortex since this study used visual tasks. However, these areas are not part of the core EMN regions, such that these results do not argue against a modality independent role for the EMN.

The most prominent similarities between the studies, in the case of the DMN, were found in the cingulate cortex and in the precuneus, which are core DMN areas. At the same time, differences were observed in the superior and middle frontal gyri and the angular operculum. These discrepancies presumably represent DMN spatial extension variation as environmental demands change since OFF-task activations likely are affected by ON-task activation (Turnbull, Wang et al., 2019).

5.3 EMN Up-regulation Independent of Task specifics

The second main finding in Study II was that the up-regulation of the task-positive EMN network was independent of the specifics of the task, i.e., generalized across the tasks as suggested by Hugdahl et al. (2019). The presented results agree with the results of Fedorenko et al. (2013) and Duncan (2013) on a non-specific task-positive network, particularly in the case of activations in the SMA, superior parietal lobule, inferior and middle frontal gyrus, and the precentral gyrus. However, there are significant differences between the current study and Fedorenko and Duncan's study. Firstly, different tasks were used to elicit activations in the two studies, and the interpretation of the findings extends beyond an attention model as a mediating factor, as suggested by Duncan (2013).

The results of study II provide evidence that the brain may shift between intrinsic and extrinsic functioning modes, corresponding to the dominating environmental demand. In line with previous suggestions (Andreou, Steinmann et al., 2018; Hugdahl et al., 2019; Lustig et al., 2003), the intrinsic mode network dominates during task-absence and the extrinsic mode network, the EMN, dominates in a task-presence. The DMN is essentially a task-negative network (Andreou et al., 2018; Gotts, Gilmore et al., 2020) that is up-regulated in the absence of specific processing demands, and therefore it can be considered as an intrinsic mode network. Recent unpublished findings from our group (Weber, Aleman et al., 2021) suggest however that the EMN and DMN may converge when external processing demands are low, i.e. when tasks are cognitively easy to perform, but diverge when demands are high, i.e. when tasks are difficult to perform. Thus, the dynamic interplay between the EMN and DMN are probably more complex than originally thought.

5.4 EMN Modulated by Environmental Demands

In Study II, joint activations across tasks, both during ON- and OFF-blocks, were not unambiguous since there were also unique single-task activations and common

activations for combinations of tasks. These results may support the hypothesis by Hugdahl et al. (2015a) that the EMN, among other non-specific general-domain networks, may be dynamically modulated depending on environmental demands. Hence, task-specific nodes in the network may transiently be modulated by dynamically stretching or shrinking. Therefore, it may be hypothesized that dynamic modulation of the DMN, seen during OFF-blocks, depends both on previous and anticipated environmental challenges, as shown in some studies (see Buckner and DiNicola (2019) for a review of DMN activations). No unique activations related to the mental arithmetic task during ON-blocks were observed in conjunction with all three tasks or compared with activations from the working memory task. The absence of unique activations for the mental arithmetic task during ON-blocks needs further investigation since it contrasts with the finding of additional activations during OFF-blocks. The absence of unique mental arithmetic activations during active periods may therefore be due to the inclusion of a transient working memory component in addition to a pure arithmetic component, making it a more demanding task. The additional activations during resting periods associated with the mental arithmetic task suggests that an arithmetic task induces a more substantial up-regulation of the DMN (in the sense of extended area) than the other two tasks. Hence, this observation may indicate that the arithmetic task is more resource-demanding during ON-blocks. Thus, it can be suggested that the level of demand embedded in a task could be operationally defined by how much rebound a task causes during intermittent rest periods (OFF-blocks).

5.5 DMN and EMN Dynamic Complexities

As briefly mentioned above, the DMN and EMN networks are sometimes positively correlated, suggesting that their relationship may be more complex than initially thought [30]. Study II focused on the precuneus/PCC and ventral SMA as ROIs when extracting the time-courses representing the EMN and DMN, respectively.

Extracted EMN and DMN time-courses showed an inverse up- and down-regulation between the two selected ROIs across task- and rest-periods. However, these two signals were not constantly anti-correlated, as would be expected from a classic EMN

DMN networks dynamics understanding (Michael D. Fox, Abraham Z. Snyder et al., 2005). A positive correlation between the two signals was observed in the middle of the ON-blocks. The positive correlations seem to be caused by the EMN BOLD-response beginning to drop shortly after an initial up-regulation at the transition points between the blocks. This result could originate from fading concentration focus across ON-blocks or a habituation effect caused by task repetitions.

5.6 DMN Activity Patterns Depend on the Experimental Design

Study III compared DMN activity patterns between two different experimental conditions, an intermittent resting-state condition, and a continuous resting-state condition, focusing on the DMN. Study III hypothesized that the general architecture of the DMN observed in these two experimental conditions should be similar. However, differences in mental states in these conditions may influence DMN activity and connectivity across the two experimental conditions may therefore vary in different ways.

When comparing ICA components from both conditions, a clear overlap in the overall DMN pattern was observed. The overlap was present regardless of the technique used for the comparison (conjunction or probability maps). As anticipated, the highest resemblance between the two DMN-maps was observed in the posterior parts of the brain, which also converged with the key DMN-nodes in the precuneus and posterior cingulate cortex,

The intermittent resting-state condition resulted in reduced activity in the medial prefrontal cortex (MPFC) compared to the continuous resting-state condition. MPFC activity is associated with self-related processing, retrieving personal knowledge, such as autobiographical memories, and simulating future personal events or social

interactions (Andrews-Hanna, 2012; D'Argembeau, 2013; Denny, Kober et al., 2012; Moran, Kelley et al., 2013; Spreng, Mar et al., 2009). These activities may reflect brain correlates of mind-wandering anticipated to be predominant in a continuous resting-state condition compared to an intermittent resting-state condition. Therefore, it may be hypothesized that participants will not manage to achieve a deep state of resting during an intermittent condition in contrast to a continuous period, and consequently less DMN activity. Activity during ON-blocks may also "carry over" and interfere with activity during OFF-blocks, reducing DMN activity in an intermittent resting condition resulting in reduced activity in the MPFC.

5.7 DMN Connectivity is Depending on the Functional MRI Experimental Design

In Study III, the functional connectivity between the DMN and other major networks was compared between an intermittent and continuous resting-state condition to test how network dynamics vary between conditions.

The comparison showed a significant difference in connectivity between the DMN and the salience network (SN), with stronger connectivity between the DMN and SN in the intermittent resting-state condition compared to the corresponding connectivity in the continuous resting-state condition. This finding may reflect that the SN is dynamically modulating brain activity while constantly transitioning between active and resting periods during the experiment.

The results of Study III seem to support the findings of other studies showing that the SN plays a significant role in switching between the central executive network (CEN) and the DMN (Goulden, Khusnulina et al., 2014; Menon, 2011; Sridharan et al., 2008). The CEN is a large-scale brain network primarily composed of the dorsolateral prefrontal cortex and posterior parietal cortex around the intraparietal sulcus (Gong, He et al., 2016; Gratton, Sun et al., 2018). It is involved in sustained attention, complex problem-solving, and working memory (Menon, 2011). The CEN is one of three

networks in the so-called triple-network model together with the SN and the DMN (van Oort et al., 2017). The ACC and the insula regions, which are central regions in the SN, have known reciprocal connectivity and connect to motor and sensory areas. This characteristic makes these regions ideal for receiving inputs required to regulate switching between resting and task-processing networks, like DMN and CEN.

While the SN and CEN are domain-specific task-positive networks, however, it has previously been shown that they share certain characteristics with general domain networks, like the EMN (Hugdahl et al., 2019). However, it is essential to remember that the SN and CEN are domain-specific while the EMN is conceptualized as a non-specific domain network. Therefore, further research is needed to understand the complexity of the relationship and dynamics between the EMN, SN, and CEN.

Additionally, increased functional connectivity between the DMN and CEN in schizophrenia patients has been reported, and further related this to the severity of hallucinations being a most prominent symptom in schizophrenia (Manoliu, Riedl et al., 2013). Therefore, understanding the role of the SN in the modulation of the CEN and DMN networks may be necessary for understanding underlying neuronal mechanisms of mental disorders such as schizophrenia.

5.8 Block-design Experiment as an Approximation for Everyday Brain activity Fluctuations

The functional role of the DMN network and its different parts in the dynamics of the network as a whole are still not fully understood despite extensive research being done. Even though the DMN was present in both resting-conditions in Study III, there were also differences in overall DMN activity and connectivity between the two conditions. Pyka et al. (2009) showed that the DMN was not only more intensely down-regulated during the performance of the more demanding tasks (working memory 2-back task), but the same network was also more intensely activated during OFF-blocks following after these tasks. This observation suggests that cognitive load may influence DMN-activity during task performance, especially after challenging tasks (Pyka et al., 2009).

The fact that corresponding "carry-over" effects were seen in Study II may indicate that the DMN may be more easily disrupted during brief intermittent resting periods compared to the "classic" DMN seen in prolonged resting periods without interruptions. Simultaneously, "classic" resting-state designs with 10-20 minutes of uninterrupted resting while in the scanner may not reflect a typical situation in everyday life. Experimental designs that are distant from everyday life dynamics may hinder a deeper understanding of the neurobiology of major large-scale brain networks. This may in turn have implications for understanding brain correlates of mental disorders, since network connectivity studies are often used as potential biomarkers of a variety of mental disorders, e.g. schizophrenia. The results of Study II may suggest a solution to the problem. The results of Study II indicate that an fMRI block-design with alternating task- and rest-periods may be seen as an experimental approximation for the alternations between brief periods of rest and stressful job situations during an ordinary day in life. However, one should note that such periods, will in reality vary regarding intensity, frequency, and length as environmental demands change, and will also vary between individuals.

5.9 Limitations

Limitations regarding Study I are firstly that patients were on antipsychotic medication throughout the study, which is always a source of confounding with the experimental factors. However, no differences were observed between the AVH+ and AVH- groups in DDD values, indicating that medication differences may not significantly have confounded the results. Secondly, it is essential to remember that FA-values carrying information about white matter integrity at the cellular level is averaged over large voxel volumes since the MRI voxel resolution is larger (mm) than the scale of the cells that are probed in μm (O'Donnell & Pasternak, 2015). Hence, the presence of, for instance, multiple fiber populations with different orientations may contribute to the average, macroscopic value of the signal. For this reason, decreased FA-values in specific brain regions cannot be assumed to result from microscopic cellular abnormalities exclusively, but may also result from the reorganization of fibers on a

macroscopic scale, or combination of changes in tissue myelination, fiber organization, or the number of axons (Mori & Zhang, 2006) . The mismatch between macroscopic information on microscopic properties is a common issue in DTI studies and this mismatch should be kept in mind when interpreting the results.

For Study II, it is essential to mention limitations regarding the time-course analysis performed. In this analysis, the BOLD time-courses were extracted from the precuneus/PCC and ventral SMA as EMN and DMN ROIs, respectively. To capture a reliable representation of the EMN and DMN networks, relatively large ROIs were used that could have caused partial volume effects shared with the other network, not contributing to the positive correlation observed. The mean framewise displacement (Power et al., 2012; Power et al., 2014) indices in the dataset used in Study II were both smaller than the “lenient” ($FD > 0.5$ mm), as well as the “stringent” ($FD > 0.2$ mm) thresholds discussed by Power et al. (2014) and under the threshold ($FD > 0.5$). Consequently, corrections like temporal masking by censoring or interpolating the data may not be optimal. Additionally, spurious activations are less likely to influence a task-based paradigm's results than in a resting-state fMRI study. Nevertheless, a simple test for the influence of motion by removing 17 of a total of 47 subjects that had $FDs \geq 0.2$ has been performed. The results showed no significant differences when comparing the two data sets. Although more complex censoring and interpolation methods may be more thorough, they were not considered necessary given the low mean framewise displacement.

In study III, a rather restrictive approach to extract the intermittent resting-state condition data from the block design data was used compared to similar studies (Damien A. Fair et al., 2007). A strategy like what was used in (Damien A. Fair et al., 2007) was not adopted in Study III for two reasons. Firstly, including the end-volumes of the OFF-blocks or beginning blocks of the ON-blocks may risk confounding the intermittent resting-state condition data due to subjects' “anticipation” of the start of the next ON-block. Moreover, using the strategy adopted by Damien A. Fair et al.

(2007) could allow for increasing the length of the intermittent resting-state blocks by only including the two first volumes of the subsequent ON-block.

Accounting for the additional difference in TR parameters between the two studies, the number of volumes included in both studies would be similar. The OFF-block duration was 17 whole-brain volumes (34 sec) in the intermittent resting-state condition. The relatively short OFF-block duration limits the number of volumes to create 4D intermittent resting-state condition data, making it necessarily to be shorter than the continuous resting-state data. However, continuous resting-state data were also relatively short (5 min). Block-fMRI experiments with relatively short resting OFF-blocks may risk limiting the range of available frequencies to extract resting-state correlation information (Damien A. Fair et al., 2007). Nonetheless, a study by Salvador, Suckling et al. (2005) showed that when isolating higher frequencies (>0.1 Hz), equivalent correlation profiles can be acquired, however with somewhat lower correlations than when using frequencies lower than 0.1 Hz. Therefore, joining resting-state epochs in a block-design may deliver similar correlation profiles as profiles obtained with continuous resting-state data. However, due to a shorter total sampling period, the lowest frequency components may be missing. The technique used in Study III to create 4D intermittent resting-state data also generated an artifact in the points where data from the OFF-blocks were joined. Nevertheless, these artifacts were present periodically and should not significantly have affected our results.

5.10 Conclusions and future directions

This thesis aims at contributing to knowledge of functional network architecture and dynamics in healthy individuals, and a corresponding contribution to knowledge about structural network architecture in mental disorders, especially schizophrenia.

The main conclusion from this work is that abnormalities in structural network architecture in schizophrenia patients with AVH is seemingly more widespread, rather than being focused to one particular brain structure. This point to the need for

optimizing means to investigate potential alternations in functional networks and the dynamics between task-dependent and task-independent brain networks. These investigations in healthy volunteers allowed us to conclude that it is possible to map an extrinsic brain network (EMN) which is independent of the sensory domain and task modality, and that external environmental demands dynamically interact with the default mode network (DMN).

Combining the findings across the three studies in this thesis, thus paves the way for further investigations of the interplay of structural (Study I) and functional abnormalities (Studies II and III). When investigated in the same patients, it could be explored how structural abnormalities in mental disorders also manifest in symptoms such as AVH in schizophrenia. Here, investigations in particular structural pathways rather than the whole white matter skeleton (Study I) could again be of particular interest, e.g. pathways and functional regions expected to be involved in generating AVH.

In particular, it is suggested that novel functional paradigms (Study II), and a simplified approach to mapping resting-state conditions (Study III), should be explored in such combined structure-functional studies in order to reveal the underlying mechanisms of symptoms. This could in addition provide potential imaging biomarkers which could be used to study potential effect of therapeutic interventions in mental disorders. We believe that the proposed block-design experiments may better reflect the everyday waxing and waning of brain activity in the course of a day. It is therefore suggested that future studies could explore this kind of experimental set-up more extensively, especially in clinical fMRI studies.

6. References

- Abdul-Rahman, M. F., Qiu, A., Woon, P. S., Kuswanto, C., Collinson, S. L., & Sim, K. (2012). Arcuate Fasciculus Abnormalities and Their Relationship with Psychotic Symptoms in Schizophrenia. *PLOS ONE*, 7(1), e29315. doi:10.1371/journal.pone.0029315
- Alves, P. N., Foulon, C., Karolis, V., Bzdok, D., Margulies, D. S., Volle, E., & Thiebaut de Schotten, M. (2019). An improved neuroanatomical model of the default-mode network reconciles previous neuroimaging and neuropathological findings. *Communications Biology*, 2(1), 370. doi:10.1038/s42003-019-0611-3
- Andreou, C., Steinmann, S., Kolbeck, K., Rauh, J., Leicht, G., Moritz, S., & Mulert, C. (2018). The role of effective connectivity between the task-positive and task-negative network for evidence gathering [Evidence gathering and connectivity]. *Neuroimage*, 173, 49-56.
- Andrews-Hanna, J. R. (2012). The brain's default network and its adaptive role in internal mentation. *The Neuroscientist*, 18(3), 251-270.
- Bandettini, P. A. (2012). Twenty years of functional MRI: the science and the stories. *Neuroimage*, 62(2), 575-588.
- Basser, P. J., & Jones, D. K. (2002). Diffusion-tensor MRI: theory, experimental design and data analysis—a technical review. *NMR in Biomedicine: An International Journal Devoted to the Development and Application of Magnetic Resonance In Vivo*, 15(7-8), 456-467.
- Bassett, D. S., & Bullmore, E. T. (2009). Human brain networks in health and disease. *Current opinion in neurology*, 22(4), 340.
- Beaulieu, C. (2002). The basis of anisotropic water diffusion in the nervous system—a technical review. *NMR in Biomedicine: An International Journal Devoted to the Development and Application of Magnetic Resonance In Vivo*, 15(7-8), 435-455.
- Bell, A. J., & Sejnowski, T. J. (1995). An information-maximization approach to blind separation and blind deconvolution. *Neural computation*, 7(6), 1129-1159.
- Birn, R. M., Molloy, E. K., Patriat, R., Parker, T., Meier, T. B., Kirk, G. R., . . . Prabhakaran, V. (2013). The effect of scan length on the reliability of resting-state

fMRI connectivity estimates. *Neuroimage*, 83, 550-558.

doi:<https://doi.org/10.1016/j.neuroimage.2013.05.099>

Bopp, M. H. A., Zöllner, R., Jansen, A., Dietsche, B., Krug, A., & Kircher, T. T. J. (2017). White matter integrity and symptom dimensions of schizophrenia: A diffusion tensor imaging study. *Schizophrenia research*, 184, 59-68.

doi:<https://doi.org/10.1016/j.schres.2016.11.045>

Brandl, F., Avram, M., Weise, B., Shang, J., Simões, B., Bertram, T., . . . Sorg, C. (2019). Specific Substantial Dysconnectivity in Schizophrenia: A Transdiagnostic Multimodal Meta-analysis of Resting-State Functional and Structural Magnetic Resonance Imaging Studies. *Biological psychiatry*, 85(7), 573-583.

doi:<https://doi.org/10.1016/j.biopsych.2018.12.003>

Braun, U., Schaefer, A., Betzel, R. F., Tost, H., Meyer-Lindenberg, A., & Bassett, D. S. (2018). From Maps to Multi-dimensional Network Mechanisms of Mental Disorders. *Neuron*, 97(1), 14-31. doi:<https://doi.org/10.1016/j.neuron.2017.11.007>

Bressler, S. L., & Menon, V. (2010). Large-scale brain networks in cognition: emerging methods and principles. *Trends in Cognitive Sciences*, 14(6), 277-290.

doi:<https://doi.org/10.1016/j.tics.2010.04.004>

Bubb, E. J., Metzler-Baddeley, C., & Aggleton, J. P. (2018). The cingulum bundle: Anatomy, function, and dysfunction. *Neuroscience & Biobehavioral Reviews*, 92, 104-127. doi:<https://doi.org/10.1016/j.neubiorev.2018.05.008>

Buckner, R. L., Andrews-Hanna, J. R., & Schacter, D. L. (2008). The brain's default network: anatomy, function, and relevance to disease.

Buckner, R. L., & DiNicola, L. M. (2019). The brain's default network: updated anatomy, physiology and evolving insights. *Nature reviews neuroscience*, 20(10), 593-608.

Calhoun, V., Eichele, T., & Pearlson, G. (2009). Functional brain networks in schizophrenia: a review. *Frontiers in Human Neuroscience*, 3(17).

doi:10.3389/neuro.09.017.2009

Catani, M., Craig, M. C., Forkel, S. J., Kanaan, R., Picchioni, M., Touloupoulou, T., . . . McGuire, P. (2011). Altered Integrity of Perisylvian Language Pathways in Schizophrenia: Relationship to Auditory Hallucinations. *Biological Psychiatry*, 70(12), 1143-1150. doi:10.1016/j.biopsych.2011.06.013

Catani, M., Jones, D. K., & Ffytche, D. H. (2005). Perisylvian language networks of the human brain. *Annals of Neurology: Official Journal of the American Neurological Association and the Child Neurology Society*, 57(1), 8-16.

Chawla, N., Deep, R., Khandelwal, S. K., & Garg, A. (2019). Reduced integrity of superior longitudinal fasciculus and arcuate fasciculus as a marker for auditory hallucinations in schizophrenia: A DTI tractography study. *Asian Journal of Psychiatry*, 44, 179-186. doi:<https://doi.org/10.1016/j.ajp.2019.07.043>

Collin, G., Turk, E., & van den Heuvel, M. P. (2016). Connectomics in Schizophrenia: From Early Pioneers to Recent Brain Network Findings. *Biological Psychiatry: Cognitive Neuroscience and Neuroimaging*, 1(3), 199-208. doi:<https://doi.org/10.1016/j.bpsc.2016.01.002>

Corbetta, M., Patel, G., & Shulman, G. L. (2008). The reorienting system of the human brain: from environment to theory of mind. *Neuron*, 58(3), 306-324.

Cunningham, S. I., Tomasi, D., & Volkow, N. D. (2017). Structural and functional connectivity of the precuneus and thalamus to the default mode network. *Human brain mapping*, 38(2), 938-956.

Ćurčić-Blake, B., Ford, J. M., Hubl, D., Orlov, N. D., Sommer, I. E., Waters, F., . . . Aleman, A. (2017). Interaction of language, auditory and memory brain networks in auditory verbal hallucinations. *Progress in neurobiology*, 148, 1-20. doi:<https://doi.org/10.1016/j.pneurobio.2016.11.002>

Ćurčić-Blake, B., Nanetti, L., van der Meer, L., Cerliani, L., Renken, R., Pijnenborg, G. H., & Aleman, A. (2015). Not on speaking terms: hallucinations and structural network disconnectivity in schizophrenia. *Brain Structure and Function*, 220(1), 407-418.

D'Argembeau, A. (2013). On the role of the ventromedial prefrontal cortex in self-processing: the valuation hypothesis. *Frontiers in Human Neuroscience*, 7, 372.

D'esposito, M., Detre, J. A., Alsop, D. C., Shin, R. K., Atlas, S., & Grossman, M. (1995). The neural basis of the central executive system of working memory. *Nature*, 378(6554), 279-281.

De Weijer, A., Mandl, R., Diederer, K., Neggers, S., Kahn, R., Pol, H. H., & Sommer, I. (2011). Microstructural alterations of the arcuate fasciculus in schizophrenia patients with frequent auditory verbal hallucinations. *Schizophrenia research*, 130(1), 68-77.

- Deng, Z., Wu, J., Gao, J., Hu, Y., Zhang, Y., Wang, Y., . . . Zuo, X. (2019). Segregated precuneus network and default mode network in naturalistic imaging. *Brain Structure and Function*, 224(9), 3133-3144.
- Denny, B. T., Kober, H., Wager, T. D., & Ochsner, K. N. (2012). A meta-analysis of functional neuroimaging studies of self-and other judgments reveals a spatial gradient for mentalizing in medial prefrontal cortex. *Journal of Cognitive Neuroscience*, 24(8), 1742-1752.
- Di, X., & Biswal, B. B. (2015). Dynamic brain functional connectivity modulated by resting-state networks. *Brain Structure and Function*, 220(1), 37-46.
- Duffau, H., Gatignol, P., Mandonnet, E., Peruzzi, P., Tzourio-Mazoyer, N., & Capelle, L. (2005). New insights into the anatomo-functional connectivity of the semantic system: a study using cortico-subcortical electrostimulations. *Brain*, 128(4), 797-810. doi:10.1093/brain/awh423
- Duncan, J. (2013). The structure of cognition: attentional episodes in mind and brain. *Neuron*, 80(1), 35-50.
- Duncan, J., & Owen, A. M. (2000). Common regions of the human frontal lobe recruited by diverse cognitive demands. *Trends in Neurosciences*, 23(10), 475-483. doi:[https://doi.org/10.1016/S0166-2236\(00\)01633-7](https://doi.org/10.1016/S0166-2236(00)01633-7)
- Eickhoff, S. B., & Müller, V. I. (2015). Functional Connectivity. In A. W. Toga (Ed.), *Brain Mapping* (pp. 187-201). Waltham: Academic Press.
- Ellison-Wright, I., & Bullmore, E. (2009). Meta-analysis of diffusion tensor imaging studies in schizophrenia. *Schizophrenia research*, 108(1), 3-10. doi:<https://doi.org/10.1016/j.schres.2008.11.021>
- Fair, D. A., Cohen, A. L., Power, J. D., Dosenbach, N. U., Church, J. A., Miezin, F. M., . . . Petersen, S. E. (2009). Functional brain networks develop from a “local to distributed” organization. *PLoS computational biology*, 5(5), e1000381.
- Fair, D. A., Schlaggar, B. L., Cohen, A. L., Miezin, F. M., Dosenbach, N. U. F., Wenger, K. K., . . . Petersen, S. E. (2007). A method for using blocked and event-related fMRI data to study “resting state” functional connectivity. *Neuroimage*, 35(1), 396-405. doi:<https://doi.org/10.1016/j.neuroimage.2006.11.051>
- Falkenberg, L. E., Westerhausen, R., Johnsen, E., Kroken, R., Løberg, E.-M., Beresniewicz, J., . . . Hugdahl, K. (2019). Positive relation between arcuate fasciculus white matter fiber structure and severity of auditory hallucinations: A DTI tractography study. *bioRxiv*, 784942. doi:10.1101/784942

Falkenberg, L. E., Westerhausen, R., Johnsen, E., Kroken, R., Løberg, E.-M., Beresniwicz, J., . . . Hugdahl, K. (2020). Hallucinating schizophrenia patients have longer left arcuate fasciculus fiber tracks: a DTI tractography study. *Psychiatry Research: Neuroimaging*, *302*, 111088.

doi:<https://doi.org/10.1016/j.psychresns.2020.111088>

Fedorenko, E., Duncan, J., & Kanwisher, N. (2013). Broad domain generality in focal regions of frontal and parietal cortex. *Proceedings of the National Academy of Sciences*, *110*(41), 16616-16621.

Fields, R. D. (2008). White matter in learning, cognition and psychiatric disorders. *Trends in Neurosciences*, *31*(7), 361-370.

doi:<https://doi.org/10.1016/j.tins.2008.04.001>

Fitzsimmons, J., Kubicki, M., & Shenton, M. E. (2013). Review of functional and anatomical brain connectivity findings in schizophrenia. *Current Opinion in Psychiatry*, *26*(2).

Fornito, A., Zalesky, A., Pantelis, C., & Bullmore, E. T. (2012). Schizophrenia, neuroimaging and connectomics. *Neuroimage*, *62*(4), 2296-2314.

doi:<https://doi.org/10.1016/j.neuroimage.2011.12.090>

Fox, M. D., Snyder, A. Z., Vincent, J. L., Corbetta, M., Van Essen, D. C., & Raichle, M. E. (2005). The human brain is intrinsically organized into dynamic, anticorrelated functional networks. *Proceedings of the National Academy of Sciences of the United States of America*, *102*(27), 9673-9678. doi:10.1073/pnas.0504136102

Fox, M. D., Snyder, A. Z., Vincent, J. L., Corbetta, M., Van Essen, D. C., & Raichle, M. E. (2005). The human brain is intrinsically organized into dynamic, anticorrelated functional networks. *Proceedings of the National Academy of Sciences*, *102*(27), 9673-9678.

Friederici, A. D. (2009). Allocating functions to fiber tracts: facing its indirectness. *Trends in Cognitive Sciences*, *13*(9), 370-371.

doi:<https://doi.org/10.1016/j.tics.2009.06.006>

Ganger, S., Hahn, A., Küblböck, M., Kranz, G. S., Spies, M., Vanicek, T., . . .

Kasper, S. (2015). Comparison of continuously acquired resting state and extracted analogues from active tasks. *Human brain mapping*, *36*(10), 4053-4063.

Geoffroy, P. A., Houenou, J., Duhamel, A., Amad, A., De Weijer, A. D., Ćurčić-Blake, B., . . . Jardri, R. (2014). The arcuate fasciculus in auditory-verbal hallucinations: A meta-analysis of diffusion-tensor-imaging studies. *Schizophrenia Research*, *159*(1), 234-237. doi:<https://doi.org/10.1016/j.schres.2014.07.014>

- Geschwind, N. (1970). The Organization of Language and the Brain. *Science*, 170(3961), 940. doi:10.1126/science.170.3961.940
- Glasser, M. F., & Rilling, J. K. (2008). DTI Tractography of the Human Brain's Language Pathways. *Cerebral Cortex*, 18(11), 2471-2482. doi:10.1093/cercor/bhn011
- Gong, D., He, H., Ma, W., Liu, D., Huang, M., Dong, L., . . . Yao, D. (2016). Functional integration between salience and central executive networks: a role for action video game experience. *Neural Plasticity*, 2016.
- Gotts, S. J., Gilmore, A. W., & Martin, A. (2020). Brain networks, dimensionality, and global signal averaging in resting-state fMRI: Hierarchical network structure results in low-dimensional spatiotemporal dynamics. *Neuroimage*, 205, 116289.
- Goulden, N., Khusnulina, A., Davis, N. J., Bracewell, R. M., Bokde, A. L., McNulty, J. P., & Mullins, P. G. (2014). The salience network is responsible for switching between the default mode network and the central executive network: Replication from DCM. *Neuroimage*, 99, 180-190. doi:<https://doi.org/10.1016/j.neuroimage.2014.05.052>
- Gratton, C., Sun, H., & Petersen, S. E. (2018). Control networks and hubs. *Psychophysiology*, 55(3), e13032.
- Greicius, M. D., Krasnow, B., Reiss, A. L., & Menon, V. (2003). Functional connectivity in the resting brain: a network analysis of the default mode hypothesis. *Proceedings of the National Academy of Sciences*, 100(1), 253-258.
- Gusnard, D. A., & Raichle, M. E. (2001). Searching for a baseline: functional imaging and the resting human brain. *Nature reviews neuroscience*, 2(10), 685-694.
- Hagmann, P., Cammoun, L., Martuzzi, R., Maeder, P., Clarke, S., Thiran, J.-P., & Meuli, R. (2006). Hand preference and sex shape the architecture of language networks. *Human brain mapping*, 27(10), 828-835. doi:10.1002/hbm.20224
- Hammar, Å., Neto, E., Clemo, L., Hjetland, G. J., Hugdahl, K., & Elliott, R. (2016). Striatal hypoactivation and cognitive slowing in patients with partially remitted and remitted major depression. *PsyCh journal*, 5(3), 191-205.
- Hjelmervik, H., Craven, A. R., Sinceviciute, I., Johnsen, E., Kompus, K., Bless, J. J., . . . Grüner, R. (2020). Intra-regional Glu-GABA vs inter-regional glu-glu imbalance: a 1H-MRS study of the neurochemistry of auditory verbal hallucinations in schizophrenia. *Schizophrenia Bulletin*, 46(3), 633-642.

-
- Honey, C. J., Sporns, O., Cammoun, L., Gigandet, X., Thiran, J. P., Meuli, R., & Hagmann, P. (2009). Predicting human resting-state functional connectivity from structural connectivity. *Proceedings of the National Academy of Sciences*, *106*(6), 2035. doi:10.1073/pnas.0811168106
- Hugdahl, K. (2009). "Hearing voices": Auditory hallucinations as failure of top-down control of bottom-up perceptual processes. *Scandinavian Journal of Psychology*, *50*(6), 553-560. doi:10.1111/j.1467-9450.2009.00775.x
- Hugdahl, K., Kazimierzczak, K., Beresniewicz, J., Kompus, K., Westerhausen, R., Ersland, L., . . . Specht, K. (2019). Dynamic up-and down-regulation of the default (DMN) and extrinsic (EMN) mode networks during alternating task-on and task-off periods. *PLoS One*, *14*(9), e0218358.
- Hugdahl, K., Løberg, E.-M., & Nygård, M. (2009). Left temporal lobe structural and functional abnormality underlying auditory hallucinations. *Frontiers in Neuroscience*, *3*(1). doi:10.3389/neuro.01.001.2009
- Hugdahl, K., Løberg, E.-M., Specht, K., Steen, V., Wagneningen, H., & Jørgensen, H. (2008). Auditory hallucinations in schizophrenia: the role of cognitive, brain structural and genetic disturbances in the left temporal lobe. *Frontiers in Human Neuroscience*, *2*, 6.
- Hugdahl, K., Raichle, M. E., Mitra, A., & Specht, K. (2015a). On the existence of a generalized non-specific task-dependent network. *Frontiers in Human Neuroscience*, *9*(430). doi:10.3389/fnhum.2015.00430
- Hugdahl, K., Raichle, M. E., Mitra, A., & Specht, K. (2015b). On the existence of a generalized non-specific task-dependent network. *Frontiers in Human Neuroscience*, *9*, 430.
- Hugdahl, K., & Sommer, I. E. (2017). Auditory Verbal Hallucinations in Schizophrenia From a Levels of Explanation Perspective. *Schizophrenia Bulletin*, *44*(2), 234-241. doi:10.1093/schbul/sbx142
- Hugdahl, K., Thomsen, T., & Ersland, L. (2006). Sex differences in visuo-spatial processing: an fMRI study of mental rotation. *Neuropsychologia*, *44*(9), 1575-1583.
- Jäncke, L., Wüstenberg, T., Schulze, K., & Heinze, H. J. (2002). Asymmetric hemodynamic responses of the human auditory cortex to monaural and binaural stimulation. *Hearing Research*, *170*(1), 166-178. doi:[https://doi.org/10.1016/S0378-5955\(02\)00488-4](https://doi.org/10.1016/S0378-5955(02)00488-4)
- Johns, P. (2014). Functional neuroanatomy. *Clinical neuroscience*, *27*.

Jordan, K., Heinze, H.-J., Lutz, K., Kanowski, M., & Jäncke, L. (2001). Cortical activations during the mental rotation of different visual objects. *Neuroimage*, *13*(1), 143-152.

Kamali, A., Flanders, A. E., Brody, J., Hunter, J. V., & Hasan, K. M. (2014). Tracing superior longitudinal fasciculus connectivity in the human brain using high resolution diffusion tensor tractography. *Brain Structure and Function*, *219*(1), 269-281.

Kay, S. R., Fiszbein, A., & Opler, L. A. (1987). The positive and negative syndrome scale (PANSS) for schizophrenia. *Schizophrenia Bulletin*, *13*(2), 261-276.

Kelly, S., Jahanshad, N., Zalesky, A., Kochunov, P., Agartz, I., Alloza, C., . . . Donohoe, G. (2017). Widespread white matter microstructural differences in schizophrenia across 4322 individuals: results from the ENIGMA Schizophrenia DTI Working Group. *Molecular Psychiatry*, *23*, 1261. doi:10.1038/mp.2017.170

<https://www.nature.com/articles/mp2017170#supplementary-information>

Kelly, S., Jahanshad, N., Zalesky, A., Kochunov, P., Agartz, I., Alloza, C., . . . Donohoe, G. (2018). Widespread white matter microstructural differences in schizophrenia across 4322 individuals: results from the ENIGMA Schizophrenia DTI Working Group. *Molecular Psychiatry*, *23*(5), 1261-1269. doi:10.1038/mp.2017.170

Köhler, S., Moscovitch, M., Winocur, G., Houle, S., & McIntosh, A. R. (1998). Networks of domain-specific and general regions involved in episodic memory for spatial location and object identity. *Neuropsychologia*, *36*(2), 129-142.

Kubicki, M., McCarley, R., Westin, C.-F., Park, H.-J., Maier, S., Kikinis, R., . . . Shenton, M. E. (2007). A review of diffusion tensor imaging studies in schizophrenia. *Journal of psychiatric research*, *41*(1-2), 15-30. doi:10.1016/j.jpsychires.2005.05.005

Kühn, S., & Gallinat, J. (2012). Quantitative Meta-Analysis on State and Trait Aspects of Auditory Verbal Hallucinations in Schizophrenia. *Schizophrenia Bulletin*, *38*(4), 779-786. doi:10.1093/schbul/sbq152

Le, H.-B., Zhang, H.-H., Wu, Q.-L., Zhang, J., Yin, J.-J., & Ma, S.-H. (2018). Neural activity during mental rotation in deaf signers: The influence of long-term sign language experience. *Ear and hearing*, *39*(5), 1015-1024.

Lee, M. H., Smyser, C. D., & Shimony, J. S. (2013). Resting-state fMRI: a review of methods and clinical applications. *American Journal of neuroradiology*, *34*(10), 1866-1872.

Leroux, E., Delcroix, N., & Dollfus, S. (2017). Abnormalities of language pathways in schizophrenia patients with and without a lifetime history of auditory verbal hallucinations: A DTI-based tractography study. *The World Journal of Biological Psychiatry, 18*(7), 528-538.

Lubrini, G., Martín-Montes, A., Díez-Ascaso, O., & Díez-Tejedor, E. (2018). Brain disease, connectivity, plasticity and cognitive therapy: A neurological view of mental disorders. *Neurología (English Edition), 33*(3), 187-191.
doi:<https://doi.org/10.1016/j.nrleng.2017.02.001>

Lustig, C., Snyder, A. Z., Bhakta, M., O'Brien, K. C., McAvoy, M., Raichle, M. E., . . . Buckner, R. L. (2003). Functional deactivations: change with age and dementia of the Alzheimer type. *Proceedings of the National Academy of Sciences, 100*(24), 14504-14509.

Madhavan, K. M., McQueeney, T., Howe, S. R., Shear, P., & Szaflarski, J. (2014). Superior longitudinal fasciculus and language functioning in healthy aging. *Brain Research, 1562*, 11-22.

Mandonnet, E., Sarubbo, S., & Petit, L. (2018). The Nomenclature of Human White Matter Association Pathways: Proposal for a Systematic Taxonomic Anatomical Classification. *Frontiers in Neuroanatomy, 12*. doi:10.3389/fnana.2018.00094

Manning, K. J., & Steffens, D. C. (2016). Chapter 11 - Systems Neuroscience in Late-Life Depression. In T. Frodl (Ed.), *Systems Neuroscience in Depression* (pp. 325-340). San Diego: Academic Press.

Manoliu, A., Riedl, V., Doll, A., Bäuml, J. G., Mühlau, M., Schwerthöffer, D., . . . Bäuml, J. (2013). Insular dysfunction reflects altered between-network connectivity and severity of negative symptoms in schizophrenia during psychotic remission. *Frontiers in Human Neuroscience, 7*, 216.

Manoliu, A., Riedl, V., Zherdin, A., Mühlau, M., Schwerthöffer, D., Scherr, M., . . . Sorg, C. (2014). Aberrant Dependence of Default Mode/Central Executive Network Interactions on Anterior Insular Salience Network Activity in Schizophrenia. *Schizophrenia Bulletin, 40*(2), 428-437. doi:10.1093/schbul/sbt037

McCarthy-Jones, S., Oestreich, L. K. L., & Whitford, T. J. (2015). Reduced integrity of the left arcuate fasciculus is specifically associated with auditory verbal hallucinations in schizophrenia. *Schizophrenia research, 162*(1), 1-6.
doi:10.1016/j.schres.2014.12.041

McCarthy-Jones, S., Smailes, D., Corvin, A., Gill, M., Morris, D. W., Dinan, T. G., . . . Donohoe, G. (2017). Occurrence and co-occurrence of hallucinations by modality in schizophrenia-spectrum disorders. *Psychiatry Research, 252*, 154-160.

Menon, V. (2011). Large-scale brain networks and psychopathology: a unifying triple network model. *Trends in Cognitive Sciences*, 15(10), 483-506.
doi:<https://doi.org/10.1016/j.tics.2011.08.003>

Moran, J. M., Kelley, W. M., & Heatherton, T. F. (2013). What can the organization of the brain's default mode network tell us about self-knowledge? *Frontiers in Human Neuroscience*, 7, 391.

Mori, S., & Zhang, J. (2006). Principles of diffusion tensor imaging and its applications to basic neuroscience research. *Neuron*, 51(5), 527-539.

Narr, K. L., & Leaver, A. M. (2015). Connectome and schizophrenia. *Current Opinion in Psychiatry*, 28(3).

Nayani, T. H., & David, A. S. (1996). The auditory hallucination: a phenomenological survey. *Psychological Medicine*, 26(1), 177-189.

Nichols, T. E., & Holmes, A. P. (2002). Nonparametric permutation tests for functional neuroimaging: a primer with examples. *Human brain mapping*, 15(1), 1-25.

O'Donnell, L. J., & Pasternak, O. (2015). Does diffusion MRI tell us anything about the white matter? An overview of methods and pitfalls. *Schizophrenia research*, 161(1), 133-141.

Oestreich, L. K., McCarthy-Jones, S., & Whitford, T. J. (2016). Decreased integrity of the fronto-temporal fibers of the left inferior occipito-frontal fasciculus associated with auditory verbal hallucinations in schizophrenia. *Brain Imaging and Behavior*, 10(2), 445-454.

Ogawa, S., Tank, D. W., Menon, R., Ellermann, J. M., Kim, S. G., Merkle, H., & Ugurbil, K. (1992). Intrinsic signal changes accompanying sensory stimulation: functional brain mapping with magnetic resonance imaging. *Proceedings of the National Academy of Sciences*, 89(13), 5951-5955.

Panksepp, J. (2004). *Affective neuroscience: The foundations of human and animal emotions*: Oxford university press.

Panksepp, J. (2005). Affective consciousness: Core emotional feelings in animals and humans. *Consciousness and Cognition*, 14(1), 30-80.
doi:<https://doi.org/10.1016/j.concog.2004.10.004>

-
- Pop, M., & Stefu, N. (2020). Diffusion Magnetic Resonance Imaging with Applications to Cardiac Muscle: Short Review. *Annals of the West University of Timisoara. Physics Series*, 62, 108-119.
- Power, J. D., Barnes, K. A., Snyder, A. Z., Schlaggar, B. L., & Petersen, S. E. (2012). Spurious but systematic correlations in functional connectivity MRI networks arise from subject motion. *Neuroimage*, 59(3), 2142-2154.
- Power, J. D., Mitra, A., Laumann, T. O., Snyder, A. Z., Schlaggar, B. L., & Petersen, S. E. (2014). Methods to detect, characterize, and remove motion artifact in resting state fMRI. *Neuroimage*, 84, 320-341.
- Pyka, M., Beckmann, C. F., Schöning, S., Hauke, S., Heider, D., Kugel, H., . . . Konrad, C. (2009). Impact of working memory load on FMRI resting state pattern in subsequent resting phases. *PLoS One*, 4(9), e7198.
- Raichle, M. E. (2009). A paradigm shift in functional brain imaging. *Journal of Neuroscience*, 29(41), 12729-12734.
- Raichle, M. E., MacLeod, A. M., Snyder, A. Z., Powers, W. J., Gusnard, D. A., & Shulman, G. L. (2001). A default mode of brain function. *Proceedings of the National Academy of Sciences*, 98(2), 676-682.
- Raichle, M. E., & Snyder, A. Z. (2007). A default mode of brain function: a brief history of an evolving idea. *Neuroimage*, 37(4), 1083-1090.
- Rilling, J. K., Glasser, M. F., Preuss, T. M., Ma, X., Zhao, T., Hu, X., & Behrens, T. E. J. (2008). The evolution of the arcuate fasciculus revealed with comparative DTI. *Nature Neuroscience*, 11(4), 426-428. doi:10.1038/nn2072
- Salvador, R., Suckling, J., Coleman, M. R., Pickard, J. D., Menon, D., & Bullmore, E. (2005). Neurophysiological Architecture of Functional Magnetic Resonance Images of Human Brain. *Cerebral Cortex*, 15(9), 1332-1342. doi:10.1093/cercor/bhi016
- Sandrone, S., & Catani, M. (2013). Journal Club: Default-mode network connectivity in cognitively unimpaired patients with Parkinson disease. *Neurology*, 81(23), e172-e175.
- Seok, J.-H., Park, H.-J., Chun, J.-W., Lee, S.-K., Cho, H. S., Kwon, J. S., & Kim, J.-J. (2007). White matter abnormalities associated with auditory hallucinations in schizophrenia: a combined study of voxel-based analyses of diffusion tensor imaging and structural magnetic resonance imaging. *Psychiatry Research: Neuroimaging*, 156(2), 93-104.

Shepard, R. N., & Metzler, J. (1971). Mental rotation of three-dimensional objects. *Science, 171*(3972), 701-703.

Shinn, A. K., Pfaff, D., Young, S., Lewandowski, K. E., Cohen, B. M., & Öngür, D. (2012). Auditory hallucinations in a cross-diagnostic sample of psychotic disorder patients: a descriptive, cross-sectional study. *Comprehensive Psychiatry, 53*(6), 718-726.

Shulman, G. L., Fiez, J. A., Corbetta, M., Buckner, R. L., Miezin, F. M., & Raichle, M. E. others. 1997. Common blood flow changes across visual tasks: II. Decreases in cerebral cortex. *J Cogn Neurosci, 9*, 648-663.

Shulman, G. L., Fiez, J. A., Corbetta, M., Buckner, R. L., Miezin, F. M., & Raichle, M. E. (1997.). Common blood flow changes across visual tasks: II. Decreases in cerebral cortex. *J Cogn Neurosci, 9*, 648-663.

Smith, S. M., Jenkinson, M., Johansen-Berg, H., Rueckert, D., Nichols, T. E., Mackay, C. E., . . . Matthews, P. M. (2006). Tract-based spatial statistics: voxelwise analysis of multi-subject diffusion data. *Neuroimage, 31*(4), 1487-1505.

Smith, S. M., Jenkinson, M., Woolrich, M. W., Beckmann, C. F., Behrens, T. E., Johansen-Berg, H., . . . Flitney, D. E. (2004). Advances in functional and structural MR image analysis and implementation as FSL. *Neuroimage, 23*, S208-S219.

Spreng, R. N., Mar, R. A., & Kim, A. S. (2009). The common neural basis of autobiographical memory, prospection, navigation, theory of mind, and the default mode: a quantitative meta-analysis. *Journal of cognitive Neuroscience, 21*(3), 489-510.

Sridharan, D., Levitin, D. J., & Menon, V. (2008). A critical role for the right fronto-insular cortex in switching between central-executive and default-mode networks. *Proceedings of the National Academy of Sciences, 105*(34), 12569-12574.

Stark, C. E. L., & Squire, L. R. (2001). When zero is not zero: The problem of ambiguous baseline conditions in fMRI. *Proceedings of the National Academy of Sciences, 98*(22), 12760-12766. doi:10.1073/pnas.221462998

Stocco, A. (2014). Coordinate-Based Meta-Analysis of fMRI Studies with R. *R Journal, 6*(2).

Sturm, W., Simone, A. d., Krause, B. J., Specht, K., Hesselmann, V., Radermacher, I., . . . Willmes, K. (1999). Functional anatomy of intrinsic alertness: evidence for a fronto-parietal-thalamic-brainstem network in the right hemisphere.

Neuropsychologia, 37(7), 797-805. doi:[https://doi.org/10.1016/S0028-3932\(98\)00141-9](https://doi.org/10.1016/S0028-3932(98)00141-9)

Sun, L., Peräkylä, J., Polvivaara, M., Öhman, J., Peltola, J., Lehtimäki, K., . . . Hartikainen, K. M. (2015). Human anterior thalamic nuclei are involved in emotion-attention interaction. *Neuropsychologia*, 78, 88-94.
doi:<https://doi.org/10.1016/j.neuropsychologia.2015.10.001>

Tagaris, G. A., Kim, S.-G., Strupp, J. P., Andersen, P., Uğurbil, K., & Georgopoulos, A. P. (1997). Mental rotation studied by functional magnetic resonance imaging at high field (4 Tesla): Performance and cortical activation. *Journal of cognitive Neuroscience*, 9(4), 419-432.

Turnbull, A., Wang, H., Murphy, C., Ho, N., Wang, X., Sormaz, M., . . . Margulies, D. (2019). Left dorsolateral prefrontal cortex supports context-dependent prioritisation of off-task thought. *Nature communications*, 10(1), 1-10.

Uddin, L. Q. (2017). Chapter 3 - Functions of the Salience Network. In L. Q. Uddin (Ed.), *Salience Network of the Human Brain* (pp. 11-16). San Diego: Academic Press.

Van Horn, J. D., & Poldrack, R. A. (2009). Functional MRI at the crossroads. *International Journal of Psychophysiology*, 73(1), 3-9.

van Oort, J., Tendolkar, I., Hermans, E. J., Mulders, P. C., Beckmann, C. F., Schene, A. H., . . . van Eijndhoven, P. F. (2017). How the brain connects in response to acute stress: A review at the human brain systems level. *Neuroscience & Biobehavioral Reviews*, 83, 281-297. doi:<https://doi.org/10.1016/j.neubiorev.2017.10.015>

Weber, S., Aleman, A., & Hugdahl, K. (2021). Challenging the notion of a task-negative network: default mode network involvement under varying levels of cognitive effort. *bioRxiv*.

Weber, S., Hjelmervik, H., Craven, A. R., Johnsen, E., Kroken, R. A., Løberg, E.-M., . . . Hugdahl, K. (2021). Glutamate-and GABA-modulated connectivity in auditory hallucinations—A combined resting state fMRI and MR spectroscopy study. *Frontiers in Psychiatry*, 12, 135.

Weber, S., Johnsen, E., Kroken, R. A., Løberg, E.-M., Kandilarova, S., Stoyanov, D., . . . Hugdahl, K. (2020). Dynamic functional connectivity patterns in schizophrenia and the relationship with hallucinations. *Frontiers in Psychiatry*, 11, 227.


Winkler, A. M., Ridgway, G. R., Webster, M. A., Smith, S. M., & Nichols, T. E. (2014). Permutation inference for the general linear model. *Neuroimage*, 92, 381-397.

Wycoco, V., Shroff, M., Sudhakar, S., & Lee, W. (2013). White matter anatomy: what the radiologist needs to know. *Neuroimaging Clinics*, 23(2), 197-216.

Zhang, X., Gao, J., Zhu, F., Wang, W., Fan, Y., Ma, Q., . . . Yang, J. (2018). Reduced white matter connectivity associated with auditory verbal hallucinations in first-episode and chronic schizophrenia: A diffusion tensor imaging study. *Psychiatry research. Neuroimaging*, 273, 63-70.

Article

White Matter Microstructural Differences between Hallucinating and Non-Hallucinating Schizophrenia Spectrum Patients

Justyna Beresiewicz^{1,2,3,*}, Alexander R. Craven^{1,2,4} , Kenneth Hugdahl^{1,5,6}, Else-Marie Løberg^{2,5,8,9}, Rune Andreas Kroken^{2,5,7}, Erik Johnsen^{2,5,7} and Renate Grüner^{3,6,10}

¹ Department of Biological and Medical Psychology, University of Bergen, 5009 Bergen, Norway; Alex.Craven@uib.no (A.R.C.); hugdahl@uib.no (K.H.)

² NORMENT Center of Excellence, Haukeland University Hospital, 5021 Bergen, Norway; else-marie.loberg@helse-bergen.no (E.-M.L.); rune.andreas.kroken@helse-bergen.no (R.A.K.); erik.johnsen@helse-bergen.no (E.J.)

³ Mohn Medical Imaging and Visualization Center, Haukeland University Hospital, 5021 Bergen, Norway; rena.te.gruner@uib.no

⁴ Department of Clinical Engineering, Haukeland University Hospital, 5021 Bergen, Norway

⁵ Division of Psychiatry, Haukeland University Hospital, 5021 Bergen, Norway

⁶ Department of Radiology, Haukeland University Hospital, 5021 Bergen, Norway

⁷ Department of Clinical Medicine, University of Bergen, 5009 Bergen, Norway

⁸ Department of Addiction Medicine, Haukeland University Hospital, 5021 Bergen, Norway

⁹ Department of Clinical Psychology, University of Bergen, 5009 Bergen, Norway

¹⁰ Department of Physics and Technology, University of Bergen, 5009 Bergen, Norway

* Correspondence: justyna.beresiewicz@uib.no



check for updates

Citation: Beresiewicz, J.; Craven, A.R.; Hugdahl, K.; Løberg, E.-M.; Kroken, R.A.; Johnsen, E.; Grüner, R. White Matter Microstructural Differences between Hallucinating and Non-Hallucinating Schizophrenia Spectrum Patients. *Diagnostics* **2021**, *11*, 139. <https://doi.org/10.3390/diagnostics11010139>

Received: 11 December 2020

Accepted: 15 January 2021

Published: 19 January 2021

Publisher's Note: MDPI stays neutral with regard to jurisdictional claims in published maps and institutional affiliations.



Copyright: © 2021 by the authors. Licensee MDPI, Basel, Switzerland. This article is an open access article distributed under the terms and conditions of the Creative Commons Attribution (CC BY) license (<https://creativecommons.org/licenses/by/4.0/>).

Abstract: The relation between auditory verbal hallucinations (AVH) and white matter has been studied, but results are still inconsistent. This inconsistency may be related to having only a single time-point of AVH assessment in many studies, not capturing that AVH severity fluctuates over time. In the current study, AVH fluctuations were captured by utilizing a longitudinal design and using repeated (Positive and Negative Symptoms Scale) PANSS questionnaire interviews over a 12 month period. We used a Magnetic Resonance Diffusion Tensor Imaging (MR DTI) sequence and tract-based spatial statistics (TBSS) to explore white matter differences between two subtypes of schizophrenia patients; 44 hallucinating (AVH+) and 13 non-hallucinating (AVH-), compared to 13 AVH- matched controls and 44 AVH+ matched controls. Additionally, we tested for hemispheric fractional anisotropy (FA) asymmetry between the groups. Significant widespread FA-value reduction was found in the AVH+ group in comparison to the AVH- group. Although not significant, the extracted FA-values for the control group were in between the two patient groups, for all clusters. We also found a significant difference in FA-asymmetry between the AVH+ and AVH- groups in two clusters, with significantly higher leftward asymmetry in the AVH- group. The current findings suggest a possible qualitative difference in white matter integrity between AVH+ and AVH- patients. Strengths and limitations of the study are discussed.

Keywords: schizophrenia; hallucinations; diffusion tensor imaging; DTI; tract-based spatial statistics; fractional anisotropy; white matter integrity

1. Introduction

Schizophrenia is a mental disorder that may lead to severe impairments of quality of life and of occupational and social functioning [1,2], and hallucinations, contributing strongly to perceived distress [3,4]. A majority of patients with schizophrenia experience auditory verbal hallucinations (AVH) [5]. The neural underpinnings of the symptoms the patient experiences have been extensively investigated, yet remain unclear. It has been suggested that AVH may involve alterations in structural and functional connectivity of

frontal and temporoparietal language-related brain areas [6–8] as well as altered internode connectivity within large-scale networks such as the default mode network (DMN) [9,10].

By using diffusion tensor imaging (DTI) to explore microstructural changes *in vivo*, a substantial number of studies have reported on a correlation between white matter integrity and schizophrenia [11–16]. However, the association between AVH, as a key symptom in schizophrenia, and white matter integrity is still not fully understood, and findings are often contradictory. Seok, Park [17] found significant reduction of fractional anisotropy (FA) values when comparing hallucinating (AVH+) and non-hallucinating (AVH-) patients, in the rostral part of the cingulum bundle, the anterior part of the superior longitudinal fasciculus, and the middle cerebellar peduncle, and additionally higher FA-values in the left superior longitudinal fasciculus. In contrast, Ćurčić-Blake, Nanetti [18] found decreased FA-values in the left inferior frontal-occipital fasciculus, uncinate fasciculus, arcuate fasciculus, corpus callosum, cingulate, corticospinal tract, and anterior thalamic radiation in hallucinating patients. Shergill, Kanaan [19], using a voxel-wise approach, showed reduced FA-values in schizophrenia patients vs. healthy controls in several white matter areas, including the right frontal and temporal-parietal portions of the superior longitudinal fasciculus, and the genu of the corpus callosum, as well as in inferior longitudinal fasciculus and tapetum. These authors also found that an increased tendency to hallucinate was related to increased FA-values in the lateral aspects of the superior longitudinal fasciculus and the anterior cingulum.

Several factors could explain the lack of convergence in the current literature. One source of variance is the fluctuating nature of AVH (“state” vs. “trait”) [20,21]. Medication treatment may reduce overt signs of AVH in many patients, such that a “state” assessment could indicate a patient as non-hallucinating, even though he/she has experienced severe and frequent AVHs during earlier periods of the illness, which would be characteristic of a “trait”. Many studies have divided their patients into hallucinating (AVH+) and non-hallucinating (AVH-) sub-groups based on a single assessment (e.g., Seok, Park [17], Psomiades, Fonteneau [22]). As AVHs may have a fluctuating course as a response to treatment [23,24], such approaches may misclassify patients in remission with patients who have never experienced hallucinations. To correctly classify patients as non-hallucinating, multiple assessments over an extended observation-period would therefore be required. In the current study, evaluation of whether a patient would be classified as AVH+ or AVH- was made throughout a 12 month period, using the P3 (third positive item in the scale measuring hallucinatory behavior) item of the Positive and Negative Syndrome Scale (PANSS) [25].

A second issue to be investigated was hemispheric asymmetry and lateralization of white matter tracts. Many studies have shown that schizophrenia patients have altered hemispheric lateralization in comparison to healthy controls. This has been observed in many forms such as handedness [26], grey matter volume [27–29], white matter, and functional connectivity [30,31]. Many studies based on DTI have reported reduced left-right asymmetry in schizophrenia patients in white matter tracts related to language processing, e.g., in the arcuate fasciculus [15,32,33], but also bilateral reduction of white matter integrity has been reported [11,18]. However, most of the studies on white matter integrity have not compared values of FA between the left and right hemispheric (e.g., Ćurčić-Blake, Nanetti [18]), have only reported on data from one hemisphere (e.g., Leroux, Delcroix [15], McCarthy-Jones, Oestreich [32]), or limited the analysis to particular fiber tracts (e.g., De Weijer, Mandl [11], Falkenberg, Westerhausen [33]). The current study investigates possible hemispheric asymmetry between groups.

DTI analysis were based on the tract-based spatial statistics (TBSS) approach, which allows for data-driven and bottom-up analysis of white matter structures of the whole brain. The advantage of such an approach is to be able to include the whole brain volume in the analysis, not restricting the analysis to a priori hypothesized structures.

2. Materials and Methods

2.1. Participants

A total of 57 schizophrenia patients were recruited via The Bergen Psychosis Project 2, and compared to 57 healthy controls. The patient and control groups were then subdivided into 44 AVH+ patients and 44 matched healthy controls, and 13 AVH- patients and 13 matched healthy controls, see Table 1 for demographics. Patients were classified as non-hallucinating (AVH-) if they scored lower than “3” on the P3 item on all available assessments for each patient, and patients were classified as hallucinating (AVH+) if they scored “3” or higher at least one out of all available assessments for each patient. For visualization purposes, the two control groups are shown as a single sample of 57 participants in Figures 1 and 2.

Table 1. Demographic and clinical information for the three groups (hallucinating patients (AVH+), non-hallucinating patients (AVH-), and healthy controls, (Cntrl)).

	AVH+	AVH-	Cntrl	<i>p</i> (Value)
Sample size (female/male)	44 (12/32)	13 (2/11)	57 (15/42)	0.72 Fisher’s Exact test
Age (mean ± SD) ^a	30.1 ± 11.4	29.5 ± 9.3	30.7 ± 9.9	0.92 ANOVA
Handedness (A/L/R) ^b	2/4/38	1/1/11	0/6/51	0.35 Fisher’s Exact test
Scanning after/before the upgrade	21/23	5/8	25/32	0.86 Fisher’s Exact test
Duration of illness	3.6 ± 4.7	2.2 ± 4.4	-	0.40 Welch Two Sample <i>t</i> -test
Defined Daily Dose (DDD)	1.02 ± 0.63	0.91 ± 0.41	-	0.51 Welch Two Sample <i>t</i> -test
Smoking/non-smoking	28/16	10/3	-	0.51 Fisher’s Exact test
Baseline PANSS ^c positive	3.0 ± 0.7	2.6 ± 0.7	-	0.04 Welch Two Sample <i>t</i> -test
Baseline PANSS negative	2.4 ± 0.8	2.0 ± 0.7	-	0.99 Welch Two Sample <i>t</i> -test
Baseline PANSS total	2.7 ± 0.6	2.3 ± 0.6	-	0.03 Welch Two Sample <i>t</i> -test

^a SD—Standard deviation, ^b A—Ambidextrous, L—Left handed, R—Right handed, ^c PANSS—Positive and Negative Syndrome Scale.

The study was approved by the Regional Committee for Medical and Health Research Ethics in Western Norway (REK-VEST, #2010/3387-6). Included patients were 18 years or older with symptoms of psychosis in the schizophrenia spectrum, or with paranoid psychosis according to the International Classification of Diseases ICD-10 diagnostic manual (F20–F29: Schizophrenia, schizotypal, and delusional disorders). All patients were on second-generation antipsychotic medication with average defined daily dose DDD = 0.99 ± 0.58.

Patients underwent psychiatric evaluations at eight time-points during a 12 month period (visit 1—baseline, visit 2—week 1, visit 3—week 3, visit 4—week 6, visit 5—month 3, visit 6—month 6, visit 7—month 9, visit 8—month 12). Due to subject attrition, not all patients were evaluated at all eight time-points, with a median of six assessments. Evaluation over a longer period gave us an overview of the fluctuating character of AVHs for a given patient. The division of the patients into subgroups (AVH+ and AVH-) was based on PANSS P3 scores from all available time-points for each patient. The AVH+ subgroup consisted of 44 hallucinating patients, with a PANSS P3 score of “3” or higher on at least one assessment over the 12 months period. The average PANSS P3 over all visits for the AVH+ group was equal to 3.02 ± 1.66. The AVH- subgroup consisted of 13 non-hallucinating patients (AVH-) with a PANSS P3 score lower than “3” on all available

assessments over the 12 months. The average PANSS P3 for AVH- group was equal to 1.13 ± 0.33 .

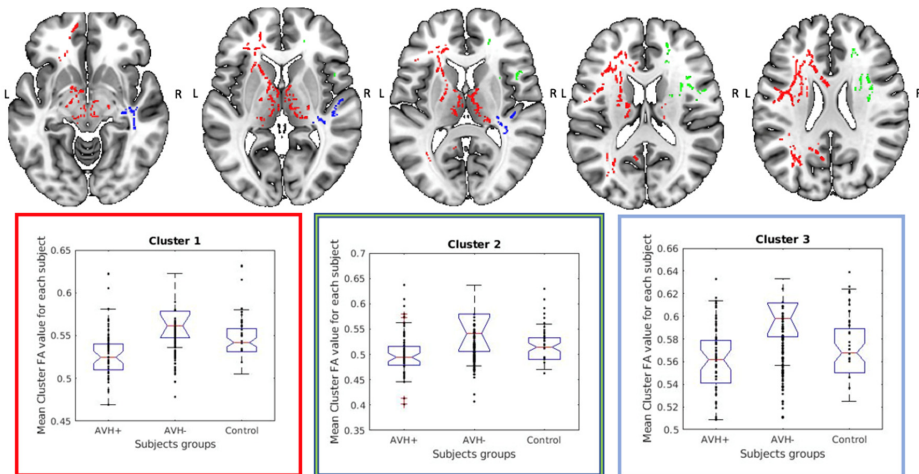


Figure 1. Upper row shows the localization and distribution for the three largest significant clusters, (cluster 1 marked in red, cluster 2 marked in green, and cluster 3 marked in blue) obtained from the comparison between the AVH+ and AVH- groups. The box plot graphs in the lower row shows the corresponding mean clusters Fractional Anisotropy (FA) values for each participant in each group (AVH+, AVH-, Control). The color of the graph frame matches the color of the cluster it belongs to. The central mark indicates the median, and the top and bottom edges of the box represent the 25th and 75th percentiles, respectively. The whiskers extend to the most extreme data points not considered outliers, while the outliers are plotted individually and marked with a plus symbol. Data were merged for the two control groups and presented as a single control group for facilitation of comparison with the patient groups.

Although the strict selection threshold for AVH- participants resulted in a small sample size, the selection assured that participants were not prone to AVHs, giving us a possibility of comparing hallucinating-prone with non-hallucinating-prone patients. We assumed that patients who experienced AVHs just once and in a mild form, nevertheless had higher chances to have experienced AVHs in the assessment period compared to patients who over the course of 12 months were not experiencing AVHs at all. Here, it is important to mention that although PANSS P3 assesses for hallucinations in a spectrum of modalities (e.g., visual, tactile, olfactory), we used it as a proxy for AVH severity since it has been shown that the auditory modality also dominates in situations with other modalities [34–36]. The value of “3” on the PANSS P3 item was chosen as a threshold since, although this indicates “mild” symptom load, such a score is nevertheless indicative of clearly formed hallucinations [25], and is typically used as a cut-off criterion in other studies (e.g., Weber, Johnsen [8]). PANSS ratings were made by certified clinicians/raters, and the number of raters were kept to a minimum, to reduce inter-rater variability. Healthy control participants were recruited from community samples via advertisement in social media and from flyers. The broad announcement was used to obtain a broad representation from the community, i.e., reflecting a randomness that is also believed to be the case for the recruited patients. Among those responding to the advertisements, control participants were continuously blindly selected to best match the recruited patients age, sex, and handedness. The enrollment of control participants was done prior to scanning and was fixed for all the analysis processes and for evaluation of results. No control participants were excluded after scanning. As part of the analysis, the selected control group was further subdivided into two sub-groups: one matched to the AVH+ patients (44 subjects) and one matched to the AVH- patients (13 subjects). Prior to enrollment, the control participants were asked to self-report any history of mental disorder using an in-house questionnaire. A full PANSS evaluation was

not performed for these participants as there was no reason to believe that they would provide erroneous answers in the self-reporting on history of mental disorders. Exclusion criteria for the Magnetic Resonance (MR) scanning were history of mental disorders, pregnancy, or standard contraindications to Magnetic Resonance Imaging (MRI), such as any ferromagnetic artefacts in the body. Participants were instructed according to current local hospital practice for all neuroimaging research scanning, i.e., abstain from drinking coffee two hours prior to scanning, to minimize potential confounders. Control participants and patients were included randomly to minimize possible changes in the technical performance of the MR systems. Neither patients nor controls were screened for drugs in urine, although use of medication was registered for both groups.

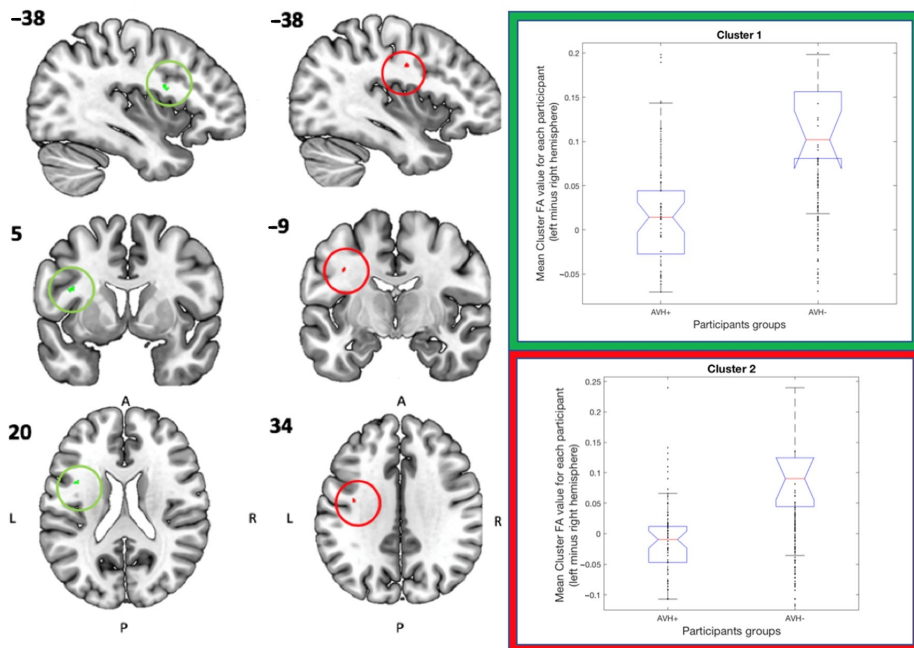


Figure 2. The localization of significant Cluster 1 is marked in green and localization of Cluster 2 is marked in red, see Table 3 for further details regarding localization and size of the two clusters. The box plot graphs represent the corresponding mean asymmetry FA-values (left minus right hemisphere, see Y-axis) for each participant in each group. The color of the graph frame matches the colors of the cluster it belongs to. The central mark indicates the median, and the top and bottom edges of the box represents 25th and 75th percentiles, respectively. The whiskers extend to the most extreme data points not considered outliers and the outliers are plotted individually and marked with a plus symbol.

2.2. Image Acquisition

Participants were scanned using a whole-body 3T GE Medical Systems Signa HDx MR scanner at the Department of Radiology, Haukeland University Hospital, Bergen, Norway. The scanner was upgraded to a Discovery MR750 in the middle of the data acquisition period, and a covariate accounting for the scanner version was therefore included in the statistical analysis. As seen in Table 1, there were no significant effects of the scanning upgrade. Imaging data for the matched controls were acquired on the same scanner version as was used for the corresponding patient groups. Head motion was restricted by using foam padding inside the head coil. Diffusion data were acquired with 30 diffusion encoding gradients, b-value 1000 s/mm², and six sets of diffusion unweighted images,

phase encoding direction anterior-posterior, FoV 220 mm, TR 14000 ms, TE 84.4 ms, flip angle 90° matrix size 128 × 128 mm, slice thickness 2.4 mm, and total scan time 8.4 min.

2.3. Image Processing

The processing pipeline for the DTI-data was performed with FMRIB Software Library (FSL) software package (version 5.0; FMRIB Software Library and the corresponding Diffusion Toolbox). Data were examined visually at all pre-processing steps to identify artifacts as well as to ensure proper data quality. First, a binary brain-mask was created for each subject by using the FSL Brain Extraction Tool (BET) [37]. Second, original data were corrected for head-movements and eddy currents using FSL eddy function with outlier replacement and slice-to-volume outlier correction. We used the eddy function *mporder* to correct for slice-to-volume movements, and the function *repol* to remove any slices judged as outliers and replaced them with predictions made by the Gaussian process. FA-maps were then calculated by using the DTIFit tool, which fits the diffusion tensor model at each voxel. After calculation of the FA-images, voxel-wise statistical analysis of the FA-data was carried out using the TBSS component of FSL [38,39]. This involved alignment of all FA-images onto a common space, using the standard Montreal Neurological Institute (MNI) space atlas, and then subsequently resampling to 1 × 1 × 1 mm³ spatial resolution. Thereafter, a mean FA-image was created and further thinned, resulting in a mean FA-skeleton. The skeletonized mean FA-image was thresholded at 0.3 to suppress areas of low mean FA-values, and low and/or high subject-variability. In a next step, the aligned FA-data for all subjects were projected onto the mean FA-skeleton by filling the skeleton with FA-values from the nearest relevant tract center. This resulted in a four-dimensional (4D) image-file which contained the projected, skeletonized FA-data, and which was then entered into statistical analyses. An example of the FA-skeletons is shown in Supplementary Materials Figure S1. For performing hemispheric asymmetry analysis between patients and controls, symmetric mean FA-skeleton images were created. In the analysis, the images were flipped and subtracted from each other to create “left minus right” images using the *tbss sym* function. A detailed description of the *tbss_sym* function is provided in the TBSS manual [40].

2.4. Statistical Analysis

In a first statistical analysis, we tested whether voxel-wise FA-values between patient subgroups and their matched control groups were significantly different from each other, with two-sided *t*-tests using the original FA-skeleton. Secondly, significant group-differences in the FA-values between the left- and right hemisphere skeleton were similarly examined, using images from the left-minus-right subtracted symmetrical skeletons. For the first statistical analysis, we performed four group comparisons: (a) comparison between AVH+ and AVH- patients; (b) comparison between AVH+ patients and their matched controls; (c) comparison between AVH- patients and their matched controls, (d) comparison between the two control groups while correcting for sex, age, handedness, and scanner version covariates. The comparison between two control groups was performed to ensure that observed FA-differences between the patient groups were not driven by the differences in sample sizes or influence of covariates of no interest. For the second statistical analysis (FA hemispheric asymmetry analysis), we performed three group-comparisons: (a) comparison between AVH+ and AVH- patients; (b) comparison between AVH+ patients and their matched controls; (c) comparison between AVH- patients and their matched controls, while correcting for sex, age, handedness, and scanner version covariates. Statistical analyses were performed using the permutation interface for general linear model (PALM) [41], which is a tool allowing for inference by using permutation testing. Permutation testing was chosen as it does not impose any assumptions on the distribution of the dependent variables and accounts for possible non-normality of FA-values [42]. All analyses were performed using 10,000 random permutations with threshold-free cluster enhancement (TFCE) [43] with correction of multiple comparisons to a familywise error

(FWE) corrected significance level of $p < 0.05$ per analysis. The resulting statistical maps with regions showing significant differences between compared groups and hemispheres were further used for anatomical localization and visualization of the results using the John Hopkins University (JHU) white matter tractography atlas supplied by FSL. A mask of significant regions was created from the images containing p-values, using a cut-off threshold of $p < 0.05$. These clusters served as a mask for the *autoaq* tool supplied by FSL for identification of corresponding anatomical atlas regions. From the significant clusters, the individual FA-values were extracted to illustrate group differences.

3. Results

3.1. Group Comparison of the Original FA-Skeletons

The comparison of the FA-values between AVH+ patients and their matching healthy controls did not show any significant differences. Similarly, comparison between AVH-patients and their matching healthy controls did not show any significant differences. The additional comparison between two groups of matching controls did not show any significant differences (this was just done to assure that these sub-groups did not differ). However, the comparison between AVH+ and AVH- patients showed widespread and significant reduction in FA-values in the AVH+ subgroup in a number of regions, including bilateral anterior thalamic radiation, bilateral corticospinal tract, bilateral inferior fronto-occipital fasciculus, bilateral superior longitudinal fasciculus, and the temporal part of the right inferior longitudinal fasciculus, forceps minor, and the cingulum bundle. For an overview, see Table 2.

Table 2. Localization and size of significantly different clusters between AVH+ and AVH- participants. The numbers after each tract label indicates the percentage probability of the cluster to belong to the given (John Hopkins University) JHU white matter tractography atlas label.

Number of Voxels	X (mm) ^a	Y (mm)	Z (mm)	Major Tracts Included in a Cluster ^b
13231	−36	−1	28	Anterior thalamic radiation L ^c : 5.9 Anterior thalamic radiation R: 2.7 Corticospinal tract L: 1.8 Corticospinal tract R: 1.0 Forceps minor: 2.0 Inferior fronto-occipital fasciculus L: 1.4 Superior longitudinal fasciculus L: 2.2 Anterior thalamic radiation R: 1.2
1752	32	7	28	Forceps minor: 3.8 Superior longitudinal fasciculus R: 6.4 Superior longitudinal fasciculus (temporal part) R: 2.4
948	45	−22	5	Inferior fronto-occipital fasciculus R: 14.4 Inferior longitudinal fasciculus R: 9.8
530	34	−59	29	Superior longitudinal fasciculus R: 7.5 Superior longitudinal fasciculus (temporal part) R: 1.3
295	17	−52	25	Cingulum (cingulate gyrus) R: 1.3
275	12	4	−7	Anterior thalamic radiation R: 14.8
89	49	−4	−12	Inferior longitudinal fasciculus R: 6.8
53	31	−32	37	Superior longitudinal fasciculus R: 16.3 Inferior fronto-occipital fasciculus R: 5.0
46	24	−54	24	Inferior longitudinal fasciculus R: 1.7 Superior longitudinal fasciculus R: 1.3
38	34	−11	−5	Inferior fronto-occipital fasciculus R: 3 9.4 Inferior longitudinal fasciculus R: 1.2

Table 2. Cont.

Number of Voxels	X (mm) ^a	Y (mm)	Z (mm)	Major Tracts Included in a Cluster ^b
30	36	−4	−5	Inferior fronto-occipital fasciculus R: 8.7 Superior longitudinal fasciculus R: 3.8 Superior longitudinal fasciculus (temporal part) R: 2.3 Anterior thalamic radiation R: 1.9
25	23	−50	32	Inferior fronto-occipital fasciculus R: 2.9 Superior longitudinal fasciculus R: 1.6
15	19	−47	35	Cingulum (cingulate gyrus) R: 4.2

^a MNI—Montreal Neurological Institute; ^b values reflect the percentage probability of the cluster to belong to the given atlas label; ^c L—abbreviation for the left hemisphere, R—abbreviation for the right hemisphere.

In a next step, we extracted the FA-values from each of the significant clusters found in the AVH+ vs. AVH- comparison to further examine the spatial extent of the findings and perform quantitative comparisons of FA-values, see Figure 1. For all significant clusters, the extracted FA-values were lowest for the AVH+ group and highest for the AVH- group with the controls falling in between. The box plot graphs showing the mean clusters FA-values for each participant in each group (AVH+, AVH-, Control) for all detected clusters is shown in Supplementary Materials Figure S2.

3.2. Hemispheric Asymmetry Comparisons

Hemispheric asymmetry analysis was performed using symmetric mean FA-skeleton images, but where the images of the right hemisphere were flipped and subtracted from the corresponding left hemisphere to create “left-minus-right” hemisphere images, using the *tbss sym* function. See Table 3 for co-ordinate localization and size, and the left side of Figure 2 for visualization of the same clusters. The FA asymmetry-analysis showed significantly stronger leftward asymmetry in the AVH- patient subgroup in comparison to the AVH+ patient subgroup in two clusters located in the superior longitudinal fasciculus tract, cfr the bar graphs to the right in Figure 2. As in the preceding analysis, FA-values (here hemispheric differences in FA-values) were lowest for the AVH+ group, highest for the AVH- group, and with the control group non-significantly falling in between.

Table 3. Montreal Neurological Institute (MNI) space co-ordinates, number of voxels, and major white matter tracts included in the two significant clusters, labeled Cluster 1 and Cluster 2, respectively. The numbers after each tract label indicates the percentage probability of the cluster to belong to the given JHU white matter tractography atlas label.

Cluster Index	Number of Voxels	X ^a (mm)	Y (mm)	Z (mm)	Major Tracts Included in a Cluster ^b
1	22	−38	5	20	Superior longitudinal fasciculus: 13.2 Superior longitudinal fasciculus (temporal part): 6.9 (marked in green on Figure 2) Superior longitudinal fasciculus: 15.4
2	20	−38	−9	34	Superior longitudinal fasciculus (temporal part): 7.0 (marked in red on Figure 2)

^a MNI—Montreal Neurological Institute; ^b values reflect the percentage probability of the cluster to belong to the given atlas label.

4. Discussion

This study aimed to investigate a possible link between alterations of white matter integrity and auditory verbal hallucinations (AVH). The results showed widespread FA-differences between the AVH+ and AVH- subgroups in several white matter pathways, which have previously been reported to be related to AVH (Bopp, Zöllner [44], Zhang, Gao [45] for examples). In all of the regions with significant findings, we found that patients with AVH had reduced FA-values compared to patients without AVH. In

contrast, the FA-values of the healthy control groups were intermediate, although not significantly different from the AVH subgroups. The comparison between two controls groups did not show any significant differences, when controlling for possible confounders. This supports the validity of our findings by confirming that the observed differences for the AVH+ vs. AVH- comparisons were not driven by the difference in sample size or other covariates of no interest between the patient subgroups. Additionally, a significant difference in hemispheric asymmetry was found between the AVH+ and AVH- subgroups in two small clusters in the superior longitudinal fasciculus.

These results partially agree with the findings in the Ćurčić-Blake, Nanetti [18] study, which showed reduced FA-values in some of the major white matter paths, such as: fronto-temporal, cortico-spinal, cingulum, and anterior thalamus tracts and pathways for patients with AVH, see also Oestreich, McCarthy-Jones [16]. On the other hand, a study by Leroux, Delcroix [15] found significantly decreased FA-values for both AVH+ and AVH- subgroups vs. a single healthy control group, but no difference between the AVH+ and AVH- groups. Additionally, they reported FA-reduction in the left arcuate fasciculus when comparing AVH+ subjects to controls, but not when comparing AVH+ vs. AVH-, or AVH- vs. controls. This is in contrast to our findings with regards to the main intra-hemispheric pathways, in particular the inferior fronto-occipital fasciculus. However, both patient selection and data analysis differed between the studies. The studies by Leroux, Delcroix [15], Oestreich, McCarthy-Jones [16], Seok, Park [17], Ćurčić-Blake, Nanetti [18] also found significant differences when comparing AVH+ and AVH- patients to healthy controls, which is in contrast to our study, which showed that the FA-values for the AVH+ group did not differ significantly from the control subjects, while the comparison of AVH+ vs. AVH- groups showed significant differences. The differences between the studies might be that different methods were used to analyze the data and to define the subject groups. Most importantly, neither Oestreich, McCarthy-Jones [16], nor Ćurčić-Blake, Nanetti [18] used healthy control subjects that were matched to their corresponding AVH+ and AVH- patient sub-groups, relying on a single control group. Other differences that could have influenced the results were that the patient sample in our study was characterized by a relatively low mean sample-age, with high variability across age, and illness duration was relatively short.

Aberrations of white matter pathways connecting frontal and temporal brain areas seem to be a frequent finding in DTI-studies of hallucinations in schizophrenia [15,16,18]. Brain structures such as the inferior fronto-occipital fasciculus and the superior longitudinal fasciculus connect frontal and temporal regions, and have essential roles in not only language and semantic speech processing (see, e.g., Duffau, Gatignol [46], Friederici [47], Glasser and Rilling [48], Rilling, Glasser [49], but also in attention, working memory, and emotions [50,51]. Hugdahl, Løberg [7] hypothesizes that the dynamic interplay between top-down (information processing) and bottom-up (stimulus processing) might be unbalanced in AVHs. Moreover, he suggested that intact and connected prefrontal and temporal areas might be the reason why healthy voice-hearers can resist being overwhelmed by their “voices” in comparison to schizophrenia patients suffering from AVH. Our finding of decreased FA-values in fronto-temporal and fronto-occipital pathways support the model proposed by Hugdahl, Løberg [7] since the aberrations of white matter pathways connecting frontal and temporal lobes might influence information flow from frontal cortex, which in turn might result in failure to inhibit bottom-up temporal lobe hyper-activity. We also observed abnormalities in the anterior thalamic radiation and in the cingulum bundle. Both of these pathways have been shown to play a role in emotion processing [52–55], a modality which is central in AVHs since AVHs typically are negatively charged. One could hypothesize that since we did not find significant differences for PANSS total negative scores between the patient groups, abnormality of these white matter tracts might also influence the emotional content of AVH.

In a study by Miyata, Sasamoto [56], schizophrenia patients exhibited overall reduced asymmetry compared to healthy controls. Following this, the current results with significantly reduced leftward FA asymmetry in the AVH+ group compared to the AVH- group,

could mean that AVHs add to the asymmetry reduction seen in schizophrenia in general. Other studies have shown leftward asymmetry of the planum temporale and auditory cortex at the back of the superior temporal gyrus in healthy populations, which has been linked to left hemispheric functional specialization for language [57,58]. Furthermore, leftward asymmetry of the anterior cingulum and the arcuate fasciculus, the corticospinal tract and the posterior limb of the internal capsule has been reported in studies of white matter hemispheric asymmetries in healthy individuals [59]. Therefore, it may be suggested that reduced leftward asymmetry in our AVH+ patients for major white matter pathways connecting frontal and temporal brain areas may be related to dysfunction of language areas in AVH. It has been previously shown that parts of the frontal superior longitudinal fasciculus, which contain the arcuate fasciculus, also connect to the frontotemporal language association cortex [60]. Several studies suggest that the left arcuate fasciculus, which is the critical pathway of the language network, show reduced FA-values in AVH+ patients [6,17,61,62]. However, none of the previous studies have demonstrated a direct link between hemispheric differences for FA-values, and for difference in asymmetry between AVH+ and AVH- patients, indicating a structural correlate to known behavioral and functional differences between AVH+ and AVH- patients (cf. Falkenberg, Westerhausen [33], Hugdahl, Løberg [63]).

Some limitations of the present study deserve discussion. Firstly, patients underwent treatment with antipsychotic medication throughout the whole duration of the study, which is always a source of confounding. However, we did not see differences between the AVH+ and AVH- groups in DDD values, which would indicate that medication differences may not have been a major source of confounding of the results. A second limitation relates to the use of DTI as a general measure of white matter integrity and functionality. It is important to remember that although FA-values carries information about white matter-state at the cellular level, this information is averaged over large voxel volumes since the MRI resolution is much larger (mm) than the scale of the cells that are probed by diffusing water (μm) size [64]. The presence of, for example, multiple fiber populations with different fiber orientations may also contribute to the average value of the signal. Therefore, while observing decreased FA-values in specific brain regions, it cannot be assumed that this exclusively results from abnormalities at the cellular level. It could as well be due to the reorganization of the fibers on a macroscopic scale. It can also be the combination of changes in tissue myelination, fiber organization, as well as the number of axons [65]. Therefore, the presented results should be interpreted with caution. It should be kept in mind that FA is a general measure of white matter integrity and observed changes can be of the multifactorial origin (e.g., cell death, edema, gliosis, inflammation, change in myelination, increase in connectivity of crossing fibers, increase in extracellular or intracellular water, etc.) [64]. It should also be mentioned that parts of the patient data included in the current study were used in the [33] study as well as [66]. However, the composition of the samples in the studies was different, as well as the hypotheses, methods, and analysis technology used.

5. Conclusions

In conclusion, the most consistent finding was the alteration of hemispheric language pathways in AVH+ patients, which has also been reported in previous studies, although the nature and direction of this relation have often differed [6,15,16,19]. Interestingly, we also found a significant difference between AVH+ vs. AVH- patients, but not for the comparison with the healthy controls. This could be an indication that non-hallucinating schizophrenia patients form a distinct subgroup from the schizophrenia spectrum. This in turn, could mean that differences between AVH+ and AVH- patients should be studied more thoroughly in the future since it might have implications for the choice of treatment options for patients with severe and persistent hallucinations. The present study provides evidence for the importance of translational studies, bridging the gap between neurobiology and psychiatry, especially for major mental illnesses [67].

Supplementary Materials: The following are available online at <https://www.mdpi.com/2075-4418/11/1/139/s1>, Figure S1: mean FA-skeleton masks derived for three comparisons, Figure S2 The box plot graphs showing the mean clusters FA-values for each participant in each group (AVH+, AVH-, Control).

Author Contributions: Conceptualization, J.B., K.H. and R.G.; Data curation, J.B. and A.R.C.; Formal analysis, J.B.; Funding acquisition, K.H., E.J.; Methodology, J.B.; Project administration, K.H., E.J. and R.G.; Resources, K.H.; Supervision, K.H. and R.G.; Visualization, J.B.; Writing—original draft, J.B.; Writing—review & editing, A.R.C., K.H., E.-M.L., R.A.K., E.J. and R.G. All authors have read and agreed to the published version of the manuscript.

Funding: The study was funded by a grant from the Research Council of Norway #213727.to Erik Johnsen. The contribution of Justyna Beresiewicz, Alexander R Craven and Kenneth Hugdahl was funded by an ERC Advanced Grant #693124 to Kenneth Hugdahl.

Institutional Review Board Statement: The study was approved by the Regional Committee for Medical Research Ethics in Western Norway (REK Vest #2010/3876-6, approved 25 February 2011 and #2016/800, approved 22 June 2016, respectively).

Informed Consent Statement: Written informed consent was obtained from all subjects in the study.

Data Availability Statement: The datasets analyzed during the current study are not publicly available. According to Norwegian law, data sharing requires approvals from the Regional Committees for Medical and Health Research Ethics, and from the Data Protection Officer at Haukeland University Hospital, on the basis of specific research proposals.

Conflicts of Interest: The co-authors Kenneth Hugdahl, Alexander R. Craven and Renate Grüner own shares in the company NordicNeuroLab, Inc. (<https://nordicneurolab.com/>) that produced add-on equipment used for MRI data acquisition. All authors declare no conflict of interest.

Abbreviations

4D	Four Dimensional
ANOVA	Analysis of Variance
AVH	Auditory Verbal Hallucinations
BET	Brain Extraction Tool
DDD	Defined Daily Dose
DMN	Default Mode Network
DTI	Diffusion Tensor Imaging
ERC	European Research Council
FA	Fractional Anisotropy
FMRIB	Functional Magnetic Resonance Imaging of the Brain
FSL	FMRIB Software Library
FWE	Familywise Error
GE	General Electrics
HD	High-definition
ICD	International Classification of Diseases
P3	Positive three
PANSS	Positive and Negative Syndrome Scale
SD	Standard Deviation
TBSS	Tract Based Special Statistics
TE	Echo Time
TFCE	Threshold Free Cluster Enhancement
TR	Repetition Time

References

1. Chaudhury, S. Hallucinations: Clinical aspects and management. *Ind. Psychiatry J.* **2010**, *19*, 5–12. [[CrossRef](#)] [[PubMed](#)]
2. Knapp, M.; Mangalore, R.; Simon, J. The Global Costs of Schizophrenia. *Schizophr. Bull.* **2004**, *30*, 279–293. [[CrossRef](#)]
3. Toh, W.L.; Thomas, N.; Hollander, Y.; Rossell, S.L. On the phenomenology of auditory verbal hallucinations in affective and non-affective psychosis. *Psychiatry Res.* **2020**, *290*, 113147. [[CrossRef](#)] [[PubMed](#)]

4. Larøi, F.; Thomas, N.; Aleman, A.; Fernyhough, C.; Wilkinson, S.; Deamer, F.; McCarthy-Jones, S. The ice in voices: Understanding negative content in auditory-verbal hallucinations. *Clin. Psychol. Rev.* **2019**, *67*, 1–10. [[CrossRef](#)] [[PubMed](#)]
5. Bauer, S.M.; Schanda, H.; Karakula, H.; Olajosy-Hilkesberger, L.; Rudaleviciene, P.; Okribelashvili, N.; Chaudhry, H.R.; Idemudia, S.E.; Gscheider, S.; Ritter, K.; et al. Culture and the prevalence of hallucinations in schizophrenia. *Compr. Psychiatry* **2011**, *52*, 319–325. [[CrossRef](#)] [[PubMed](#)]
6. Čurčić-Blake, B.; Ford, J.M.; Hubl, D.; Orlov, N.D.; Sommer, I.E.; Waters, F.; Allen, P.; Jardri, R.; Woodruff, P.W.; David, O.; et al. Interaction of language, auditory and memory brain networks in auditory verbal hallucinations. *Prog. Neurobiol.* **2017**, *148*, 1–20. [[CrossRef](#)]
7. Hugdahl, K.; Løberg, E.-M.; Nygård, M. Left temporal lobe structural and functional abnormality underlying auditory hallucinations. *Front. Neurosci.* **2009**, *3*, 1. [[CrossRef](#)]
8. Weber, S.; Johnsen, E.; Kroken, R.A.; Løberg, E.-M.; Kandilarova, S.; Stoyanov, D.; Kompus, K.; Hugdahl, K. Dynamic Functional Connectivity Patterns in Schizophrenia and the Relationship with Hallucinations. *Front. Psychiatry* **2020**, *11*, 227. [[CrossRef](#)]
9. Garrity, A.; Pearson, G.D.; McKiernan, K.; Lloyd, D.; Kiehl, K.; Calhoun, V. Aberrant “Default Mode” Functional Connectivity in Schizophrenia. *Am. J. Psychiatry* **2007**, *164*, 450. [[CrossRef](#)]
10. Sambataro, F.; Blasi, G.; Fazio, L.; Caforio, G.; Taurisano, P.; Romano, R.; Di Giorgio, A.; Gelao, B.; Bianco, L.L.; Papazacharias, A.; et al. Treatment with Olanzapine is Associated with Modulation of the Default Mode Network in Patients with Schizophrenia. *Neuropsychopharmacology* **2009**, *35*, 904–912. [[CrossRef](#)]
11. De Weijer, A.D.; Mandl, R.; Diederer, K.; Neggers, S.; Kahn, R.S.; Pol, H.H.; Sommer, I. Microstructural alterations of the arcuate fasciculus in schizophrenia patients with frequent auditory verbal hallucinations. *Schizophr. Res.* **2011**, *130*, 68–77. [[CrossRef](#)] [[PubMed](#)]
12. Ellison-Wright, I.; Bullmore, E. Meta-analysis of diffusion tensor imaging studies in schizophrenia. *Schizophr. Res.* **2009**, *108*, 3–10. [[CrossRef](#)] [[PubMed](#)]
13. Kelly, S.; Jahanshad, N.; Zalesky, A.; Kochunov, P.; Agartz, I.; Alloza, C.; Andreassen, O.A.; Arango, C.; Banaj, N.; Bouix, S.; et al. Widespread white matter microstructural differences in schizophrenia across 4322 individuals: Results from the ENIGMA Schizophrenia DTI Working Group. *Mol. Psychiatry* **2018**, *23*, 1261–1269. [[CrossRef](#)] [[PubMed](#)]
14. Kubicki, M.; McCarley, R.; Westin, C.-F.; Park, H.-J.; Maier, S.; Kikinis, R.; Jolesz, F.A.; Shenton, M.E. A review of diffusion tensor imaging studies in schizophrenia. *J. Psychiatr. Res.* **2007**, *41*, 15–30. [[CrossRef](#)] [[PubMed](#)]
15. Leroux, E.; Delcroix, N.; Dollfus, S. Abnormalities of language pathways in schizophrenia patients with and without a lifetime history of auditory verbal hallucinations: A DTI-based tractography study. *World J. Biol. Psychiatry* **2017**, *18*, 528–538. [[CrossRef](#)]
16. Oestreich, L.K.; Australian Schizophrenia Research Bank; McCarthy-Jones, S.; Whitford, T.J. Decreased integrity of the fronto-temporal fibers of the left inferior occipito-frontal fasciculus associated with auditory verbal hallucinations in schizophrenia. *Brain Imaging Behav.* **2016**, *10*, 445–454. [[CrossRef](#)]
17. Seok, J.-H.; Park, H.-J.; Chun, J.-W.; Lee, S.-K.; Cho, H.S.; Kwon, J.S.; Kim, J.-J. White matter abnormalities associated with auditory hallucinations in schizophrenia: A combined study of voxel-based analyses of diffusion tensor imaging and structural magnetic resonance imaging. *Psychiatry Res. Neuroimaging* **2007**, *156*, 93–104. [[CrossRef](#)]
18. Čurčić-Blake, B.; Nanetti, L.; Van Der Meer, L.; Cerliani, L.; Renken, R.; Pijnenborg, G.H.M.; Aleman, A. Not on speaking terms: Hallucinations and structural network disconnectivity in schizophrenia. *Brain Struct. Funct.* **2013**, *220*, 407–418. [[CrossRef](#)]
19. Shergill, S.S. A diffusion tensor imaging study of fasciculi in schizophrenia. *Am. J. Psychiatry* **2007**, *164*, 467–473. [[CrossRef](#)]
20. Kühn, S.; Gallinat, J. Quantitative Meta-Analysis on State and Trait Aspects of Auditory Verbal Hallucinations in Schizophrenia. *Schizophr. Bull.* **2010**, *38*, 779–786. [[CrossRef](#)]
21. Hugdahl, K.; Sommer, I.E. Auditory Verbal Hallucinations in Schizophrenia from a Levels of Explanation Perspective. *Schizophr. Bull.* **2018**, *44*, 234–241. [[CrossRef](#)] [[PubMed](#)]
22. Psomiades, M.; Fonteneau, C.; Mondino, M.; Luck, D.; Haesebaert, F.; Suaud-Chagny, M.-F.; Brunelin, J. Integrity of the arcuate fasciculus in patients with schizophrenia with auditory verbal hallucinations: A DTI-tractography study. *NeuroImage Clin.* **2016**, *12*, 970–975. [[CrossRef](#)] [[PubMed](#)]
23. Case, M.; Stauffer, V.L.; Ascher-Svanum, H.; Conley, R.; Kapur, S.; Kane, J.M.; Kollack-Walker, S.; Jacob, J.; Kinon, B.J. The heterogeneity of antipsychotic response in the treatment of schizophrenia. *Psychol. Med.* **2010**, *41*, 1291–1300. [[CrossRef](#)] [[PubMed](#)]
24. Levine, S.Z.; Rabinowitz, J.; Faries, D.; Lawson, A.H.; Ascher-Svanum, H. Treatment response trajectories and antipsychotic medications: Examination of up to 18 months of treatment in the CATIE chronic schizophrenia trial. *Schizophr. Res.* **2012**, *137*, 141–146. [[CrossRef](#)] [[PubMed](#)]
25. Kay, S.R.; Fiszbein, A.; Opler, L.A. The Positive and Negative Syndrome Scale (PANSS) for Schizophrenia. *Schizophr. Bull.* **1987**, *13*, 261–276. [[CrossRef](#)]
26. Hirnstein, M.; Hugdahl, K. Excess of non-right-handedness in schizophrenia: Meta-analysis of gender effects and potential biases in handedness assessment. *Br. J. Psychiatry* **2014**, *205*, 260–267. [[CrossRef](#)]
27. Bilder, R.M.; Wu, H.; Bogerts, B.; Degreif, G.; Ashtari, M.; Alvir, J.M.; Snyder, P.J.; Lieberman, J.A. Absence of regional hemispheric volume asymmetries in first-episode schizophrenia. *Am. J. Psychiatry* **1994**, *151*, 1437–1447. [[CrossRef](#)]
28. Falkai, P. Loss of sylvian fissure asymmetry in schizophrenia: A quantitative post mortem study. *Schizophr. Res.* **1992**, *7*, 23–32. [[CrossRef](#)]
29. Takao, H.; Abe, O.; Yamasue, H.; Aoki, S.; Kasai, K.; Ohtomo, K. Cerebral asymmetry in patients with schizophrenia: A voxel-based morphometry (VBM) and diffusion tensor imaging (DTI) study. *J. Magn. Reson. Imaging* **2009**, *31*, 221–226. [[CrossRef](#)]

30. Dollfus, S.; Razafimandimby, A.; Delamillieure, P.; Brazo, P.; Joliot, M.; Mazoyer, B.; Tzourio-Mazoyer, N. Atypical hemispheric specialization for language in right-handed schizophrenia patients. *Biol. Psychiatry* **2005**, *57*, 1020–1028. [[CrossRef](#)]
31. Oertel-Knöchel, V.; Linden, D.E.J. Cerebral Asymmetry in Schizophrenia. *Neuroscience* **2011**, *17*, 456–467. [[CrossRef](#)] [[PubMed](#)]
32. McCarthy-Jones, S.; Oestreich, L.K.; Whitford, T. Reduced integrity of the left arcuate fasciculus is specifically associated with auditory verbal hallucinations in schizophrenia. *Schizophr. Res.* **2015**, *162*, 1–6. [[CrossRef](#)] [[PubMed](#)]
33. Falkenberg, L.E.; Westerhausen, R.; Johnsen, E.; Kroken, R.; Løberg, E.-M.; Beresniewicz, J.; Kazimierczak, K.; Kompus, K.; Ersland, L.; Sandøy, L.B.; et al. Hallucinating schizophrenia patients have longer left arcuate fasciculus fiber tracks: A DTI tractography study. *Psychiatry Res. Neuroimaging* **2020**, *302*, 111088. [[CrossRef](#)] [[PubMed](#)]
34. McCarthy-Jones, S.; Smailes, D.; Corvin, A.; Gill, M.; Morris, D.W.; Dinan, T.G.; Murphy, K.C.; O’neill, F.A.; Waddington, J.L.; null Australian Schizophrenia Research Bank; et al. Occurrence and co-occurrence of hallucinations by modality in schizophrenia-spectrum disorders. *Psychiatry Res.* **2017**, *252*, 154–160. [[CrossRef](#)] [[PubMed](#)]
35. Nayani, T.H.; David, A.S. The auditory hallucination: A phenomenological survey. *Psychol. Med.* **1996**, *26*, 177–189. [[CrossRef](#)]
36. Shinn, A.K.; Pfaff, D.; Young, S.; Lewandowski, K.E.; Cohen, B.M.; Öngür, D. Auditory hallucinations in a cross-diagnostic sample of psychotic disorder patients: A descriptive, cross-sectional study. *Compr. Psychiatry* **2012**, *53*, 718–726. [[CrossRef](#)]
37. Smith, S.M. Fast robust automated brain extraction. *Hum. Brain Mapp.* **2002**, *17*, 143–155. [[CrossRef](#)]
38. Smith, S.M.; Jenkinson, M.; Woolrich, M.W.; Beckmann, C.F.; Behrens, T.E.; Johansen-Berg, H.; Bannister, P.R.; De Luca, M.; Drobnjak, I.; Flitney, D.E.; et al. Advances in functional and structural MR image analysis and implementation as FSL. *NeuroImage* **2004**, *23*, S208–S219. [[CrossRef](#)]
39. Smith, S.M.; Jenkinson, M.; Johansen-Berg, H.; Rueckert, D.; Nichols, T.E.; Mackay, C.E.; Watkins, K.E.; Ciccarelli, O.; Cader, M.Z.; Matthews, P.M.; et al. Tract-based spatial statistics: Voxelwise analysis of multi-subject diffusion data. *NeuroImage* **2006**, *31*, 1487–1505. [[CrossRef](#)]
40. Jenkinson, M. TBSS User Guide. 2013. Available online: https://fsl.fmrib.ox.ac.uk/fsl/fslwiki/TBSS/UserGuide#Testing_left_vs._right_in_TBSS (accessed on 1 January 2019).
41. Winkler, A.M.; Ridgway, G.R.; Webster, M.A.; Smith, S.M.; Nichols, T.E. Permutation inference for the general linear model. *NeuroImage* **2014**, *92*, 381–397. [[CrossRef](#)]
42. Nichols, T.E.; Holmes, A.P. Nonparametric permutation tests for functional neuroimaging: A primer with examples. *Hum. Brain Mapp.* **2002**, *15*, 1–25. [[CrossRef](#)] [[PubMed](#)]
43. Smith, S.M.; Nichols, T.E. Threshold-free cluster enhancement: Addressing problems of smoothing, threshold dependence and localisation in cluster inference. *NeuroImage* **2009**, *44*, 83–98. [[CrossRef](#)]
44. Bopp, M.; Zöllner, R.; Jansen, A.; Dietsche, B.; Krug, A.; Kircher, T. White matter integrity and symptom dimensions of schizophrenia: A diffusion tensor imaging study. *Schizophr. Res.* **2017**, *184*, 59–68. [[CrossRef](#)] [[PubMed](#)]
45. Zhang, X.; Gao, J.; Zhu, F.; Wang, W.; Fan, Y.; Ma, Q.; Ma, X.; Yang, J. Reduced white matter connectivity associated with auditory verbal hallucinations in first-episode and chronic schizophrenia: A diffusion tensor imaging study. *Psychiatry Res. Neuroimaging* **2018**, *273*, 63–70. [[CrossRef](#)]
46. Duffau, H.; Gatignol, P.; Mandonnet, E.; Peruzzi, P.; Tzourio-Mazoyer, N.; Capelle, L. New insights into the anatomo-functional connectivity of the semantic system: A study using cortico-subcortical electrostimulations. *Brain* **2005**, *128*, 797–810. [[CrossRef](#)] [[PubMed](#)]
47. Friederici, A.D. Allocating functions to fiber tracts: Facing its indirectness. *Trends Cogn. Sci.* **2009**, *13*, 370–371. [[CrossRef](#)]
48. Glasser, M.F.; Rilling, J.K. DTI Tractography of the Human Brain’s Language Pathways. *Cereb. Cortex* **2008**, *18*, 2471–2482. [[CrossRef](#)] [[PubMed](#)]
49. Rilling, J.K.; Glasser, M.F.; Preuss, T.M.; Ma, X.; Zhao, T.; Hu, X.; Behrens, T.E.J. The evolution of the arcuate fasciculus revealed with comparative DTI. *Nat. Neurosci.* **2008**, *11*, 426–428. [[CrossRef](#)]
50. Geschwind, N. The Organization of Language and the Brain: Language disorders after brain damage help in elucidating the neural basis of verbal behavior. *Science* **1970**, *170*, 940–944. [[CrossRef](#)]
51. Hagmann, P.; Cammoun, L.; Martuzzi, R.; Maeder, P.; Clarke, S.; Thiran, J.-P.; Meuli, R.A. Hand preference and sex shape the architecture of language networks. *Hum. Brain Mapp.* **2006**, *27*, 828–835. [[CrossRef](#)]
52. Bubb, E.J.; Metzler-Baddeley, C.; Aggleton, J.P. The cingulum bundle: Anatomy, function, and dysfunction. *Neurosci. Biobehav. Rev.* **2018**, *92*, 104–127. [[CrossRef](#)] [[PubMed](#)]
53. Panksepp, J. *Affective Neuroscience: The Foundations of Human and Animal Emotions*; Oxford University Press: New York, NY, USA, 2004.
54. Panksepp, J. Affective consciousness: Core emotional feelings in animals and humans. *Conscious. Cogn.* **2005**, *14*, 30–80. [[CrossRef](#)] [[PubMed](#)]
55. Sun, L.; Peräkylä, J.; Polvivaara, M.; Öhman, J.; Peltola, J.; Lehtimäki, K.; Huhtala, H.; Hartikainen, K.M. Human anterior thalamic nuclei are involved in emotion-attention interaction. *Neuropsychology* **2015**, *78*, 88–94. [[CrossRef](#)] [[PubMed](#)]
56. Miyata, J.; Sasamoto, A.; Koelkebeck, K.; Hirao, K.; Ueda, K.; Kawada, R.; Fujimoto, S.; Tanaka, Y.; Kubota, M.; Fukuyama, H.; et al. Abnormal asymmetry of white matter integrity in schizophrenia revealed by voxelwise diffusion tensor imaging. *Hum. Brain Mapp.* **2011**, *33*, 1741–1749. [[CrossRef](#)] [[PubMed](#)]
57. Jäncke, L.; Wustenberg, T.; Schulze, K.; Heinze, H.J. Asymmetric hemodynamic responses of the human auditory cortex to monaural and binaural stimulation. *Heart Res.* **2002**, *170*, 166–178. [[CrossRef](#)]
58. Hugdahl, K.; Heiervang, E.; Ersland, L.; Lundervold, A.; Steinmetz, H.; Smievoll, A.I. Significant relation between MR measures of planum temporale area and dichotic processing of syllables in dyslexic children. *Neuropsychology* **2003**, *41*, 666–675. [[CrossRef](#)]

59. Ribolsi, M.; Daskalakis, Z.J.; Siracusanano, A.; Koch, G. Abnormal Asymmetry of Brain Connectivity in Schizophrenia. *Front. Hum. Neurosci.* **2014**, *8*, 1010. [[CrossRef](#)]
60. Kamali, A.; Flanders, A.E.; Brody, J.; Hunter, J.V.; Hasan, K.M. Tracing superior longitudinal fasciculus connectivity in the human brain using high resolution diffusion tensor tractography. *Brain Struct. Funct.* **2014**, *219*, 269–281. [[CrossRef](#)]
61. Abdul-Rahman, M.F.; Qiu, A.; Woon, P.S.; Kuswanto, C.; Collinson, S.L.; Sim, K. Arcuate Fasciculus Abnormalities and Their Relationship with Psychotic Symptoms in Schizophrenia. *PLoS ONE* **2012**, *7*, e29315. [[CrossRef](#)]
62. Catani, M.; Craig, M.C.; Forkel, S.J.; Kanaan, R.; Picchioni, M.; Toulopoulou, T.; Shergill, S.; Williams, S.; Murphy, D.G.; McGuire, P. Altered Integrity of Perisylvian Language Pathways in Schizophrenia: Relationship to Auditory Hallucinations. *Biol. Psychiatry* **2011**, *70*, 1143–1150. [[CrossRef](#)]
63. Hugdahl, K.; Løberg, E.-M.; Falkenberg, L.E.; Johnsen, E.; Kompus, K.; Kroken, R.A.; Nygård, M.; Westerhausen, R.; Alptekin, K.; Özgören, M. Auditory verbal hallucinations in schizophrenia as aberrant lateralized speech perception: Evidence from dichotic listening. *Schizophr. Res.* **2012**, *140*, 59–64. [[CrossRef](#)] [[PubMed](#)]
64. O'Donnell, L.J.; Pasternak, O. Does diffusion MRI tell us anything about the white matter? An overview of methods and pitfalls. *Schizophr. Res.* **2015**, *161*, 133–141. [[CrossRef](#)] [[PubMed](#)]
65. Mori, S.; Zhang, J. Principles of Diffusion Tensor Imaging and Its Applications to Basic Neuroscience Research. *Neuron* **2006**, *51*, 527–539. [[CrossRef](#)] [[PubMed](#)]
66. Tønnesen, S.; Kaufmann, T.; De Lange, A.-M.G.; Richard, G.; Doan, N.T.; Alnæs, D.; Van Der Meer, D.; Rokicki, J.; Moberget, T.; Maximov, I.I.; et al. Brain Age Prediction Reveals Aberrant Brain White Matter in Schizophrenia and Bipolar Disorder: A Multi-sample Diffusion Tensor Imaging Study. *Biol. Psychiatry Cogn. Neurosci. Neuroimaging* **2020**, *5*, 1095–1103. [[CrossRef](#)] [[PubMed](#)]
67. Stoyanov, D. A linkage of mind and brain: Towards translational validity between neurobiology and psychiatry. *Biomed. Rev.* **2014**, *22*, 65. [[CrossRef](#)]



OPEN

Dynamic switching between intrinsic and extrinsic mode networks as demands change from passive to active processing

Frank Riemer^{1,2✉}, Renate Grüner^{1,2,3}, Justyna Beresniewicz⁴, Katarzyna Kazimierczak^{1,4}, Lars Erstrand^{4,5} & Kenneth Hugdahl^{2,4,6}

In this study we report on the relationship between default and extrinsic mode networks across alternating brief periods of rest and active task processing. Three different visual tasks were used in a classic fMRI ON–OFF block design where task (ON) blocks alternated with equal periods of rest (OFF) blocks: mental rotation, working memory and mental arithmetic. We showed the existence of a generalized task-positive network, labelled the extrinsic mode network (EMN) that is anti-correlated with the default mode network (DMN) as processing demands shifted from rest to active processing. We then identified two key regions of interest (ROIs) in the supplementary motor area (SMA) and precuneus/posterior cingulate cortex (PCC) regions as hubs for the extrinsic and intrinsic networks, and extracted the time-course from these ROIs. The results showed a close to perfect anti-correlation for the SMA and Precuneus/PCC time-courses for ON- and OFF-blocks. We suggest the existence of two large-scale networks, an extrinsic mode network and an intrinsic mode network, which are up- and down-regulated as environmental demands change from active to passive processing.

Ever since the discovery and identification of the default mode network (DMN) by Marcus Raichle and colleagues^{1–3}, the study of network interactions has been a major issue in imaging neuroscience⁴. This has in particular concerned intrinsic interactions and anti-correlations between the DMN and other resting-state networks, and task-positive networks which are activated during active task-processing^{5–8}. Other studies have focused on the decomposition of the DMN into sub-networks typically activated in task-processing situations^{9–13}. At around the same time as the discovery of the DMN, Duncan and Owen¹⁴ suggested that regions in the dorsolateral and anterior cingulate frontal cortex were activated during multiple processing demands. Duncan and Owen¹⁴ described their discovery as a "regional specialization of function within prefrontal cortex" (p. 475), which generalised across a variety of cognitive tasks and situations. The initial discovery by Duncan and Owen¹⁴ was later replicated and extended by Fedorenko et al.¹⁵, who found a common network structure across seven memory, executive, and attention tasks, and by Duncan¹⁶ who now labelled these activations a multiple demand (MD) system. Adding to this, Hugdahl et al.¹⁷ performed a retrospective analysis using nine separate fMRI experiments and found a generalized task non-specific network, which was activated across all nine tasks. This network involved the SMA/anterior cingulate, lateral prefrontal cortex, and inferior parietal lobule. Hugdahl et al.¹⁷ labelled this network the extrinsic mode network (EMN) to distinguish it from the intrinsic DMN. It is therefore clear that not only is there a linked set of network activations during resting periods, which collectively could be called non-specific task-negative networks, but also a set of similar non-specific task-positive networks. This set of networks has been labelled by different groups as the multiple demand system¹⁶, frontal-lobe network¹⁴, or extrinsic mode network¹⁷. We will use the term "extrinsic mode network (EMN)" in the following to describe this generalised task-positive network. Although the EMN and other task non-specific networks

¹Mohn Medical Imaging and Visualization Centre, University of Bergen and, Haukeland University Hospital, Bergen, Norway. ²Department of Radiology, Haukeland University Hospital, Bergen, Norway. ³Department of Physics and Technology, University of Bergen, Bergen, Norway. ⁴Department of Biological and Medical Psychology, University of Bergen, Bergen, Norway. ⁵Department of Clinical Engineering, Haukeland University Hospital, Bergen, Norway. ⁶Division of Psychiatry, Haukeland University Hospital, Bergen, Norway. ✉email: F.Riemer@web.de

show overlapping features with task-specific networks, there are also essential differences, in particular that the EMN and other general-domain networks^{15,16} are observed in a wide range of tasks across cognitive domains¹⁷ -while task-specific networks are more specific to a particular cognitive domain, such as attention or executive functions^{10,12}. The interaction between task non-specific and task specific networks is however complex and not fully understood. There are overlapping activations in fronto-parietal areas between the network categories, which could be perceived as nodes in task-specific networks that are also existing in task non-specific networks, and may modulate the strength of the latter depending on the nature of the task. An important question is how the DMN and EMN networks interact with regard to dominant up- and down-regulations across time when environmental demands repeatedly change from active to passive task-processing, i.e., change from engagement to rest and vice versa, on a short-term basis. Most studies of the relationship between task-negative and task-positive networks are either conducted during prolonged resting-periods, or by having subjects solve a single task. A single-task paradigm is usually performed by only addressing a single cognitive domain^{1,10,18}, like working memory or attention as examples. An experimental set-up like this would however not capture the question of the dynamics of resting-state and non-specific task-positive network interactions, where tasks change from one processing period to another across the experimental session. Hugdahl et al.¹⁹ suggested an experimental proxy to the everyday switching between periods of task engagement alternated with periods of rest, where tasks moreover will differ in terms of cognitive domain and processing load from one processing period to another. In the confines of an fMRI experiment, this can be obtained by alternating task-presence and task-absence periods, using a traditional fMRI block-design²⁰. In such an experiment, ON- and OFF-blocks represent active versus passive processing periods, respectively. Such an approach was taken by Hugdahl et al.¹⁹ who used an auditory dichotic listening task^{21–23} with ON-blocks and pseudo-random presentations of three different cognitive tasks involving perception, attention, and executive function that were interspersed with OFF-blocks and no task present. The results showed statistically significant anti-correlations between the DMN and EMN, particularly in the inferior frontal and posterior cingulate cortex regions. Moreover, EMN up-regulations at the transition from an OFF- to an ON-block were steeper and more prolonged, than the corresponding up-regulation of the DMN in the transition from an ON- to an OFF-block. The study by Hugdahl et al.¹⁹ was however confined to the auditory modality, and had the different cognitive domains embedded within a single task, the so called "forced-attention dichotic listening task"²². Thus, it is not known if a similar pattern of interactions between the DMN and EMN would hold for; (a) the visual modality, (b) when splitting the cognitive domains across tasks, and (c) expanding the tasks to more complex cognition, like number arithmetic, working memory, and mental rotation. The three tasks chosen represent three cognitive domains typically encountered during an ordinary day. To activate visuo-spatial processing, a mental rotation task²⁴ was chosen because this task is shown to provide significant fronto-parietal activations^{25–27}. A working memory task was chosen because working memory is a central cognitive concept, which includes attention and executive control in addition to short-term memory^{28,29}, and would thus be a valid proxy for the varying processing demands during an ordinary working-day. A mental arithmetic task with adding numbers was chosen because it draws on a common cognitive ability encountered every day, the ability for mental arithmetic and to manipulate numbers. Previous research has shown that this task in isolation produces reliable activation in inferior frontal cortex and anterior cingulate^{30,31}. In addition to whole brain analysis, we chose two region-of-interests (ROIs) for comparisons and correlations between the DMN and EMN networks, respectively. For the DMN we chose the precuneus as an ROI, since this region is consistently activated during DMN up-regulations^{5,32}. For the EMN we chose the intersection of anterior cingulate (ACC) and supplementary motor area (SMA), since this region is consistently activated during periods of EMN up-regulation^{15,17}. The justification for the choice of the SMA as the key hub for the ROI analysis was also to allow a direct comparison to our previous study with auditory tasks¹⁹. A second justification was to contrast this region with the precuneus region for the DMN. The aim of the present study was therefore to provide an extension of the Hugdahl et al.¹⁹ study by including different tasks, and cognitive processing strategies, while staying within the same ON–OFF experimental approach as the one used in Hugdahl et al.¹⁹. Considering the current replication crisis in neuroscience and psychology³³, an extended replication is a necessary first step for establishing a solid factual basis for new findings.

Results

Behavioural data. Mean response accuracy was calculated as the ratio of correct responses to overall number of responses and expressed as a hits-ratio. For the mental rotation task, the hits ratio was 0.560, for the working memory task it was 0.769 and for the mental arithmetic task it was 0.843. The corresponding Cohen's *d* values were: 0.55, 0.91, and 1.84 for the mental rotation, working memory, and mental arithmetic tasks, respectively. Following a standard interpretation of corresponding effect sizes, all three tasks showed medium to strong effect size. Mean response latency, also known as reaction-time (RT), for the three tasks were 404.2 ms (SD 143.0) for the mental rotation task, 168.4 ms (SD 56.5) for the working memory task and 218.3 ms (SD 38.0) for the mental arithmetic task. These results confirm that the subjects had understood and performed the tasks as expected.

fMRI data. Mean framewise displacement (FD) indices for all subjects were $=0.19 \pm 0.08$ mm. 17 out of the 47 subjects had $FDs \geq 0.20$ and were excluded for a re-analysis to compare to the results of the whole data-set. The activation maps for the re-analysis of the subset confirmed the results of the whole-dataset. We therefore decided not to remove any subjects due to motion. Adding the estimated motion parameters as a regressor did also not affect any of the results significantly.

Figure 1 shows the results from the inclusive conjunction analysis of mean joint activations across the three tasks, $p < 0.05$, family-wise-error (FWE) corrected, with significant activations for the ON–OFF contrast seen

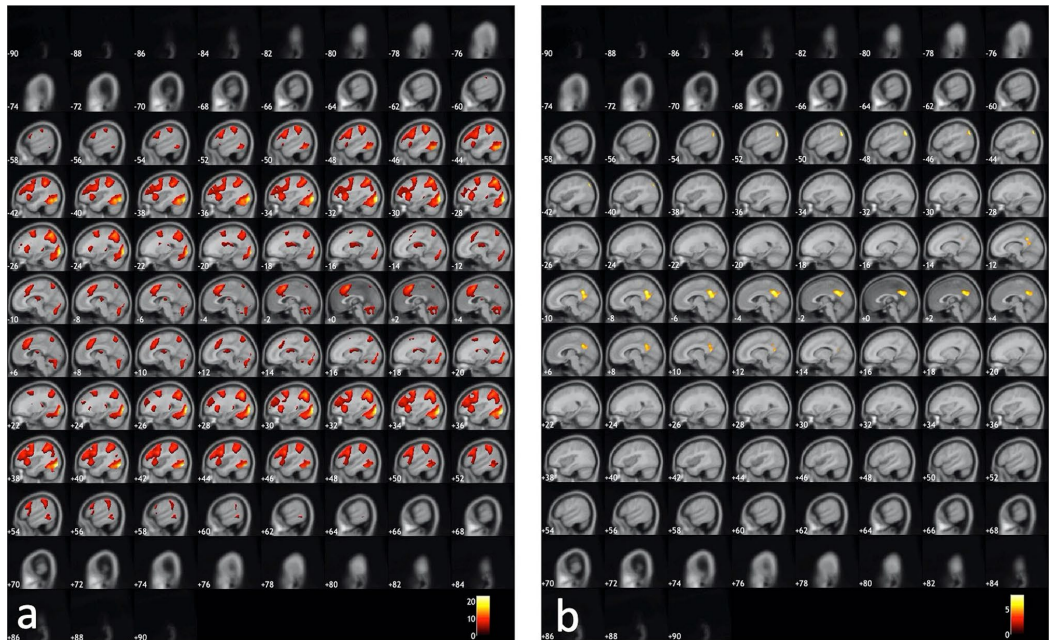


Figure 1. Activations that passed the .05 FWE-corrected significance threshold, shown on sagittal slices of the MNI-template. The panel (a) to the left shows activations obtained during ON-blocks contrasted with activations obtained during OFF-blocks (ON-OFF). The panel (b) to the right shows activations obtained with the contrast flipped, i.e. obtained during OFF-blocks contrasted with activations obtained during ON-blocks (OFF-ON). See “Results” for further details.

in the left-hand panel and corresponding activations for the OFF-ON contrast seen in the right-hand panel. A cluster size of minimum 20 voxels was used and slices are shown with 2 mm spacing.

The ON-OFF contrast produced significant, $p = 0.05$, FWE-corrected activations in the right SMA (MNI coordinates: $x 4, y 14, z 50$), right inferior occipital gyrus ($x 32, y - 85, z - 32$), right angular gyrus ($x 30, y - 64, z 44$), left superior parietal lobule ($x - 26, y - 58, z 54$), right and left precentral gyrus ($x 46, y 10, z 32$, and $x - 46, y 4, z 30$, respectively), left anterior insula ($x - 30, y 18, z 6$) and left middle frontal gyrus ($x - 26, y - 4, z 50$). All t -values were > 7.46 , critical $0.05 t$ -value was $= 4.40$ with 447 df. The OFF-ON contrast produced corresponding activations in the left precuneus/posterior cingulate gyrus (PCC) ($x - 6, y - 54, z 32$), $x 0, y 52, z 31$), left and right angular gyrus ($x - 48, y - 70, z 36$ and $x 50, y - 68, z 30$) and in the right central operculum ($x 38, y - 14, z 18$). All t -values were > 4.97 with a critical $0.06 t$ -value $= 4.40$. Figure 2 shows the results split for the three tasks, with activations overlaid on the MRIcron anatomical template (ch2.better.niftii) as different layers and colours: As seen in Fig. 2, the main findings from the overall conjunction analysis were confirmed in the separate analyses, with essentially similar patterns of activations for all three tasks. Activation caused by the working memory task is shown in blue and activations caused by the mental rotation task is shown in green. Common activations across all three tasks are correspondingly indicated in white colour. Common activations for the mental rotation and working memory tasks are indicated in violet colour. Common activations for the mental rotation and mental arithmetic tasks are indicated in cyan colour, and common activations for the working memory and mental arithmetic tasks are indicated in yellow colour.

Analysing the contrasts separately for each task also yielded activations beyond what was seen in the conjunction analysis across tasks. For the ON-OFF contrast, the mental rotation task yielded additional activation in the right thalamus ($x 24, y - 30, z 4$), and the mental arithmetic yielded additional activations in right and left thalamus ($x 26, y - 30, z 2$, and $x - 24, y - 30, z 0$, respectively). For the OFF-ON contrast, the corresponding additional activations for the working memory task were seen in the left and right lingual gyrus ($x - 24, y - 44, z - 8$ and $x 30, y - 38, z - 12$, respectively), in the left medial and lateral superior frontal gyrus ($x - 2, y 58, z 8$ and $x - 16, y 38, z 52$, respectively) and in the right posterior insula ($x 38, y - 12, z 16$). For the mental arithmetic task, the corresponding additional activations were seen in the right cerebellum ($x 30, y - 74, z - 40$), left middle temporal gyrus ($x - 62, y 34, z 48$) and in the left superior frontal gyrus ($x - 22, y 34, z 48$).

We then identified overlapping activations for all three tasks in the SMA and precuneus/PCC and defined them as new ROIs for the subsequent analysis, as these regions are key nodes in the EMN and DMN networks, respectively^{2,17}. The ROIs are shown on top of the anatomy template in the upper panel of Fig. 3a,b. The mean

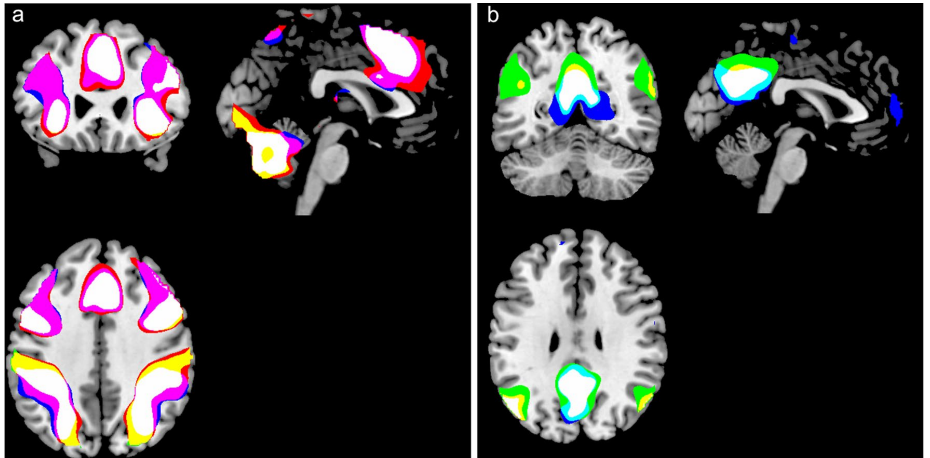


Figure 2. Activations for the three separate tasks overlaid on top of each other demonstrating significant overlap. The panel (a) to the left shows activations obtained during ON-blocks contrasted with activations obtained during OFF-blocks (ON–OFF). The panel (b) to the right shows activations obtained with the contrast flipped, i.e. obtained during OFF-blocks contrasted with activations obtained during ON-blocks (OFF–ON). For both panels (a) and (b), activation caused by the working memory task is shown in red, activation caused by the mental rotation task is shown in blue and activations caused by the mental arithmetic task is shown in green. Common activations across all three tasks are correspondingly indicated in white colour. Common activations for the mental rotation and working memory tasks are indicated in violet colour. Common activations for the mental rotation and mental arithmetic tasks are indicated in cyan colour, and common activations for the working memory and mental arithmetic tasks are indicated in yellow colour.

time-course from these regions was extracted separately for ON- and OFF-blocks across the whole scanning session (lower panel of Fig. 3c). Windowed correlation coefficients were calculated using a time-window of 17 s with 50% overlap (half the length of one ON- or OFF-block). Development of correlation coefficients across time is shown as an intermittent black line in Fig. 3c. The black line in Fig. 3c demonstrates that there was a strong negative correlation at the beginning and end of each task-related ON-block (mean Pearson r -coefficients at points of inflection was -0.56 ± 0.21) and corresponding strong positive correlation was seen at approximately the middle of each task ON- and rest OFF-periods (mean peak Pearson R 's was $+0.68 \pm 0.19$).

Discussion

We demonstrated that switching between resting and active processing periods results in two distinct networks that were up- and down-regulated as environmental demands changed from passive to active. In this respect, the present results resemble the results from a similar study where the processing tasks were auditory in nature¹⁹. We therefore conclude that the existence of a generalised task-positive network is not dependent on sensory modality. The most conspicuous similarities between the current and the Hugdahl et al.¹⁹ study were in the overlapping activations in the SMA and insula regions. There were however also differences between the previous Hugdahl et al.¹⁹ and the current study. In the Hugdahl et al.¹⁹ study, activations during ON-blocks were seen in auditory regions in the temporal lobes, while the present study showed activations in visual regions in the occipital cortex, as expected due to difference in task modality. Other differences were in the pre-central motor area, because a motor task was used in the current study, and in the superior parietal and middle frontal gyrus. These latter differences most likely refer to the wider range of cognitive tasks used in the current study in addition to targeting the visual modality. For the DMN, the most conspicuous similarities between the studies were found for the cingulate cortex and the precuneus, while differences were found for the superior and middle frontal gyri, and the angular operculum. Again, these differences probably reflect variation in DMN spatial extension as environmental demands vary, since OFF-task activation is affected by ON-task activations³⁴. The behavioural results confirmed that the subjects were performing the tasks required throughout the scanning session. A second finding was that the up-regulation of the task-positive network was independent of the specifics of the task, and as seen in Figs. 2 and 3, i.e. generalised across the tasks. In this respect, the present results are in line with the findings of Fedorenko et al.¹⁵ and Duncan¹⁶ pointing to the existence of a task non-specific network, which we have labelled the EMN, following the nomenclature from Hugdahl et al.¹⁷. There are several notable similarities between the current findings, the previously suggested EMN network and the findings reported in the Fedorenko et al. and Duncan papers: Most notably are the agreement of activations in the SMA, superior parietal lobule, inferior and middle frontal gyrus, and the precentral gyrus. A major difference between our and the previous studies is in the tasks being used to elicit these activations, and the interpretation of the significance of the findings as extending beyond an attention model as a mediating factor. Considering that the DMN in essence is a task-negative network^{2,5,35,36} being up-regulated in periods of absence of specific processing demands, it is an

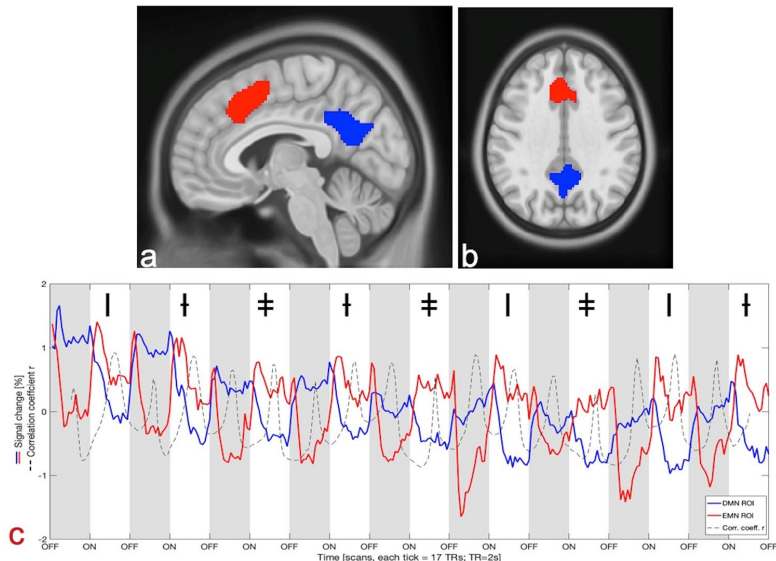


Figure 3. Sagittal (a) and axial (b) views of the ROIs shown on the MNI-T1 template. The DMN ROI is shown in blue and the EMN ROI in red. The ROIs were used for the time-series extraction shown in (c): The tasks alternated randomly between mental rotation (marked with the symbol I), working memory (marked with the symbol †) and mental arithmetic (marked with the symbol ‡). Signal change is shown as percentage of total signal change and keeping in line with the colour coding for the ROIs as in panels (a) and (b). Onsets and offsets of the task and rest periods are shown on the x-axis as ON and OFF respectively with OFF-blocks also being marked in grey. The black intermittent line in panel (c) shows the Pearson correlation coefficients continuously calculated on the mean of a 17 s sliding-window through the whole session.

intrinsic mode network. We now provide more evidence that the brain may alternate between an intrinsic and extrinsic mode of function, corresponding to the dominating environmental demand, with the intrinsic mode network dominating during task-absence, and the extrinsic mode network dominating during task-presence as has been previously suggested^{18,19,35}. Interestingly, our results also show that the two networks are sometimes positively correlated, suggesting that the relationship between DMN and EMN may be more complex than we originally thought¹⁹. We would also like to suggest that intrinsic and extrinsic mode networks operate at a superordinate level with regard to domain-specific networks, like the salience network^{10,11,37}, dorsal attention network^{3,38}, or central executive network^{12,39}.

We focused on the precuneus/PCC and ventral SMA as ROIs when extracting the time-courses representing the extrinsic and intrinsic mode networks, respectively, since the SMA was overlapping in activation for all three cognitive tasks, and has previously been implicated in a variety of cognitive operations, including visuo-spatial processing, working memory, and mental arithmetic⁴⁰. The precuneus region was chosen because it was strongly activated during OFF-blocks, and has previously been shown to be implicated in the default mode network^{1,11,41,42}. Thus, the time-course dynamics seen in Fig. 3 from the SMA and precuneus ROIs is taken as a proxy for the up- and down-regulation of the corresponding extrinsic and intrinsic mode networks. We suggest that the role of the SMA, and in particular the ventral portion, is overlapping with the pre-SMA. While Fig. 3 shows a clear inverse up- and down-regulation between the two ROIs for the alternating task and rest periods, the signals are not anti-correlated at all time (see dotted line in Fig. 3). During the middle of the task-blocks, a positive correlation can be seen, despite the rate of change of the two signals seeming static (a plateau or equilibrium is reached in the middle of the task block). This is in conflict with findings by Fox et al.³, who used a paradigm of three alternating rest periods (visual fixation, eyes open and eyes closed) instead of alternating rest and active periods, as employed in our study. The results of the Fox et al. study are therefore not directly comparable with the current results since the paradigm used in their study did not involve periods of active task-processing. Moreover, as seen in Fig. 3, the positive correlations seem to be driven by the EMN BOLD-response (red line) beginning to dip slightly after an initial up-regulation at the transition points. This could imply a corresponding fading of concentration focus across active blocks, or a habituation effect due to task repetitions. Further investigation is necessary to sort out these inconsistencies. In addition, to capture a good surrogate for the EMN and DMN networks, we used relatively large ROIs, which could have introduced a partial volume effect with a different network that does contribute to the positive correlation observed at times. Our mean framewise displacement^{43,44} indices are both smaller than the “lenient” ($FD > 0.5$ mm), as well as the “stringent” ($FD > 0.2$ mm) thresholds discussed

by Power et al.⁴⁴. Similarly, the popular resting-state functional connectivity MRI (rs-fcMRI) toolbox CONN only gives an outlier warning if $FD > 0.5$ (<https://web.conn-toolbox.org/fmri-methods/preprocessing-pipeline>)⁴⁵. Therefore, corrections such as temporal masking by censoring or interpolation of the data are not likely to give any significantly different results in our study. In addition, spurious activations are less likely to impact the results in a task-based paradigm as opposed to a rs-fcMRI study. Nevertheless, we performed a simple test for influence of motion by removing 17 of the total of 47 subjects that had $FDs \geq 0.2$. The results yielded no major differences to the activations patterns observed from the full dataset. More complex censoring and interpolation approaches may be more thorough but were not deemed necessary given the low mean framewise displacement.

The conjunction analysis revealed in addition the other following areas activated during ON-blocks: The angular gyrus, superior parietal lobule, anterior insula, and the middle frontal gyrus. All these regions are implicated in higher-order cognition, including mental arithmetic, visuo-spatial processing, mental rotation and working memory^{27,46–48}. In addition, the occipital activation, which most likely reflects the fact that the tasks were all visual in nature. Likewise, the activation bilaterally in the pre-central region would be related to the motor-response and button-pressing. The OFF-blocks were characterised by activations in the angular gyrus and central operculum, which are regions previously implicated in the DMN^{32,49}. Looking at Fig. 2, which shows areas with overlapping and non-overlapping activations for the three tasks reveals a remarkable similarity in activation patterns across all three tasks during ON-blocks (see white-coloured areas in Fig. 2). This is evident for all activations, except for the left inferior parietal lobule, which was more strongly activated to the mental rotation and working memory tasks than in the mental arithmetic task. A similar pattern emerged from looking at the overlapping activations for OFF-blocks, i.e. whether activations during resting periods associated with the three tasks differed (see white-coloured areas in Fig. 2). Again, as for ON-block periods, the pattern of activations for the OFF-blocks were quite similar across resting periods, especially for the precuneus with centre of gravity showing similar overlapping activations. Activation related to the mental rotation task did however extend in the inferior axis, and was also seen with a small area in the medial-ventral frontal lobe. The patterns of overlapping activations differed however for ON- and OFF-blocks when it comes to overlapping areas for only two tasks. For ON-blocks, the mental rotation and working memory tasks showed overlapping activations (shown in violet colour in Fig. 2) to a greater extent than the other task-combinations, which was not the case for OFF-blocks. For OFF-blocks, most of the activations were overlapping for all three tasks, with mental arithmetic (shown in green colour) in addition activating the middle temporal and superior frontal gyri. These areas are implicated in working memory tasks⁵⁰ and may be overshooting from the ON-periods for this particular task. The ON–OFF contrast resulted in unique activations in the thalamus for mental rotation and mental arithmetic tasks, as well as in left lateral superior frontal gyrus. Thalamus activations have previously been reported for both mental arithmetic and mental rotation^{51,52} and may be related to the role of basal ganglia in number processing and visuo-spatial processing in general. Figures 1 and 2 clearly demonstrate that joint activations across tasks, both during ON- and OFF-blocks were not perfect, showing unique single-task activations, as well as joint activations for combinations of two tasks. This suggests that the EMN and other non-specific general-domain networks may be dynamically modulated depending on environmental demands, such that task-specific nodes in the network may transiently be modulated by dynamically stretching or shrinking. We suggest a similar dynamic modulation of the DMN, seen during OFF-blocks, in that its shape and level of up-regulated modulation depends both on previous and anticipated environmental challenges, which has been shown in several studies (see Bruckner et al.⁴ for a recent review of DMN activations). The absence of unique activations for the mental arithmetic task during ON-blocks, not subsumed either under the conjunction of all three tasks (white color in Fig. 2a), or overlapping with activations associated with the working memory task (yellow color in Fig. 2a), needs further investigation since it is in contrast to the additional activations during OFF-blocks associated with the mental arithmetic task (green color in Fig. 2b). We suggest that the reason for the absence of unique mental arithmetic activations during ON-blocks is that this task contains a transient working memory component in addition to a pure arithmetic component, making it a doubly-demanding task. The additional extended activations during resting periods (OFF-blocks) associated with the mental arithmetic task would in contrast imply that an arithmetic task results in stronger up-regulation of the DMN (at least defined as an extended area) than the other two tasks, which in turn could indicate that this task is more resource demanding, despite being subsumed during ON-blocks. We now suggest that a way of defining task-demands could be defined by its extent from "side to side", i.e. how much of rebound a task causes during intermittent rest-periods.

In conclusion, the present results have shown the existence of a generalized task-non-specific network, which is upregulated during periods of active task-processing, but is essentially independent of the specifics of the task. By following the nomenclature introduced by Hugdahl et al.¹⁷ we have labelled this network the Extrinsic Mode Network (EMN), as an extrinsic mode network in contrast to the default mode network, which is an intrinsic mode network, and should perhaps also be labelled so. Secondly, building on our previous research with auditory tasks¹⁹, the current results have shown that similar network dynamics exist for visual tasks, which in isolation has been shown previously^{1,18}. We now show that this also occurs across different tasks in a single scanning session. For these reasons, we now suggest that a standard, classic, fMRI block-design with alternating task- and rest-periods, may be an experimental proxy for alternating rest-periods combined with task processing requirement periods that we encounter in the course of an ordinary day in life. Having said that, it should be noted that such periods in reality will vary with regard to intensity, frequency and length as environmental demands vary, and will also vary between individuals.

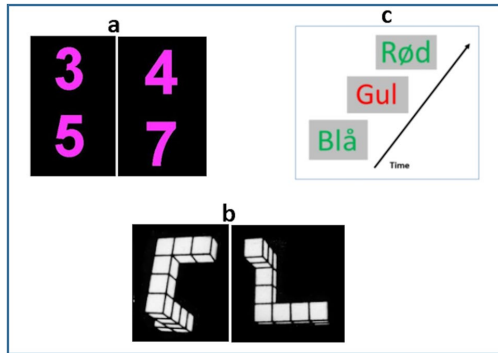


Figure 4. Examples of the stimuli used in the three cognitive tasks. (a) Shows examples of the digit pairs shown on each trial: The left part of the example shows two digits that do not match the target since the sum of the two is < 11 . To the right are shown two numbers that match the target since the sum is 11, and the subject should then correspondingly press the response button. (b) Shows two of the 3D objects that should be compared for similarity: The example shows two object shapes that are the same but rotated horizontally with regard to each other. The subject should press the response button in this example if the shape is the same. (c) Shows an example of the 2-back Stroop working memory task in Norwegian, where the instruction is to press the button when the colour of the word matches with the colour shown two items before.

Methods

Subjects. The subjects were 47 healthy, adult individuals, 27 males and 20 females, mean age 34.9 years (SD 13.9). The subjects were recruited in the Bergen city area through general, open announcements. Absence of any psychiatric and neurological disorder was an inclusion criteria and information was obtained from self-reports. Information about education and mathematical skills level was not formally collected. There is however no reason to assume major differences in education among the subjects, since they all were young adults having been through the obligatory 10 year school system in Norway. Visual acuity and colour-vision was not formally tested, but the behavioural results show that these factors could not have been a confounding factor.

Stimuli and design. There were three different cognitive tasks and stimuli: a mental arithmetic task, a working memory task and a mental rotation task. The tasks were each repeated three times in 30 s ON-blocks in a random order, alternated with 30 s OFF-blocks (Fig. 4).

The stimuli were constructed with graphics software (MS-paint and Corel PaintShop) and stored as bitmaps for presentation through high-resolution LCD HD goggles (NordicNeuroLab Inc., Norway, <https://nordicneurolab.com/>) mounted to the MR head-coil. The timing, duration and sequencing of the stimuli, as well control of overall timing parameters of the experiment was done in the E-Prime (Psychology Software Tools, Inc., USA, <https://pstnet.com/>) software platform. Synchronization timing of presentation of the stimuli with acquisition of the MR data was done through a NordicNeuroLab SyncBox (NordicNeuroLab Inc., Norway, <https://nordicneurolab.com/>). There were nine ON-blocks with task presentations (three repetitions of each task), alternated with nine black screen OFF-blocks without task-presentations. The OFF-blocks had a fixation-cross in the middle of the visual field, and the subjects were instructed to keep their eyes open during OFF-blocks. Each ON- and OFF-block lasted for 60 s, making up a total of 18 min.

The mental arithmetic task consisted of two digits that could vary between the digits 1–9, written on top of each other, in purple font against black background (see Fig. 4a for examples). Each pair of digits was presented for 1200 ms with a blank gap of 300 ms between trials and 20 pseudo-random trials in each ON-block. The instruction to the subject was to mentally add the two numbers and press a hand-held button whenever the sum was "11". There were five target trials randomly interspersed among the 20 trials (25%), with the restriction of not allowing two or more consecutive targets by random selection. Thus, there were 15 target trials in total.

The mental rotation task (Fig. 4b) was tailored on the classic Shepard and Metzler mental rotation task²⁴ with images of two 3D non-configurative objects in white against black background, that were displayed on each trial. The task of the subject was to decide by pressing the hand-held button whether the two shapes were two different objects, or two shapes of the same object, which were rotated horizontally with regard to each other (rotation varied between 20° and 180°). Each presentation trial lasted for 1500 ms, with 20 trial presentations during an ON-block, and where the two shapes were the same on 10 trial presentations and different on 10 trial presentations. The instruction was to press on "same", thus there were a total of 30 targets across the Mental rotation task.

The working memory task (Fig. 4c) was an n-back task with presentations of incongruent Stroop colour-words, like the word "red" written in blue ink. The instruction to the subject was to remember the colour of the word presented two items back (2-back paradigm), and to press the hand-held when the item currently seen in the goggles matched the one presented two items back. This task adds an executive function process to the working memory process, making it cognitively more demanding. It has previously been shown to discriminate

between healthy and depressed patients²⁸ and reliably elicits demands for working memory processing. Each presentation lasted for 1500 ms, with 20 presentations in total, and with five (25%) pseudo-randomly interspersed target trials where the two displays matched. Thus, there were a total of 15 targets for the working memory task.

Behavioural data statistics. Behavioural data for the three tasks were available for 46 participants, with one data set missing. Behavioural data were automatically collected and stored by the E-prime software, for later statistical analysis of response accuracy and response latency (RT ms).

For all three tasks, response accuracy and RT was evaluated statistically for means, standard deviations, and hits ratio of correct responses to false alarms. Hits ratios were converted to Cohen's d-statistic for effect sizes in each task.

Procedure. The subjects were first interviewed for body implants such as pace-makers and any signs of claustrophobia after they were presented with the informed consent form to sign. Females were in addition asked about pregnancy, which was an exclusion criterion. The study was approved by the Regional Committee for Medical Research Ethics in Western Norway (2014/1641/REK Vest). The study was conducted according to the Declaration of Helsinki regarding ethical standards and in agreement with the good clinical practice framework in accordance with all rules and guidelines at our institution for human research. Subjects who agreed to take part in the study were then informed about the experiment and shown examples of the stimuli and familiarized with the tasks to be presented when in the scanner, before being placed in the scanner. Written informed consent was obtained from all participants. To facilitate direct communication with the MR-technicians in the control-room, a balloon was placed on the chest, which should be squeezed in case of an emergency. There was also direct audio contact between the scanner chamber and the control room. The E-Prime stimulus program was run from a stand-alone PC and operated by a research assistant.

MR scanning and data acquisition. The experiment was conducted on a 3 T Magnetom Prisma MR scanner (Siemens Healthcare, Germany). An anatomical T1-weighted image was acquired prior to the functional imaging with the following sequence parameters: MPRAGE 3D T1-weighted sagittal volume, TE/TR/TI = 2.28 ms/1.8 s/900 ms, acquisition matrix = 256 × 256 × 192, field of view (FOV) = 256 × 256 mm², 200 Hz/px readout bandwidth, flip angle = 8 degrees and total acquisition duration of 7.40 min. 2D gradient echo planar imaging (EPI) was performed with the following parameters: TE/TR = 30 ms/2 s, 306 volumes in time, acquisition matrix = 64 × 64, slice thickness = 3.6 mm, 35 slices, FOV = 230 × 230 mm².

fMRI data processing. All pre-processing and analysis were performed in Matlab 9.5 (the MathWorks, Natick, MA) using SPM12-r7219 (the Wellcome Centre for Human Neuroimaging, UCL, London, UK, <https://www.fil.ion.ucl.ac.uk/spm/>). Pre-processing consisted of rigid-realignment, normalisation to MNI space and smoothing with an 8 × 8 × 8 mm³ Gaussian kernel. After pre-processing, first level analysis of all subjects was performed using a general linear model (GLM) implementation of the block-based paradigm. The estimated motion parameters from the re-alignment process were used as a regressor. Framewise displacement was calculated from the re-alignment parameters^{43,44}. For this, projection to the surface of a sphere of 50 mm radius was used to convert rotational displacements from degrees into mm after motion parameter de-meaning and de-trending⁴⁴. Activation maps were re-calculated after removing subjects that had mean FDs ≥ 0.20 mm and compared to the full data-set to test for the impact of motion on the results. Using the standard haemodynamic response (HRF) function, t-contrast images for all three tasks were created with an FWE-corrected *p*-value threshold of *p* = 0.05 yielding a t-contrast image for each condition.

Conjunction analysis. The resultant contrast images (one for each condition) were then used to perform a second level conjunction (one-way ANOVA random effects) analysis across all contrast images of the individual tasks. Briefly, the steps resemble those of a general second-order analysis: All first-order contrast images (one for each subject and each condition) were added into a second-order analysis (one-way ANOVA). The images were grouped by condition. After estimation of the model, contrasts for each condition were defined as usual. To compute the joint-conjunction, multiple contrasts at a time were selected. Statistical maps were calculated with correction for multiple comparisons (FWE), a *p*-value of 0.05 and cluster extent of 20 voxels.

The tasks were also studied individually adjunct to the conjunction analysis to assess the effect of each task. These individual maps were processed in MRICron (ch2.better.niftii) and superimposed on each other.

ROI time course analyses. A third analysis concerned comparing and contrasting activity in ROI that were functionally defined from the activation patterns seen in the conjunction analyses. These ROI were chosen because those regions have shown significant activations during resting- and task-absent periods^{45,32,53}. Similarly, they have shown ROI-activations during active processing and task-presence^{15,19,28,29,54} including tasks and processes covered by the current three tasks.

For this time-course analysis, the ROI were created using MarsBaR v0.44⁵⁵ from the thresholded SPM clusters. Mean voxel values over the ROI were then extracted for each subject from the motion-corrected intensity images in MNI-space. These images represent the actual BOLD signal change at each voxel, rather than the modelled, HRF-corrected response. The images were then averaged over the cohort into a single time-course curve. This resultant time-course curve was rescaled as a percentage of total BOLD signal change, see Fig. 3.

Received: 16 March 2020; Accepted: 23 November 2020
 Published online: 08 December 2020

References

- Shulman, G. L. *et al.* Common blood flow changes across visual tasks: II. Decreases in cerebral cortex. *J. Cogn. Neurosci.* <https://doi.org/10.1162/jocn.1997.9.5.648> (1997).
- Raichle, M. E. *et al.* A default mode of brain function. *Proc. Natl. Acad. Sci. U. S. A.* <https://doi.org/10.1073/pnas.98.2.676> (2001).
- Raichle, M. E. Two views of brain function. *Trends Cogn. Sci.* <https://doi.org/10.1016/j.tics.2010.01.008> (2010).
- Buckner, R. L. & DiNicola, L. M. The brain's default network: Updated anatomy, physiology and evolving insights. *Nat. Rev. Neurosci.* <https://doi.org/10.1038/s41583-019-0212-7> (2019).
- Fox, M. D. *et al.* The human brain is intrinsically organized into dynamic, anticorrelated functional networks. *Proc. Natl. Acad. Sci. U. S. A.* <https://doi.org/10.1073/pnas.0504136102> (2005).
- Corbetta, M. & Shulman, G. L. Control of goal-directed and stimulus-driven attention in the brain. *Nat. Rev. Neurosci.* <https://doi.org/10.1038/nrn755> (2002).
- Uddin, L. Q., Kelly, A. M. C., Biswal, B. B., Castellanos, F. X. & Milham, M. P. Functional connectivity of default mode network components: correlation, anticorrelation, and causality. *Hum. Brain Mapp.* <https://doi.org/10.1002/hbm.20531> (2009).
- Keller, K. & Menon, V. Gender differences in the functional and structural neuroanatomy of mathematical cognition. *Neuroimage* <https://doi.org/10.1016/j.neuroimage.2009.04.042> (2009).
- Keller, J. B. *et al.* Resting-state anticorrelations between medial and lateral prefrontal cortex: Association with working memory, aging, and individual differences. *Cortex* <https://doi.org/10.1016/j.cortex.2014.12.001> (2015).
- Corbetta, M., Patel, G. & Shulman, G. L. The reorienting system of the human brain: From environment to theory of mind. *Neuron* <https://doi.org/10.1016/j.neuron.2008.04.017> (2008).
- Greicius, M. D., Krasnow, B., Reiss, A. L. & Menon, V. Functional connectivity in the resting brain: A network analysis of the default mode hypothesis. *Proc. Natl. Acad. Sci. U. S. A.* <https://doi.org/10.1073/pnas.0135058100> (2003).
- Bressler, S. L. & Menon, V. Large-scale brain networks in cognition: Emerging methods and principles. *Trends Cogn. Sci.* <https://doi.org/10.1016/j.tics.2010.04.004> (2010).
- Lee, M. H. *et al.* Clustering of resting state networks. *PLoS ONE* <https://doi.org/10.1371/journal.pone.0040370> (2012).
- Duncan, J. & Owen, A. M. Common regions of the human frontal lobe recruited by diverse cognitive demands. *Trends Neurosci.* [https://doi.org/10.1016/S0166-2236\(00\)01633-7](https://doi.org/10.1016/S0166-2236(00)01633-7) (2000).
- Fedorenko, E., Duncan, J. & Kanwisher, N. Broad domain generality in focal regions of frontal and parietal cortex. *Proc. Natl. Acad. Sci. U. S. A.* <https://doi.org/10.1073/pnas.1315235110> (2013).
- Duncan, J. The structure of cognition: Attentional episodes in mind and brain. *Neuron* <https://doi.org/10.1016/j.neuron.2013.09.015> (2013).
- Hugdahl, K., Raichle, M. E., Mitra, A. & Specht, K. On the existence of a generalized non-specific task-dependent network. *Front. Hum. Neurosci.* <https://doi.org/10.3389/fnhum.2015.00430> (2015).
- Lustig, C. *et al.* Functional deactivations: Change with age and dementia of the Alzheimer type. *Proc. Natl. Acad. Sci. U. S. A.* <https://doi.org/10.1073/pnas.2235925100> (2003).
- Hugdahl, K. *et al.* Dynamic up- and down-regulation of the default (DMN) and extrinsic (EMN) mode networks during alternating task-on and task-off periods. *PLoS ONE* <https://doi.org/10.1371/journal.pone.0218358> (2019).
- Huettel, A. S., Song, A. W. & McCarthy, G. Functional Magnetic Resonance Imaging, Second Edition. *Book* (2004).
- Bryden, M. P., Munhall, K. & Allard, F. Attentional biases and the right-ear effect in dichotic listening. *Brain Lang.* [https://doi.org/10.1016/0093-934X\(83\)90018-4](https://doi.org/10.1016/0093-934X(83)90018-4) (1983).
- Hugdahl, K. & Andersson, L. The "Forced-Attention Paradigm" in dichotic listening to CV-syllables: A comparison between adults and children. *Cortex* [https://doi.org/10.1016/S0010-9452\(86\)80005-3](https://doi.org/10.1016/S0010-9452(86)80005-3) (1986).
- Westerhausen, R. A primer on dichotic listening as a paradigm for the assessment of hemispheric asymmetry. *Laterality* <https://doi.org/10.1080/1037650X.2019.1598426> (2019).
- Shepard, R. N. & Metzler, J. Mental rotation of three-dimensional objects. *Science (80-)*. <https://doi.org/10.1126/science.171.3972.701> (1971).
- Jordan, K., Heinze, H. J., Lutz, K., Kanowski, M. & Jäncke, L. Cortical activations during the mental rotation of different visual objects. *Neuroimage* <https://doi.org/10.1006/nimg.2000.0677> (2001).
- Tagaris, G. A. *et al.* Mental rotation studied by functional magnetic resonance imaging at high field (4 Tesla): Performance and cortical activation. *J. Cogn. Neurosci.* <https://doi.org/10.1162/jocn.1997.9.4.419> (1997).
- Hugdahl, K., Thomsen, T. & Erslund, L. Sex differences in visuo-spatial processing: An fMRI study of mental rotation. *Neuropsychologia* <https://doi.org/10.1016/j.neuropsychologia.2006.01.026> (2006).
- Hammar, Å. *et al.* Striatal hypoactivation and cognitive slowing in patients with partially remitted and remitted major depression. *Psych J.* <https://doi.org/10.1002/pcbj.134> (2016).
- Desposito, M. *et al.* The neural basis of the central executive system of working memory. *Nature* <https://doi.org/10.1038/378279a0> (1995).
- Hinault, T., Larcher, K., Bherer, L., Courtney, S. M. & Dagher, A. Age-related differences in the structural and effective connectivity of cognitive control: A combined fMRI and DTI study of mental arithmetic. *Neurobiol. Aging* <https://doi.org/10.1016/j.neurobiolaging.2019.06.013> (2019).
- Hugdahl, K. *et al.* Brain activation measured with fMRI during a mental arithmetic task in schizophrenia and major depression. *Am. J. Psychiatry* <https://doi.org/10.1176/appi.ajp.161.2.286> (2004).
- Cunningham, S. I., Tomasi, D. & Volkow, N. D. Structural and functional connectivity of the precuneus and thalamus to the default mode network. *Hum. Brain Mapp.* <https://doi.org/10.1002/hbm.23429> (2017).
- Chambers, C. *The Seven Deadly Sins of Psychology. The Seven Deadly Sins of Psychology* (2019). <https://doi.org/10.2307/j.ctvc779w5>.
- Turnbull, A. *et al.* Left dorsolateral prefrontal cortex supports context-dependent prioritisation of off-task thought. *Nat. Commun.* <https://doi.org/10.1038/s41467-019-11764-y> (2019).
- Andreou, C. *et al.* The role of effective connectivity between the task-positive and task-negative network for evidence gathering [Evidence gathering and connectivity]. *Neuroimage* <https://doi.org/10.1016/j.neuroimage.2018.02.039> (2018).
- Gotts, S. J., Gilmore, A. W. & Martin, A. Brain networks, dimensionality, and global signal averaging in resting-state fMRI: Hierarchical network structure results in low-dimensional spatiotemporal dynamics. *Neuroimage* <https://doi.org/10.1016/j.neuroimage.2019.116289> (2020).
- Downar, J., Crawley, A. P., Mikulis, D. J. & Davis, K. D. A cortical network sensitive to stimulus salience in a neutral behavioral context across multiple sensory modalities. *J. Neurophysiol.* <https://doi.org/10.1152/jn.00636.2001> (2002).
- Mitra, A. & Raichle, M. E. Principles of cross-network communication in human resting state fMRI. *Scand. J. Psychol.* <https://doi.org/10.1111/sjop.12422> (2018).
- Power, J. D. & Petersen, S. E. Control-related systems in the human brain. *Curr. Opin. Neurobiol.* <https://doi.org/10.1016/j.conb.2012.12.009> (2013).

40. Cona, G. & Semenza, C. Supplementary motor area as key structure for domain-general sequence processing: A unified account. *Neurosci. Biobehav. Rev.* <https://doi.org/10.1016/j.neubiorev.2016.10.033> (2017).
41. Binder, J. R. *et al.* Conceptual processing during the conscious resting state: A functional MRI study. *J. Cogn. Neurosci.* <https://doi.org/10.1162/089892999563265> (1999).
42. Gusnard, D. A. & Raichle, M. E. Searching for a baseline: Functional imaging and the resting human brain. *Nat. Rev. Neurosci.* <https://doi.org/10.1038/35094500> (2001).
43. Power, J. D., Barnes, K. A., Snyder, A. Z., Schlaggar, B. L. & Petersen, S. E. Spurious but systematic correlations in functional connectivity MRI networks arise from subject motion. *Neuroimage* <https://doi.org/10.1016/j.neuroimage.2011.10.018> (2012).
44. Power, J. D. *et al.* Methods to detect, characterize, and remove motion artifact in resting state fMRI. *Neuroimage* <https://doi.org/10.1016/j.neuroimage.2013.08.048> (2014).
45. Whitfield-Gabrieli, S. & Nieto-Castanon, A. Conn: A functional connectivity toolbox for correlated and anticorrelated brain networks. *Brain Connect.* <https://doi.org/10.1089/brain.2012.0073> (2012).
46. Artemenko, C., Soltanlou, M., Ehlis, A. C., Nuerk, H. C. & Dresler, T. The neural correlates of mental arithmetic in adolescents: A longitudinal fNIRS study. *Behav. Brain Funct.* <https://doi.org/10.1186/s12993-018-0137-8> (2018).
47. Harris, I. M. *et al.* Selective right parietal lobe activation during mental rotation. A parametric PET study. *Brain* <https://doi.org/10.1093/brain/123.1.65> (2000).
48. Ke, Y. *et al.* The effects of transcranial direct current stimulation (tDCS) on working memory training in healthy young adults. *Front. Hum. Neurosci.* <https://doi.org/10.3389/fnhum.2019.00019> (2019).
49. Schilbach, L. *et al.* Transdiagnostic commonalities and differences in resting state functional connectivity of the default mode network in schizophrenia and major depression. *NeuroImage Clin.* <https://doi.org/10.1016/j.nicl.2015.11.021> (2016).
50. Miró-Padilla, A. *et al.* Long-term brain effects of N-back training: An fMRI study. *Brain Imaging Behav.* <https://doi.org/10.1007/s11682-018-9925-x> (2019).
51. Potvin, S. *et al.* The neural correlates of mental rotation abilities in cannabis-abusing patients with schizophrenia: An fMRI study. *Schizophr. Res. Treat.* <https://doi.org/10.1155/2013/543842> (2013).
52. Delazer, M. *et al.* Number processing and basal ganglia dysfunction: A single case study. *Neuropsychologia* <https://doi.org/10.1016/j.neuropsychologia.2003.12.009> (2004).
53. Deng, Z. Z. *et al.* Segregated precuneus network and default mode network in naturalistic imaging. *Brain Struct. Funct.* <https://doi.org/10.1007/s00429-019-01953-2> (2019).
54. Le, H. B. *et al.* Neural activity during mental rotation in deaf signers: The influence of long-term sign language experience. *Ear Hear.* <https://doi.org/10.1097/AUD.0000000000000540> (2018).
55. Brett, M., Anton, J. L., Valabregue, R. & Poline, J. B. Region of interest analysis using an SPM toolbox. *Neuroimage* [https://doi.org/10.1016/S1053-8119\(02\)90010-8](https://doi.org/10.1016/S1053-8119(02)90010-8) (2002).

Acknowledgements

The present study was funded by grants to R.G. from the Trond Mohn Foundation (#BFS2017TMT06) and to K.H. from the European Research Council (#693124) and the Health Authorities of Western Norway Helse-Vest #912045). The authors want to thank all subjects participating in the study, and the MR technicians and research assistants who assisted in acquiring the data and formatting of the manuscript.

Author contributions

F.R. carried out analysis of the data, manuscript writing and figure preparation. R.G. conceived and conducted the experiments. J.B. developed the fMRI tasks and analysed response data. K.K. contributed to analysis of the data. L.E. conceived and conducted the experiments. K.H. conceived and conducted the experiment and carried out analysis of the data. All authors reviewed the manuscript.

Competing interests

The co-authors R.G., L.E. and K.H. own shares in the NordicNeuroLab Inc. company (<https://nordicneurolab.com>), which produces some of the add-on equipment used during data acquisition. All other authors declare no competing interests.

Additional information

Correspondence and requests for materials should be addressed to F.R.

Reprints and permissions information is available at www.nature.com/reprints.

Publisher's note Springer Nature remains neutral with regard to jurisdictional claims in published maps and institutional affiliations.



Open Access This article is licensed under a Creative Commons Attribution 4.0 International License, which permits use, sharing, adaptation, distribution and reproduction in any medium or format, as long as you give appropriate credit to the original author(s) and the source, provide a link to the Creative Commons licence, and indicate if changes were made. The images or other third party material in this article are included in the article's Creative Commons licence, unless indicated otherwise in a credit line to the material. If material is not included in the article's Creative Commons licence and your intended use is not permitted by statutory regulation or exceeds the permitted use, you will need to obtain permission directly from the copyright holder. To view a copy of this licence, visit <http://creativecommons.org/licenses/by/4.0/>.

© The Author(s) 2020



Graphic design: Communication Division, UIB / Print: Skjipes Kommunikasjon AS



uib.no

ISBN: 9788230854082 (print)
9788230864524 (PDF)